Distinct outcomes of oscillatory and sustained Dll1 expression on muscle stem cell fate

Inaugural-Dissertation
to obtain the academic degree
Doctor rerum naturalium (Dr. rer. nat.)

submitted to the Department of Biology, Chemistry, Pharmacy
of Freie Universität Berlin

by

Yao Zhang

July, 2021

This work was carried out under the supervision of Prof. Dr. Carmen Birchmeier at Max-Delbrück-Center for Molecular Medicine from July 2016 to June 2021.

1st Reviewer: Prof. Dr. Carmen Birchmeier

2nd Reviewer: Prof. Dr. Sigmar Stricker

Date of defense: 27-Sep-2022

Acknowledgements

I would like to thank my supervisor, Prof. Dr. Carmen Birchmeier, for her supervision and support in her lab. I also want to thank Prof. Dr. Sigmar Stricker for being my thesis reviewer.

I also want to thank the people in the lab that I have worked with: Dr. Ines Lahmann, Petra Stallerow, Dr. Thomas Müller, Dr. Minchul Kim, Elijah Lowenstein, Dr. Pierre-Louis Ruffault, Sven Buchert, Bettina Brandt. Additionally, many thanks to my former colleagues: Dr. Joscha Griger, Dr. Kun Song, Dr. Shiqi Jia, Dr. Jie-Shin Chen.

Besides, I also want to give special thanks to the people that I have collaborated with. Dr. Katharina Baum and Dr. Jana Wolf, who performed a nice mathematical model, help me to understand the project deeply. Dr. Hiromi Shimojo and Dr. Ryoichiro Kageyama, who generated the *Dll1-luc* and *Dll1type2* mice, also gave me useful advice.

Last but not least, I would thank my family: my wife Lu Wang and my daughter Silin Joceline Zhang. Thanks for their daily encouragement and emotional support during the past years.

Declaration of Independence

I herewith declare that this thesis has

1) been written and composed by myself independently.

2) depended on solely the results of my own work.

3) not been submitted for any other degree.

This work has been published in *Nature Communications* as the title: Oscillations of Delta-like1 regulate the balance between differentiation and maintenance of muscle stem cells.

Table of Contents

1. Introduction

1.1. Skeletal muscle development and regeneration

Skeletal muscle is the largest organ in the body, constituting around 30-40% of the body weight (female 30.6% vs male 38.4%) (Janssen et al., 2000). Skeletal muscle is essential for movement. Disorders of muscle development and regeneration result in disease like congenital myopathies, a group of rare congenital diseases. The most frequent congenital myopathy is Duchenne muscular dystrophy. However, also in other conditions like cancer (cachexia) or very old age (sarcopenia) muscle weakness is common. Skeletal muscle is composed of many bundles of myofibers, i.e. multi-nucleated cells that arise by fusion of single cells. An extracellular matrix surrounds each myofiber. Many myofibers are arranged together in bundles, which are again surrounded by connective tissue. In addition, the skeletal muscle contains blood vessels and so-called interstitial cells that lie outside of the muscle fiber. A further cell type associated with the skeletal muscle is the muscle stem cell that is also called satellite cell. These cells attach to the myofibers, and locate between the myofiber membrane and the extracellular matrix. This location is referred to as the muscle stem cell niche (Brohl et al., 2012). Muscle stem cells can regenerate the muscle fibers, and they derive from progenitor cells that generate muscle during development.

1.1.1. Development of the skeletal muscle in the vertebrate embryo

Skeletal muscles arise from the somites, ball-like structures that lie on both sides of the embryonic axis and derive from paraxial mesoderm. Subsequently, the different parts of the somites can be distinguished, a ventral and a dorsal part called sclerotome and dermomyotome, respectively. The sclerotome will form the vertebrae and ribs, while the dermomyotome will generate the skeletal musculature of the body (Christ et al., 1992; Christ and Ordahl, 1995).

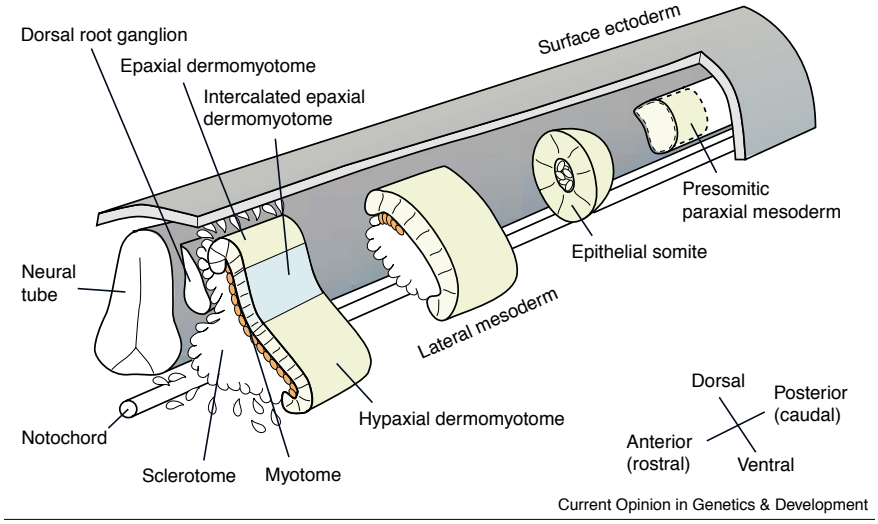

Figure 1. Schematic representation of vertebrate somitogenesis.
Details see text. (Adapted from Buckingham et al 2001)

The dermomyotome can be divided into epaxial and hypaxial dermomyotome. The epaxial dermomyotome is next to the neural tube and notochord, and it will form hypaxial (deep back) muscles. The remainder of the musculature of the body and limbs is formed by the hypaxial dermomyotome. The myotome is generated by the dermomyotome, is located below it, and represents the first differentiated myogenic cells (Tajbakhsh and Buckingham, 2000).

The paraxial muscles, i.e. muscles of the ventral body and limbs, are generated by progenitor cells from the hypaxial dermomyotome (Denetclaw and Ordahl, 2000; Ordahl and Ledouarin, 1992). On the levels of the limbs, the ventral dermomyotome undergoes an epithelial-mesenchymal transition, i.e. cells are delaminating from the epithelium, and they migrate into the limb to form a progenitor pool that eventually generates the muscle of the extremities (Christ et al., 1977). This process depends on *Pax3*, a transcription factor of the paired- and homeodomain family. It is expressed throughout the dermomyotome, but at higher levels in the ventral portion (Daston et al., 1996; Goulding et al., 1994). In splotch (*Pax3*-/-) embryos, the limb muscles fail to develop because cells from the somites fail to migrate into the limbs. In addition, the ventral dermomytome fails to express the tyrosine kinase receptor *Met* (Daston et al., 1996).

Met is expressed in the ventral dermomyotome and in cells located at the dorsal tips of the dermomyotome (Bladt et al., 1995; Yang et al., 1996). In mutant embryos which lack a functional Met receptor, skeletal muscle is absent in the limbs (Bladt et al., 1995). A similar phenotype is also apparent in mutant embryos that lack *HGF*, the Met ligand (Schmidt et al., 1995). This is due to the fact that in *Met* mutant mice cells of the dermomyotome are unable to undergo an epithelial-mesenchymal transition, and do not migrate. In addition, Gab1, an adaptor molecule that transduces Met signals, has a similar phenotype when it is ablated, i.e. the *Gab1* mutation interferes with migration of muscle progenitors (Sachs et al., 2000). The *Met* gene is a direct target of Pax3 (Epstein et al., 1996; Keller et al., 2004).

Lbx1, which encodes a homeodomain transcription factor, is also an important factor in migrating progenitors. *Lbx1* and *Pax3* are co-expressed in all migrating hypaxial progenitors, and *Lbx1* is regulated in part by Pax3 (Mennerich et al., 1998). In mice that lack *Lbx1*, cells can delaminate from the dermomyotome but do not migrate into limbs and instead get stuck on their way, ending up in the wrong position (Brohmann et al., 2000; Gross et al., 2000). Misplaced muscle progenitors are found at the posterior-ventral and dorsal margins of the limbs, thereby generating residual hypaxial muscles. Met was also shown to cooperate with Cxcr4 in muscle stem cell proliferation and migration during muscle development (Vasyutina et al., 2005).

After the cells migrate into the limbs, proliferation is necessary for amplification of the progenitors, which is required to generate sufficient cells for the formation of limb muscles. Many genes, which are involved in migration also function in proliferation and survival. Increasing the activity of *Pax3* and *Met* results in hypertrophic muscle (Keller et al., 2004; Relaix et al., 2003). Myogenic regulatory factors (MRFs) like *Myf5* and *MyoD* play an important role in progenitor amplification and also are important for the initiation of the terminal differentiation program. In mutant embryos lacking both *Myf5* and *MyoD*, the formation of all skeletal muscle in the body is severely impaired

(Rudnicki et al., 1993). Loss of both *Myf5* and *MyoD* activates *Mrf4*, but *Mrf4* alone only incompletely rescues muscle formation (Kassar-Duchossoy et al., 2004). Moreover, loss of *Myf5* results in the delay of skeletal muscle development (Braun et al., 1992). Mutation of *MyoD* allows seemingly normal skeletal muscle, but muscle differentiation is delayed and *Myf5* is upregulated. These results led to the hypothesis that *Myf5* and *MyoD* have similar roles and can functionally compensate for each other (Rudnicki et al., 1992).

Even after myogenic differentiation has initiated, only a part of the progenitor cells undergoes terminal differentiation and exit from the cell cycle, whereas other progenitor cells remain in undifferentiated state. Early myofibers (primary myofibers) are formed, that act as a scaffold, and later myofibers are added to form the bulk of skeletal muscle at birth (Wigmore and Evans, 2002). The exit from the cell cycle and entry into the terminal differentiation program depends on the presence of *Myogenin (MyoG)*. Mice lacking functional *MyoG* are immobile and die because of a complete lack of skeletal muscle (Hasty et al., 1993; Nabeshima et al., 1993). *MyoG* mutant mice have the normal number of myoblasts, but they cannot undergo efficient fusion to form functional muscle fibers.

1.1.2. Growth of the skeletal muscle in the fetal and early postnatal periods in vertebrates

After E12.5, the expression of *Pax3* in the limb is downregulated, but expression of *Pax7*, a related factor, is expressed in muscle progenitors of the limbs. Thus, in the late fetal period muscle stem cells only express *Pax7* (Vasyutina et al., 2007). By E16.5, Pax7+ cells locate to the muscle stem cell niche underneath a basal lamina and outside the myofiber (Kassar-Duchossoy et al., 2005). Colonization of the muscle stem cells niche is important for further muscle growth (Brohl et al., 2012).

The growth of the skeletal muscle is faster during neonatal period than during any other stage of postnatal life (Davis and Fiorotto, 2009). Mostly, this is due

to the fusion of myoblasts to existing myofibers. Interestingly, fetal myoblasts display a distinct genetic signature from embryonic myoblasts, for example expressing higher levels of Jag1 and Notch1 (Biressi et al., 2007). After myofibers have ceased to grow by the accretion of nuclei, which in mice is mostly completed around three weeks of age, the growth of skeletal muscle fibers is regulated by protein synthesis. Thus, the rate of synthesis of muscle proteins is higher than the degradation rate during this process (Davis et al., 1989).

When the muscle matures, the muscle stem cells (Pax7+) acquire a quiescent state. These non-cycling cells can be identified as Pax7+/MyoD- or Pax7+/Ki67- cells (Griger et al., 2017). However, cellular quiescence or G0 of muscle stem cells cannot be simply described as a withdrawal from the cell cycle. It is characterized by an increased nucleocytoplasmic ratio, a decrease in cell size, altered protein synthesis and metabolism, as well as a distinct gene expression profile (Coller et al., 2006; Dell'Orso et al., 2019; Machado et al., 2017; van Velthoven et al., 2017). Two cell surface molecules, *Calcr* (Calcitonin receptor) and *Odz4*, are highly expressed and used for FACS isolation of quiescent muscle stem cells (Fukada et al., 2013; Yamaguchi et al., 2012). In *Calcr* mutant muscle stem cells, Ki67 and other cell cycle related genes like Ccnd1 are expressed at higher levels, but myogenic factors as MyoD are expressed at similar level, suggesting that the loss of quiescence does not impact myogenic differentiation (Yamaguchi et al., 2012). Similarly, *Odz4* mutant mice showed increased numbers of activated muscle stem cells, prolonged cell proliferation and enhanced differentiation (Ishii et al., 2015). Pathways such as MAPK/ERK signaling have been explored in the context of muscle stem cell quiescence. For example, Src-homology 2-domain containing tyrosine phosphatase (Shp2) regulates the quiescent state through controlling MAPK/ERK and exit of the cell cycle (Griger et al., 2017). In quiescent muscle stem cells, myogenic differentiation factors like MyoD and Myf5 are absent. Interestingly, *Myf5* transcripts are present, and indeed repression of translation is important to maintain quiescence of muscle stem cells. This may be mediated by selected translation via phosphorylation of translation

initiation factor eIF2□. When the phosphorylation site in eIF2a is mutated, the Myf5 protein accumulates in muscle stem cells, which results in the exit from quiescence (Zismanov et al., 2016). It is more and more clear that muscle stem cell activation occurs in several steps and rapidly. For example, the gene expression profile changes within 3h after activation of muscle stem cells and thus earlier than cell cycle markers and proteins like MyoD appear (Machado et al., 2021). Following exit from quiescence, muscle stem cells can proliferate, and subsequently either differentiate to generate new muscle fibers, or self-renew to replenish the stem cell pool. Additional possible fates of muscle stem cells are death through apoptosis, or the loss of the ability to proliferate through senescence.

1.1.3. Regeneration of the skeletal muscle in adult vertebrates

In the adult skeletal muscle of sedentary vertebrates (i.e. an individuum that moves little), muscle stem cells are relatively stable and there is little turnover of myonuclei (Schmalbruch and Lewis, 2000). However, when the muscle is used, muscle stem cells can become activated. Moreover, skeletal muscles are very susceptible to injuries (Huard et al., 2002). In response to various injury types, the muscle can be regenerated. In mice this is experimentally assessed by injections of a toxin (e.g. cardiotoxin, barium chloride) into a small muscle, which damages the muscle fibers severely.

In the injured muscle, the sarcolemma of muscle fibers is disrupted, making the muscle fiber permeable (Wooddell et al., 2011). The intracellular material, for instance creatine kinase and microRNAs, are released into the extracellular environment (Baird et al., 2012; Mizuno et al., 2011; Zaharieva et al., 2013). This activates inflammatory cells residing in the muscle, which release cytokines and recruit additional inflammatory cells, such as neutrophils and macrophages, to the damaged areas by chemotactic mechanisms (Arnold et al., 2007; Pizza et al., 2005). In the early phase of regeneration, macrophages remove the debris in the injured tissue. In addition, neutrophils and macrophages play important roles in the regeneration process because they

regulate the behavior of muscle stem cells. Neutrophils can activate muscle stem cells and attract them to the injury site, and macrophages can regulate muscle stem cell proliferation and differentiation (Merly et al., 1999; Ratnayake et al., 2021; Schneider et al., 2002).

Cytokines produced during this process are also thought to activate the muscle stem cells. Activated muscle stem cells start to express MyoD and are then often referred to as myoblasts. They can extensively proliferate to increase cell numbers, which is very important for regeneration, and the regeneration efficiency is reduced if the proliferation process is inhibited (Quinlan et al., 1995; Wakeford et al., 1991; Weller et al., 1991). Activated stem cells have the ability to differentiate and to fuse to existing muscle fibers for repair, or they can fuse with each other to form new myofibers. Finally activated stem cells can also return to a quiescence state (Darr and Schultz, 1987; Griger et al., 2017; Snow, 1978).

Besides muscle stem cells, there are other cells types that participate in muscle regeneration and that can contribute to the myogenic lineage. They are muscle side population cells, PW1+ interstitial cells, mesoangioblasts, pericytes, CD133+ cells and Twist2+ cells (Lee et al., 2000; Liu et al., 2017; Peault et al., 2007; Peng and Huard, 2004). It is little studied how extensive these cell types contribute to the formation of new muscle tissue during regeneration.

1.2. Notch signaling in muscle development and regeneration

Multicellular development needs crosstalk between cells. Cells need to sense cues from extracellular environment and from neighboring cells, and integrate this information into developmental and physiological responses. There are many evolutionarily conserved signaling pathways that transmit the information, such as Wnt, Shh, BMP, PI3K/AKT, JAK/STAT and Notch signaling (Andersson et al., 2011; Gazave et al., 2009).

1.2.1. The Notch signaling pathway

Notch was described more than 100 years ago as sex-linked lethal mutation in *D. melanogaster* (Bridges, 1916). The essential components of Notch signaling are highly conserved and function in a similar manner in vertebrates and invertebrates (D'Souza et al., 2010).

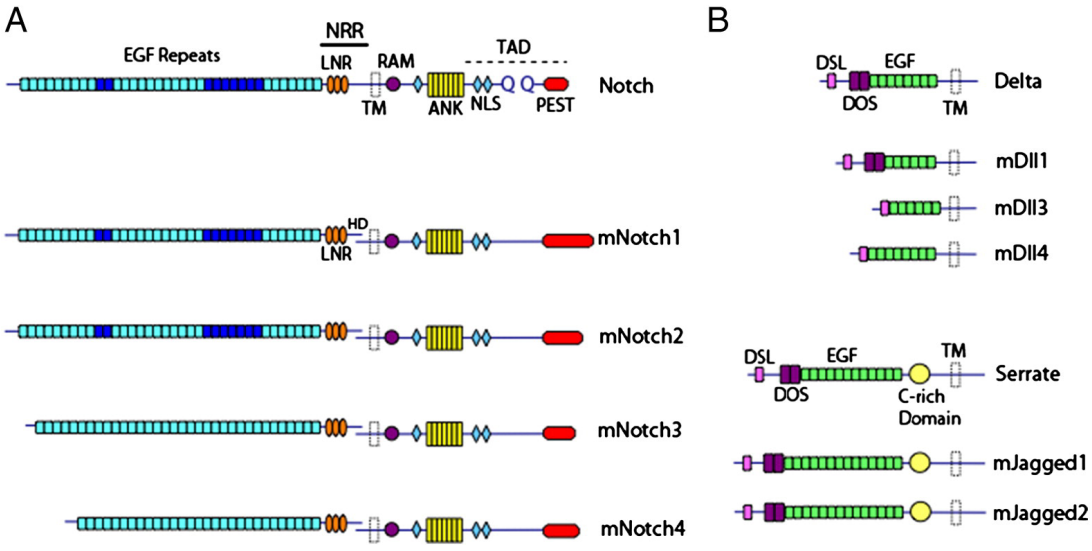

Figure 2. Structural domains of canonical ligands and Notch receptors in Drosophila and mammals.

(A) Structure of Notch receptors in *Drosophila* (Notch) and mouse (mNotch1-4). (B) Notch ligands in *Drosophila* (Delta, Serrate) and mouse (mDll1-3, mJagged1-2). (Adapted from Perdigoto et al 2013).

Notch receptors can be activated by DSL (Delta, Serrate and Lag) ligands, which are characterized by the presence of a DSL domain (Delta, Serrate and Lag) and multiple EGF repeats. In most ligands, the DSL motif is followed by a DOS motif (Delta and OSM-11-like proteins). mJagged1/2 proteins contain an additional cysteine-rich domain. The mature Notch receptors at the plasma membrane have been cleaved into a heterodimer, one subunit containing the large Notch extra cellular domain (NECD), and the second subunit the trans-membrane domain (TM) and the Notch intracellular domain (NICD) (Blaumueller et al., 1997).

The activation of Notch signaling by ligand binding leads to an additional processing step, the cleavage of Notch receptor by ADAM/TACE family metalloproteases (ADAM: short for a disintegrin and metalloproteinase; TACE: short for TNF-alpha converting enzyme). This results in formation of an activated, membrane-tethered intermediate, which is cleaved by γ-secretase to release the intracellular NICD (Brou et al., 2000; De Strooper et al., 1999; Rooke et al., 1996; Struhl and Adachi, 2000; Struhl and Greenwald, 1999). NICD then translocates into the nucleus and forms a complex with the DNA binding protein CSL/RBP-J and the co-activator Mastermind (Mam). This complex can bind specific regulatory DNA sequences to activate the expression of Notch target genes, including Hairy/enhancer of split (Hes) and Hes-related with YRPW motif (Hey) family genes (Bray, 2006; Kopan and Ilagan, 2009). When *NICD* is absent, the complex forms a transcription repressor complex to suppress Notch target genes transcription (Bray and Bernard, 2010).

DSL ligands and Notch receptors are widely expressed in various cell types and used for the communication between cells. Most cell types express both, ligands and receptors. However, the signal stream is highly regulated. Normally, Notch signaling occurs when membrane-bound ligands on one cell activate Notch receptors on neighboring cells (trans-activation) (Artavanis-Tsakonas et al., 1999; Bray, 2016; Nichols et al., 2007). Interactions between Notch1 and Jag1 can block the trans-activation during angiogenesis (trans-inhibition) (Benedito et al., 2009; Golson et al., 2009). Additionally, Dll1 can bind to Notch1 produced by the same cell, which can generate two different outcomes, cis-inhibition or cis-activation (Fiuza et al., 2010; Jacobsen et al., 1998; Lowell et al., 2000; Micchelli et al., 1997; Nandagopal et al., 2019; Sprinzak et al., 2010). This mechanism constitutes an ultrasensitive switch between signal-sending (high ligand/low receptor) and signal-receiving (high receptor/low ligand) states (Bocci et al., 2020; Nandagopal et al., 2019).

1.2.2. The function of Notch signaling in muscle

Notch signaling plays a central role in the maintenance of muscle stem cells during development and in the adult. Continuous Notch signaling is required for correct myogenesis and adult muscle homeostasis. At different stages of muscle stem cell life, different receptors and ligands are required for appropriate muscle homeostasis.

1.2.2.1. The function of Notch signaling in muscle progenitors during development

When muscle progenitors lack *Rbp-J* in the embryo, they undergo myogenic differentiation, which results in a fast depletion of the progenitor pool. Because of this, only tiny muscles are formed (Vasyutina et al., 2007). Thus, Notch signaling is required to maintain the muscle progenitor pool.

Delta-like1 (Dll1) is a major player in myogenesis during development. In the limb buds, *Dll1* is well expressed in Myf5+ and MyoG+ cells, but present at lower levels in Pax3+ and Lbx1+ progenitor cells that migrate from the hypaxial somite (Schuster-Gossler et al., 2007). The muscle progenitors (MyoD+) induce the expression of *Dll1,* which sustains the progenitor pool (Wittenberger et al., 1999). Moreover, Dll1 represses myogenesis by reducing *MyoD* expression (Kuroda et al., 1999). This gene regulatory network between myogenic factor and Notch signaling balances the maintenance of muscle progenitors. Hypomorphic *Dll1* mutation in mice results in severe muscle hypotrophy due to premature differentiation of muscle progenitors (Schuster-Gossler et al., 2007), resembling the phenotype observed when *Rbp-J* is mutated in myogenic cells. This phenotype can be rescued by the additional mutation of *MyoD*, indicating that an important outcome of Notch signaling during myogenesis is to suppress *MyoD* (Brohl et al., 2012). In hypomorphic *Dll1* and *MyoD* double mutant mice and in *Rbp-J* and *MyoD* double mutants, muscle progenitors are retained but do not locate to their niche (Brohl et al., 2012). Thus, Dll1-triggered Notch signaling is important for developmental myogenesis, and it controls two aspects: Maintenance of the progenitor pool by

suppression of MyoD, and the colonization of the stem cell niche by controlling adhesion and extracellular matrix formation (Brohl et al., 2012).

1.2.2.2. The function of Notch signaling in muscle stem cells in the adult

In the adult, muscle stem cells require Notch signaling to sustain a quiescent state (Bjornson et al., 2012; Mourikis et al., 2012). *RBP-J* null muscle stem cells exit spontaneously from the quiescent state in adult mice, leading to the hypothesis that active Notch signaling is essential for quiescent muscle stem cells. p38/mitogen activated protein kinase (MAPK) pathway activation switches the quiescent state to activated state of muscle stem cells (Jones et al., 2005). Notch signaling inhibits the p38/MAPK pathways through induction of MAPK phosphatase-1 (Kondoh et al., 2007). Notch ligands, Dll4 and Jagged1 can induce Hey1 and HeyL in human myogenic cells efficiently *in vitro* (Sakai et al., 2017). Moreover, Hes1, Hey1 and HeyL are important for generation of undifferentiated quiescent muscle stem cells (Fukada et al., 2011; Lahmann et al., 2019). Despite the fact that the mechanism that keeps muscle stem cells quiescent is not fully understood, it is sure that Notch signaling has a main role.

Muscle injury results in activation of muscle stem cells and regeneration. Dll1 is quickly up-regulated in activated muscle stem cells after muscle injury, while *Hes1* is down-regulated (Conboy et al., 2003; Conboy and Rando, 2002). When Notch signaling is blocked by Jag1-Fc, muscle regeneration is impaired (Brack et al., 2008). In *Hes1* or *Rbp-J* mutant muscle stem cells, premature differentiation occurs, resulting in muscle stem cell loss and regeneration failure (Bjornson et al., 2012; Lahmann et al., 2019; Mourikis et al., 2012). *MyoD* expression is suppressed by Hes1, while *MyoG* promoter activity can be directly suppressed by Hey1 (Buas et al., 2010; Lahmann et al., 2019; Shawber et al., 1996). Therefore, the Notch pathway has an important role in regulation of activation and differentiation of muscle stem cells. However, Notch signaling does not affect proliferation. In cultured *Rbp-J* null muscle stem cells, the time required to the first mitosis is similar to control muscle stem cells (Mourikis et al., 2012). Moreover, *Rbp-J* and *Hes1* mutant muscle stem cells showed similar

proliferation index *in vivo* (Lahmann et al., 2019; Vasyutina et al., 2007). Interestingly, *Notch3* knock-out mice have a opposite phenotype, a muscle hyperplasia. It was suggested that Notch3 acts as a Notch1 repressor (Kitamoto and Hanaoka, 2010). Recently, a report showed the function of Notch on dedifferentiation of muscle stem cells. Constitutive activation of Notch in differentiated myocytes forces them to return to an undifferentiated state and to re-express stem cell markers (Bi et al., 2016). Taken all together, Notch signaling is important for the muscle stem cell fate decision during muscle regeneration in the adult.

However, the source of the Notch ligand that keeps muscle stem cells quiescent is still unclear. Based on the location of muscle stem cells that directly contact the muscle fiber *in vivo*, the myofibers are considered as a main source of Notch ligands. *Dll4* transcripts have been detected by RNAscope in myofibers, indicating that myofibers are the source (Kann and Krauss, 2019). Recently, a report showed that deletion of *Dll4* in myofibers promotes muscle stem cell loss, but the phenotype is not as strong as the one observed after mutation of *Rbp-J* in the stem cells (Eliazer et al., 2020). It suggested that not only Dll4 from myofibers regulates muscle stem cells. By single cell sequencing, Dll1 was found to be upregulated in differentiating MyoG+ muscle stem cells. A block of Dll1 activity by an antibody resulted in smaller muscle and less muscle stem cells (Yartseva et al., 2020). Moreover, when isolated muscle stem cells are cultured *in vitro*, a proper density is necessary for healthy growth, suggesting that cell-cell communication between muscle stem cells may also be important, and Notch signals might be among the signals that are used in such cultures .

1.3. Oscillation of Notch signaling genes

Many genes can be expressed in an oscillatory manner, which means in a rhythmic pattern or in periodic cycles. The most famous oscillating genes are those that determine circadian rhythms, which oscillate with a period of about 24 hours. Recently, Notch related gene oscillation was found in the presomitic mesoderm (PSM), where oscillations occur synchronously, and in neural stem

cells, where oscillations occur asynchronously (Shimojo et al., 2016; Yoshioka-Kobayashi et al., 2020). The oscillatory expression has important roles in somite formation and in neural stem cell proliferation and differentiation (Imayoshi et al., 2013; Shimojo et al., 2016). Oscillatory gene expression needs an oscillator to drive the dynamic expression. Transcription factors can expresse in an oscillatory manner, and proteins encoded by their target genes can either oscillate or not depending on variables like the stability of the mRNA or protein (Kobayashi and Kageyama, 2011).

1.3.1. Modeling of Notch related oscillators

The Goodwin oscillator is the first and simplest biological oscillator that was mathematically modeled. The circuit is composed of a single gene, whose protein product can bind its own promoter and repress its expression, using an appropriate delay time for the generation of the functional protein, binding to the DNA and regulating its own expression (Goodwin, 1965). Hes1 functions according to this model: in its promoter, four N-boxes are located, which are the binding sites for proteins of the Hes family (Sakagami et al., 1994). Through this mechanism, Hes1 can repress its own expression. Also other proteins of the Hes/Hey family can repress transcription through binding to such an N-box. The WRPW domains of Hes/Hey interact with the Groucho-related gene (Grg), a co-repressor, which can switch off gene expression (Fisher et al., 1996; Paroush et al., 1994). Hes/Hey factors function as dimers, they can either form homodimers or heterodimers, for instance Hes1 can heterodimerize with Hey1 or Hey2, and the heterodimers possess higher repressive activity than homodimers (Iso et al., 2001). Hes1 expression oscillates in many cell types, for instance in myogenic C2C12 cells, fibroblasts, neural stem cells and muscle stem cells (Hirata et al., 2002; Lahmann et al., 2019; Shimojo et al., 2008; Yoshiura et al., 2007). The expression of Hes1 target genes *Mash1*, *MyoD* and *Dll1* can also oscillate, because Hes1 rhythmically represses their transcription (Imayoshi et al., 2013; Lahmann et al., 2019).

Whether the expression of a gene oscillates or not depends on many variables. One of them is the delay time. In mammals, introns constitute on average 95% of sequence of a gene. Many introns have regulatory functions, and their length regulates time needed for the transcription of a gene (Cravchik et al., 2001; Venter, 2001). Oscillatory systems can be synthesized by generating genes whose products repress their own transcription. When such genes possess different intron lengths, oscillations with different periods are observed, and the period correlates with the gene length (Swinburne et al., 2008). *In vivo*, intron deletion of *Hes7,* an oscillatory gene like Hes1, accelerates the transcription and abolishes the oscillation (Takashima et al., 2011). Gene expression delay time also determines whether oscillations occur in synchronized or asynchronized manners. Null mutations of the glycosyltransferase *Lfng* in cells of the presomitic mesoderm (PSM) resulted in a faster transport of Dll1 to the plasma membrane. This decreased the delay time for sending the Dll1 signal, and abolished the synchronized oscillations in the PSM (Yoshioka-Kobayashi et al., 2020).

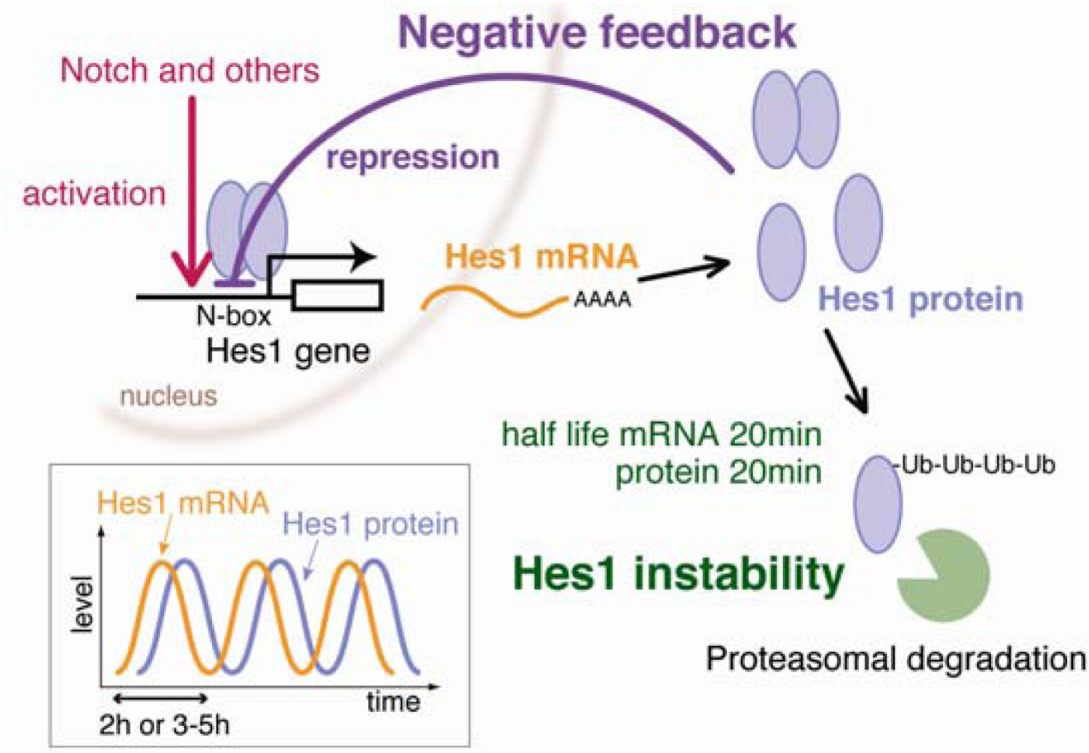

Figure 3. Hes1 oscillation and its negative feedback regulation

Hes1 protein binds N-boxes in its own gene and thereby can repress its own transcription. Hes1 mRNA and protein are both instable. Activation of Hes1 transcription (red) induces Hes1 mRNA and protein production. Hes1 protein then represses the production of its mRNA. At the same time, Hes1 and mRNA protein are degraded. This reduces the transcriptional repression leading to renewed Hes1 mRNA and protein production. As a result, Hes1 mRNA and protein oscillate.
(Adapted from Taeko Kobayashi and Ryoichiro Kageyama, 2011)

Another important regulator of oscillations is biological reaction speed. The Notch related oscillation periods in different species are distinct and range from 30 min in zebrafish, 2-3 hours in mice, to 5 hours in humans (Chedotal, 2020; Diaz-Cuadros et al., 2020; Matsuda et al., 2020b). This difference was reported be related to differential biochemical reaction speeds and protein stability. Biochemical reactions, including protein degradation and delays in gene expression processes, are two times slower in human than mouse cells. This accounts for the two times longer oscillatory period in human than in mouse cells (Matsuda et al., 2020a; Rayon et al., 2020).

Notch signaling can cross-talk with other pathways. In the PSM, other pathways can also regulate the oscillation of Notch related genes (Dequeant et al., 2006). For example, blocking the bFGF pathway with the inhibitor U0126 abolishes Hes1 oscillation in C2C12 cells (Nakayama et al., 2008). Yap signaling may change the excitation threshold for the expression of Notch oscillatory genes. Lfng and Hes7 oscillate in single PSM cell only when Yap signaling is reduced by inhibitor latrunculinA (Diaz-Cuadros et al., 2020; Hubaud et al., 2017; Yoshioka-Kobayashi et al., 2020).

1.3.2. Functions of oscillatory gene expression

The PSM is located in the posterior part of embryos, and its anterior part forms the somites. This process is repeated every 2-3 hours in mouse embryos. Hes7 is expressed in an oscillatory manner in the PSM cells, with an oscillatory period of 2-3 hours (Bessho et al., 2001). Each cycle of Hes7 expression leads to formation of one pair of somites. Lack of Hes7 results in fused somites, which

subsequently results in deformed spines and ribs (Bessho et al., 2001). Thus, Hes7 controls segmentation and somite formation, and it is therefore also called segmentation clock gene. Deletion of all three introns of Hes7 accelerates the negative feedback and results in constant and steady expression of Hes7, which also leads to fused somites (Takashima et al., 2011). If only two introns are deleted, Hes7 still oscillates but faster, resulting in the formation of supernumerous somites and vertebrae (Harima et al., 2013). In the PSM, Hes7 oscillations in neighboring cells occur in a synchronized manner. This is regulated by Lfng (Okubo et al., 2012; Yoshioka-Kobayashi et al., 2020). Lfng is regulated by Hes7 (Bessho et al., 2003). Lfng enhances Dll1-Notch1 signaling through glycosylation of the receptor (Moloney et al., 2000). When treated with secretase inhibitor, Notch signal transmission between coupled PSM cells is impaired, which results in desynchronized oscillations in neighboring PSM cells, despite the fact that Lfng still oscillates in an uncoupled single cell (Delaune et al., 2012; Ozbudak and Lewis, 2008; Riedel-Kruse et al., 2007).

Oscillation of Notch components in neural progenitor cells promotes cell proliferation and progenitor maintenance. In the developing and adult neural progenitors, Notch signals keep neural progenitors in an un-differentiation state (Ables et al., 2010; Basak et al., 2012; Giachino et al., 2014; Imayoshi et al., 2013; Shimojo et al., 2008). On the contrary, sustained expression of the Notch target gene Hes1 inhibits proliferation of neural stem cells and neurogenesis (Imayoshi et al., 2013; Pfeuty, 2015). *Hes1* type1 and type2 mutations lengthen or shorten the transcription time of Hes1 by lengthening or shortening introns. *Hes1* type1 and type2 mutant mice showed dampened oscillations, resulting in loss and premature differentiation of neural stem cells (Ochi et al., 2020). Dll1, as a downstream target of Hes1, also oscillates in coupled PSM and neural stem cells in a synchronous or asynchronous manner. Dampened Dll1 oscillations that did not affect overall Dll1 expression levels resulted in fusion of somites and accelerated differentiation of neural stem cells (Shimojo et al., 2016). Our lab recently showed that Hes1 protein is expressed in an oscillatory manner in muscle stem cells, where it drives MyoD oscillation. Null mutation of Hes1 in muscle stem cells leads to a dampened MyoD oscillation, and in an

uncontrolled differentiation of muscle stem cells (Lahmann et al., 2019). However, whether other Notch signaling related genes oscillate in muscle stem cells and control the balance of self-renewal and differentiation was not investigated yet.

1.4. The purpose of the project

When I started this project, oscillations of MyoD and Hes1 had been described in skeletal muscle stem cells (Lahmann et al., 2019). Moreover, Dll1 was known to oscillate in the PSM and neural progenitor cells (Shimojo et al., 2016). However, whether Dll1 oscillates in muscle stem cells had not been investigated. In this study, I analyzed the Dll1 expression dynamics in muscle progenitor cells of developing mice and in activated muscle stem cells of adult mice. I observed that Dll1 oscillates in such muscle cells. I characterized how the *Dll1* gene expression is regulated, and I identified Hes1 as the crucial transcription factor that regulates the Dll1 oscillation. Using a mutation that interferes with Dll1 oscillations (*Dll1type2*), I found that oscillatory expression of Dll1 could functionally not be replaced by sustained Dll1 expression in myogenesis and muscle regeneration. For this, I analyzed Dll1 expression levels and expression dynamics in *Dll1type2* mutant cells, and found that the mutation interferes with Dll1 oscillation but did not change the overall Dll1 expression level in muscle progenitor and activate muscle cells. Nevertheless, mice that carry the *Dll1type2* mutation display abnormal muscle development and repair. In summary, my data show that oscillating Dll1 regulates muscle formation in development and muscle regeneration in the adult.

2. Materials and Methods

2.1. Abbreviations

BSA	bovine serum albumin
cDNA	complementary deoxyribonucleic acid
DMEM	Dulbecco's Modified Eagle Medium
DMSO	dimethylsufoxide
DNA	deoxyribonucleic acid
dNTP	deoxyribonucleoside triphosphate
EDTA	ethylene-diaminetetraacetic acid
FACS	fluorescence activated cell sorting
FCS	fetal calf serum
GFP	green fluorescent protein
HEPES	4-(2-Hydroxyethyl)-piperazin-1-ethansulfonic acid
HS	horse serum
LIF	leukemia inhibitory factor
ON	overnight
PBS	phosphate-buffered saline
PBT	PBS+0.1% Tween-20
PBX	PBS+0.1% Triton X-100
PCR	polymerase chain reaction
PFA	paraformaldehyde
PI	propidium iodide
RNA	ribonucleic acid
RNAse	ribonuclease
RT	room temperature
SDS	sodium dodecyl sulphate
Tris	Tris-(hydroxymethyl)aminoethane
UTR	untranslated region

2.2. Materials

2.2.1. Chemicals and enzymes

Chemicals, enzymes and kits for molecular biology, oligonucleotides, probes and antibodies were purchased from the following companies: Abcam (Cambridge, UK), ACDBio (California, USA), Ambion (Huntingdon, UK), Bioline (London, UK), Cell Signaling, Dianova (Humburg, Germany), Clontech (Heidelberg, Germany), Gibco BRL (Karlsruhe, Germany), Invitrogen (Karlsruhe, Germany), Jackson Laboratories (Baltimore, USA), Merck (Darmstadt, Germany), Millipore (Billerica, USA), Molecular Probes (Eugene, USA), NEB (Frankfurt, Germany), PerkinElmer Life Science (Boston, USA), Promega (Mannheim, Germany), Qiagen (Hilden, Germany), Roche (Mannheim, Germany), Roth (Karlsruhe, Germany), Santa Cruz (Heidelberg, Germany), Shandon (Frankfurt, Germany), Sigma-Aldrich (Steinheim, Germany), Vector Laboratory (Burlingame, USA). Oligonucleotides were ordered from Eurofins genomics (Ebersberg, Germany).

2.2.2. Buffers and medium

2.2.2.1. Genotyping buffer

Lysis buffer

Tris pH8.0	100	mM
SDS	0.2	%(w/v)
EDTA	5	mM
Proteinase K	100	µg/mL

PCR mix

Sucrose	15.3	%(w/v)
β-Mercaptoethanol	0.0012	%
DMSO	0.04	%

dNTP(5mM)	0.625	mM
Tris pH8.8	45	mM
Cresol red solution	5	%
H2O	0.15	mL
MgCl2	3.5	mM
(NH4)SO4	1.274	mM
NaOH	0.00266	mM
EDTA	0.0001	mM

TAE

Tris pH8.0	40	mM
EDTA	1	mM
Acetic acid	0.1	%

2.2.2.2. Medium for cell and myofiber isolation and culture

NB4 collagenase buffer

HEPES	25	mM
DMEM	1	x
Gentamycin	0.5	%

FACS staining buffer

HBSS(-Ca2+,-Mg2+)	1	x
HEPES	25	mM
BSA	1	%
Gentamycin	0.5	%

Myofiber isolation buffer

DMEM	1	x
L-Glutamax	2	x
Penicillin/Streptomycin	1	%

Myofiber growth medium

Myofiber isolation buffer	1	x
Chicken embryo extract	0.5	%
Horse serum	10	%
Penicillin/Streptomycin	1	%

Stem cell growth medium

DMEM/F12	1	x
FCS	15	%
bFGF	1	‰
LIF	1	‰
Penicillin/Streptomycin	1	%

Cell differentiation medium

DMEM/F12	1	x
Horse serum	2	%
Penicillin/Streptomycin	1	%

2.2.2.3. Buffers for immunostaining

4% PFA

p-Formaldehyde	4	%
PBS	1	x
NaOH	0.64	mM

Dissolve p-Formaldehyde in heated PBS, add NaOH. Stir it until PFA is completely dissolved. Aliquot and store it at -20°C

IF buffer

PBS	1	x
Horse serum	10	%
BSA	0.3	%
Triton X-100	0.1	%

PBX

PBS	1	x
Triton X-100	0.1	%

Antigen retrieval buffer

Tri-sodium citrate	10	mM
Tween 20	0.05	%
pH	6.0	

2.2.2.4. Buffers for protein analysis

RIPA

Tris pH8.0	10	mM
EDTA	1	mM
EGTA	0.5	mM
Triton X100	1	%
NaCl	140	mM
SDS	0.1	%
Na-Deoxycholat	0.1	%

Cell scrape buffer

PBS	1	x
EDTA	1	mM

4x protein loading buffer

Tris pH6.8	240	mM
Glycerol	40	%
SDS	8	%
Bromphenol blue	0.04	%
β-Mercaptoethanol	5	%

SDS running buffer

Tris pH8.3	25	mM
Glycine	192	mM
SDS	0.1	%

PVDF membrane blotting buffer

Tris pH8.3	25	mM
Glycine	192	mM
SDS	0.01	%
Methanol	20	%

PBST

PBS	1	x
Tween 20	0.01	%

Western blocking buffer

PBST	1	x
Nonfat milk powder	5	%

2.2.2.5. Buffers for chromatin immunoprecipitation (ChIP)

11% PFA buffer

Formaldehyde	11	%
EDTA	1	mM
EGTA	0.5	mM
HEPES	50	mM
NaCl	100	mM

Lysis buffer 1

HEPES	50	mM
EDTA	1	mM
Glycerol	10	%

NP40	0.5	%
NaCl	140	mM
Triton X100	0.25	%
Proteinase inhibitor	1	x

Lysis buffer 2

Tris pH8.0	10	mM
EDTA	1	mM
EGTA	0.5	mM
NP40	0.5	%
NaCl	200	mM
Proteinase inhibitor	1	x

Lysis buffer 3

Tris pH8.0	10	mM
EDTA	1	mM
EGTA	0.5	mM
SDS	1	%
Proteinase inhibitor	1	x

IP dilution buffer

Tris pH8.0	10	mM
EDTA	1	mM
EGTA	0.5	mM
Na-deoxycholate	0.1	%
NaCl	140	mM
Triton X100	1	%
Proteinase inhibitor	1	x

LiCl RIPA wash buffer

HEPES	50	mM
EDTA	1	mM

Na-deoxycholate	0.7	%
NP40	1	%
LiCl	500	mM

TE buffer

EDTA	1	mM
Tris pH8.0	10	mM

Elution buffer

EDTA	10	mM
Tris pH8.0	50	mM
SDS	1	%

2.2.3. Mouse strains

2.2.3.1. *Pax7creERT2*

This knock-in stain was provided by Gabrielle Kardon, University of Utah. An internal ribosome entry site (IRES)-CreERT2 fusion protein was inserted downstream of Pax7 stop codon (Murphy et al., 2011). It allows CreERT2 expression and therefore specific conditional gene deletion in muscle stem cells.

2.2.3.2. *Pax7-nGFP*

This BAC transgenic stain was provided by Shahragim Tajbakhsh, Institut Pasteur, Paris. In the strain, a *Pax7* promoter drives expression of nuclear localized EGFP. (Sambasivan et al., 2009) This allows the expression of a nuclear localized EGFP in muscle stem cells.

2.2.3.3. *Dll1flox*

This stain was provided by Michael Owen, Lymphocyte Molecular Biology Laboratory, London. LoxP sites was inserted upstream of exon 3 and downstream of exon 4. The two exons can be deleted by transient Cre-mediated excision.

2.2.3.4. *Dll1type2*

This stain was provided Ryoichiro Kageyama, Kyoto University, Japan. A cassette of *Dll1* cDNA, firefly luciferase, stop codon and 3'UTR was inserted into exon 1 after 5'UTR of *Dll1* gene. The neo cassette was removed by germ line, flippase mediated recombination. The insertion increases the length of transcript, but does not alter the encoded protein (Shimojo et al., 2016).

2.2.3.5. *MyoD-/-*

This stain was provided Rudolf Jaenisch, Whitehead Institute, Boston, USA. A PGK-neo cassette replaced exon 1 and eliminates MyoD function (Rudnicki et al., 1992).

2.2.3.6. *Hes1flox*

This stain was provided Ryoichiro Kageyama, Kyoto University, Japan. LoxP sites were inserted upstream of exon 2 downstream of exon 4 (Imayoshi et al., 2008). It allows deletion of functional Hes1 protein by Cre-mediated excision.

2.2.3.7. *Dll1-luc*

This stain was provided Ryoichiro Kageyama, Kyoto University, Japan. Firefly luciferase cDNA was inserted into exon 11 of *Dll1*. The modified gene encodes a Dll1-luciferase fusion protein (Shimojo et al., 2016).

2.2.4. Antibodies

The primary antibodies used in this study were:

Antibodies	SOURCE	IDENTIFIER
Rabbit monoclonal Hes1 (1:500)	Cell Signaling Technology	#11988
Guinea pig polyclonal Pax7 (1:100)	Reference (Brohl et al., 2012)	
Mouse monoclonal Pax7 (1:1000)	DSHB	AB_528428
Rabbit polyclonal Laminin (1:500)	Abcam	ab14055-50
Goat polyclonal Desmin (1:500)	Santa Cruz	SC-34201
Mouse monoclonal MyoD (5.8A) (1:500)	Santa Cruz	SC-32758
Rabbit polyclonal MyoD (1:500)	Santa Cruz	SC-304
Mouse monoclonal Myogenin (1:500)	ThermoFisher	AB1835
Rabbit polyclonal Myogenin (1:500)	Santa Cruz	SC-576
Goat polyclonal Collagen IV (1:500)	Millipore	AB769
Mouse monoclonal Luciferase (1:500)	DSHB	AB_2722110
DAPI (1:1000)	Sigma-Aldrich	D9542
Rat polyclonal Pax3(1:500)	Homemade	
Rat polyclonal CD31-PE(1:200)	BD Pharmingen	553373
Rat polyclonal CD45-PE(1:200)	BD Pharmingen	553081
Rat polyclonal ScaI-PE(1:200)	BD Pharmingen	553336
Goat polyclonal Vcam1(1:100)	R&D	AF643
Mouse monoclonal Delta1(1:500)	Santa Cruz	SC-377310
Chick polyclonal GFP(1:400)	Homemade	

Primary antibodies were detected with fluorescent fragment conjugated secondary antibodies. The stock solutions were diluted 1:500 in staining buffer.

2.2.5. Probes for RNAscope

The probes used in RNAscope were:

Probes	SOURCE	IDENTIFIER
Mm-Dll1-C1	Bio-Techne	425071

Mm-Pax7-C2	Bio-Techne	314181-C2
Mm-Myod1-C3	Bio-Techne	316081-C3
Mm-Myog-C3	Bio-Techne	492921-C3

2.2.6. Oligonucleotides

The following oligonucleotides were used in this study.

Oligonucleotides	SOURCE	IDENTIF
siRNA targeting Hes1 5'-GCTACCCGTAAAGTCCCTA-3'	Eurofins	N/A
siRNA targeting Dll1	Thermo Fisher	61067
ChIP-PCR NC1: Forward: 5'-GCGTGGCTGTCATTAAGG-3' Reverse: 5'-GGTGCTGTCTGCATTACC-3'	Eurofins	N/A
ChIP-PCR NC2: Forward: 5'-GCCCCGGATTATCGCCTCAC-3' Reverse: 5'-TGTCTCCTGCTTTCTGGTTTTGTCTT-3'	Eurofins	N/A
ChIP-PCR Mymk: Forward: 5'-GAGGCAAGTGCATACCACATGGTAC-3' Reverse: 5'-GGACCAGGAGGAAGGCACTGAC-3'	Eurofins	N/A
ChIP-PCR MyoD: Forward: 5'-GGGTCTTCTCCGGTTTCTCT-3' Reverse: 5'-CAATCTCAAAGCCCTGGAAC-3'	Eurofins	N/A

ChIP-PCR Hes1: Forward: 5'-GCAGAGAGCAGGTGCTGTCTGCATTACC-3' Reverse: 5'-GGGAGATTTTCAACCAACACCACCTTCAC-3'	Eurofins	N/A
RT-PCR Myf5: Forward: 5'-TGAGGGAACAGGTGGAGAAC-3' Reverse: 5'-TGGAGAGAGGGAAGCTGTGT-3'	Eurofins	N/A
RT-PCR MyoD: Forward: 5'- GCCGCCGCCTGAGCAAAGTGAATG-3' Reverse: 5'- GGGGCGCGGCGTCCTGGTC-3'	Eurofins	N/A
RT-PCR Dll1: Forward: 5'-GCCCCGGATTATCGCCTCAC-3' Reverse: 5'-TGTCTCCTGCTTTCTGGTTTTGTCTT-3'	Eurofins	N/A
RT-PCR Hes1: Forward: 5'- GTGGGTCCTAACGCAGTGTC-3' Reverse: 5'- ACAAAGGCGCAATCCAATATG-3'	Eurofins	N/A
RT-PCR Hey1: Forward: 5'-GCCGACGAGACCGAATCAATAACA-3' Reverse: 5'-TCCCGAAACCCCAAACTCCGATAG-3'	Eurofins	N/A

RT-PCR Hes5: Forward: 5'-GCTCCGCTCGCTAATCGCCTCCAG-3' Reverse: 5'-GTCCCGACGCATCTTCTCCACCAC-3'	Eurofins	N/A
RT-PCR ß-Actin Forward: 5'-GTCCACACCCGCCACCAGTTC-3' Reverse: 5'-GGCCTCGTCACCCACATAG-3'	Eurofins	N/A
Genotyping Dll1 flox Forward: 5'-GCCCCGGATTATCGCCTCAC-3' Reverse: 5'-GCCCAAGGGGCAATGGCAGG-3'	Eurofins	N/A
Genotyping Dll1-luc Forward1: 5'-CGAGAAGAGCAGCTTTAAGGTCCG-3' Forward2: 5'-CGAGAAGAGCAGCTTTAAGGTCCG-3' Reverse: 5'-AGCAGTCCCTGGGTTTCCTCTCCC-3'	Eurofins	N/A
Genotyping Dll1-type2 Forward: 5'-TCCTCTTTCCCTCCGCGAAGAAGC-3' Reverse: 5'-TTGCGAGGTCATCGGGAGAGTCTG-3'	Eurofins	N/A
Genotyping Cre Forward: 5'-GTTTGCCGGTCGTGGGCGGCATGGTG-3' Reverse: 5'-CACGGGCACTGTGTCCAGACCAGGCCAG-3'	Eurofins	N/A

Genotyping Hes1 flox Forward: 5'-CAGCCAGTGTCAACACGACACCGGACAAAC-3' Reverse: 5'-TGCCCTTCGCCTCTTCTCCATGATA-3'	Eurofins	N/A
Genotyping EGFP Forward1: 5'-CACCATGGTGCACGTGGATC-3' Reverse: 5'-TTACTTGTACAGCTCGTCC -3'	Eurofins	N/A

2.3. Methods

2.3.1. Cell culture

Cells were cultured in an incubator at 37°C under 5% CO2 (Binder). C2C12 cells were cultured in stem cell growth medium, and split 1:10 every two days. 75000 cells were seeded in 6-well plates and cultured overnight for siRNA experiments. 50 pmol siRNA was incubated with 5µl Lipofectamine RNAiMAX for 5 min at room temperature. The complex was added to the cultured cells. After 24 hours and 48 hours, the cells were harvested for protein analysis using western blot.

Primary muscle stem cells isolated by FACS were cultivated with stem cell growth medium. 50000 cells (events) were seeded in a silicon ring for live cell imaging. Before seeding, the glass bottom dish was coated with matrigel. The cells were cultured overnight until they attached the dish and 1 µM luciferin was added. Afterwards, the cells were imaged under an inverted microscope (Olympus, IX83-ZDC with Hamamatsu 9100B camera) in a dark room.

2.3.2. Single myofiber culture

Extensor digitorum longus (EDL) muscle was dissected from a mouse. Two EDL muscles were incubated in 1mL 0.2% Collagenase I/myofiber isolation buffer at 37°C for around 1.5 hours (depends on the age of the mouse). After digestion, the muscle was transferred into myofiber isolation buffer for 20 mins at 37°C in a 5% CO2 atmosphere. The muscle was gently triturated with blunt Pasteur glass pipettes which was pre-coated with 5% BSA. The dishes were also pre-coated with 5% BSA to prevent attachment of the myofibers. Single myofibers were picked and transferred to a new medium, and the trituration was repeated several times until enough single myofibers were obtained. Myofibers were fixed with 4% PFA for 10 mins, or cultured in myofiber growth medium for several days.

For imaging, myofibers cultured for about 16 hours (single cell) or 42 hours (coupled cells), were transferred to a glass bottom dish. For immunostaining, the myofibers were fixed with 4% PFA for 10 mins at room temperature, and washed three times with PBS. Then they were transferred to low-binding Eppendorf tube and blocked with IF buffer (see Materials) at room temperature for at least 1 hour. Subsequently, the fibers were incubated with primary antibodies in IF buffer overnight at 4°C. After three washes with PBX buffer (see Materials), myofibers were incubated with the secondary antibodies for 1 hour at room temperature, washed three times and mounted for microscopy.

2.3.3. Myosphere culture

The dishes were coated with anti-adherence rinsing buffer (STEMCELL) or polyHEMA to prevent the attachment of the cells. Cells transfected with plasmids were isolated after 0.05% trypsin treatment. For 6-well plates, 50000 cells were seeded. The cells spontaneously formed clusters after overnight culture in myofiber growth medium. Under the stereo microscope, clusters containing GFP cells were picked and transferred to glass bottom dish pre-coated with anti-adherence rinsing buffer. 700 µl myofiber growth medium and 1x furimazine (Promega, 4377) was added for luciferase imaging.

For chimeric sphere culture, cells co-transfected with nGFP and EpDll1-NanoLuc plasmids and nontransfected cells were mixed at a ratio of 1:50, an cultured as described above. For analysis of the differentiation of cells in the spheres, the cell clusters were dissociated into single cells by Trypsin-EDTA, and FACS analysis was performed to determine the ratio of cell that expressed Pax7 and MyoG. Briefly, after 10 min fixation at room temperature, the cells were incubated with guinea pig anti-Pax7, mouse anti-MyoG and chick anti-GFP overnight at 4°C. Subsequently, the cells were washed and secondary antibodies conjugated with Cy2, Cy3 or Cy5 were added for 1 h at room temperature. The cells were analyzed with a FACSAria II (BD, New Jersey, US) sorter. Wild-type cells not treated with primary antibodies were used as a negative control for gating. Results are presented as the percentage of MyoG+ and Pax7+ cells in the GFP+ cell fraction.

2.3.4. Organic slice culture

E11.5 embryos were dissected in PBS. *Pax7-nGFP* embryos were picked under the stereo microscope and embedded in 4% low temperature melting agarose. Then the samples were put in cold HBSS buffer (+Ca2+, +Mg2+; Gibco)/Penicillin Streptomycin/HEPES buffer. 100 µm slices were prepared using a vibratome (Leica, Nussloch, Germany). Slices containing the limb were transferred to a glass-bottom dish containing 1 mg/ml collagen (Sigma-Aldrich, St. Louis, USA) in DMEM and neutralizing buffer, and incubated for 10 min in a 37 °C incubator. Myofiber growth medium with 1 µM luciferin (PJK GmbH, Kleinblittersdorf, Germany) was added, the dish was placed on the stage of an inverted microscope (IX83-ZDC, Olympus, Tokyo, Japan) and maintained at 37 °C in a 5% CO2 atmoshere. The nGFP signal from the *Pax7-nGFP* transgene was used to focus and to track the cells. Bioluminescence was acquired using a EM-CCD camera (Hamamatsu, Shizuoka, Japan).

2.3.5. Genotyping

Tissue biopsies were put in 60 µl lysis buffer and digested at 55°C overnight. After digestion, the samples were put into 95°C incubator for 10 mins to inactive proteinase K. Samples were diluted with 200 µl water. 1 µl was used for PCR.

PCRs were performed in a Biometra Thermal cycler and the conditions were as follows:

PCR reaction:

PCR Mix	17	µl	
PrimerF(10 µM)	1	µl	
PrimerR(10 µM)	1	µl	
Sample	1	µl	
	20	µl	

Cycler conditions:

95 °C	3	min	
95 °C	30	sec	40 cycles
55 °C	30	sec	
72 °C	1	min	
72 °C	3	min	

PCR products were loaded onto 1.5%-4% Agarose gel containing ethidium bromide in an electrophoresis chamber filled with TAE buffer. Gel running condition was 100-150V until the dye line had migrated approximately 75-80% of the way down the gel. DNA bands were visualized with UV imaging system (Vilber Lourmat).

2.3.6. RT-PCR

Cells were lyzed in 1 ml TRIzol (Life Technology) and incubated at room temperature for 5 min. 200 µl chloroform was added to separate the aqueous phase containing the total RNA. The sample was vortexed vigorously and

centrifuged at maximum speed (>12000g) for 20 mins at 4 °C. The upper phase was transferred to a new 1.5 ml EP tube, and 1 µl polyacrylcarrier and 700 µl isopropanol were added, incubated at room temperature for 10 min and then centrifuged. The total RNA was washed with 75% ethanol, and solved with 30 µl RNAse-free water.

2 µg total RNA was used for reverse transcription according to the manufacturer's instructions. The condition was as follows:

RT reaction:

total RNA	2	µg
Random primer	50	ng
dNTP mix (10 mM)	1	µl
H2O up to	10	µl

Incubate the tube at 65 °C for 5 min, and immediately put on ice for 1 min. Then add:

10X RT buffer	2	µl
MgCl2 (25mM)	4	µl
DTT (100 mM)	1	µl
RNaseOUT	1	µl
SuperScript III	1	µl

Reaction conditions:

25 °C	10	min	
50 °C	50	min	1 cycle
85 °C	5	min	
4 °C	3	min	

80 µl H2O was added to each tube.

Quantitative PCR was performed on a Biorad C1000 Thermal cycler. β-actin was used for internal control.

PCR reaction:

2xPCR Mix	10	µl
PrimerF(10 µM)	1	µl
PrimerR(10 µM)	1	µl
Sample	8	µl

Cycler conditions:

95 °C	15	min	
95 °C	30	sec	45 cycles
60 °C	30	sec	
72 °C	30	sec	
72 °C	Imaging		
65-95 °C	0.5°C/10s Imaging		

Ct values were normalized to β-actin Ct values. Relative expression was calculated with the 2^(-ΔΔCt).

2.3.7. ChIP-PCR

Dynabeads (ThermoFisher, 26162) were mixed with 0.5%BSA in PBS. 5 µg MyoD or Hes1 specific antibody was added. IgG of the same species was used for control. The beads were incubated overnight at 4°C. C2C12 cells were cultured to around 70% density in a cell culture dish. Formaldehyde was added to the dish and the concentration was 1% for 15 min at room temperature. 2M glycine was added to stop the reaction. After 5 min, cold PBS was added to wash twice.

The cells were scraped into a Falcon tube and centrifuged down. 6 ml lysis buffer 1 (see Materials) was added to lysis cells for 20 min at 4 °C on a rotor. After collecting the cells by centrifugation, 6 ml lysis buffer 2 (see Materials) was added to wash cells for 10 min at room temperature on a rotor. After collecting the cells by centrifugation, lysis buffer 3 (see Materials) was added

and then sonication was performed. The process was 30s on, 30s off, 20 cycles. The samples were incubated with beads overnight at 4°C. They were washed with LiCl RIPA buffer seven times and TE twice to release the bound DNA. Standard phenol-chloroform DNA extraction was performed. Purified DNA was used for qPCR.

2.3.8. Western blot

Cells were lysed in RIPA buffer (see Materials) using a scraper and incubated for 30 min at 4°C. Protein was quantified using a Brandford assay. A 12% SDS-PAGE gel was prepared and 30 µg protein was loaded. After electrophoresis, the gel was equilibrated in transfer buffer for 20 min. A Methanol treated 0.45 µm PVDF membrane was used to transfer the protein. Transferring was performed using a 90V setting for 1.5 hours at 4 °C. The membrane was washed once with PBS. The membrane was blocked with 5% milk in PBST (see Materials) for 1 hour at room temperature, and then incubated with the primary antibody in 5% milk in PBST overnight at 4°C. To wash out non-specific bound antibodies, the membrane was washed three times with PBST. Horseradish peroxidase (HRP) or peroxidase (POD) conjugated secondary antibodies dissolved in 5% milk in PBST was used to detect the primary antibody. After three washes with PBST, the membrane was incubated with ECL Luminol Reagent (ThermoFisher, 32109), and the developed western blot was documented with a Chemismart 5100 imaging system.

2.3.9. RNAscope

In situ hybridization was performed using the RNAscope Multiplex fluorescent V2 assay kit as recommended by the producer (ACD Biotech, CA, USA). The fresh frozen tissue sections were fixed with 4% PFA for 10 min, then washed 3x with PBS. The slides were transferred in several steps to 50%, then to 75% and 100% methanol, incubating each step for 5 mins. After the sections were dried at room temperature, drops of hydrogen peroxide was added to cover the entire sections for 10 min at room temperature. The slides were washed in 1x

washing buffer three times, and covered by pretreatment solution for 30 min at room temperature. After two washes with 1x washing buffer from the kit, the sections were covered with probes (1:50 of C2 and C3 in C1 probe solution as instructed by the manual) at 40°C for 2 hours. The sections were incubated with drops of v2 AMP1 solution from the kit for 30 min at 40°C, followed by two washes. Subsequently, v2 AMP2 solution from the kit was incubated for 30 min at 40°C, and washed twice with the washing buffer from the kit. V2 AMP3 solution from the kit was incubated 15 min at 40°C, followed by two washes. For every fluorescent channel, the following process was performed: the sections were incubated at 40°C with HRP conjugated probes specific for the distinct channels for 15 min, washed twice with the washing buffer from the kit, incubated with the TSA fluorophore for 30 min at 40°C, followed by a incubation with HRP blocker solution from the kit for 15 min. DAPI solution from the kit was added to stain the nuclei. Subsequently, the sections were mounted ProLong Gold Antifade Mountant (ThermoFisher, P10144) for microscopy.

2.3.10. Immunostaining of sections

Embryos were fixed using 4% PFA/PBS for 2 hours at 4°C. After washing with PBS, the samples were incubated in 30%Sucrose/PBS overnight at 4°C, until the embryos sink in the solution, and then embedded in OCT compound at -80 °C. For adult muscle section, fresh frozen tissue was used. Briefly, TA muscle was dissected and embedded in OCT, immediately frozen the samples with liquid nitrogen.

Tissue specimen were sectioned with a cryostat (10-12 μm), and attached to an adhesive glass slide. Slides were dried at 37°C for 15 min, and kept in -80°C. Before staining, adult TA muscle sections were fixed with 4%PFA/PBS. When sections of embryos were used, this step was omitted and the antigen retrieval step was directly performed. Antigen retrieval was done with Vector antigen unmasking solution (Vector laboratories) at 80°C for 20 mins for the sections from embryos and TA muscle. Then the sections were incubated with IF

staining buffer (see Materials) for 1 hour at room temperature. Primary antibodies were diluted in IF staining buffer and covered the sections overnight at 4 °C. The sample was washed three times with PBX before the secondary antibodies solution (1:500 in IF staining buffer; DAPI) was used to cover the sections, and incubated for 1 hour at room temperature. The sections were washed with PBX three times and then mounted.

2.3.11. EdU analysis

5-ethynyl-2 deoxyuridine (EdU) analysis was used to assay proliferation. The mice were injected i.p. with EdU (50 μg/gram body weight) 3 hour before the dissection. The sections for EdU staining were washed with PBS and permeabilized by 0.5% Triton X100/PBS for 20 min at room temperature. After washed with PBS twice, the cocktail reaction solution was used to cover the section, and incubated for 30 min at room temperature. The cocktail reaction solution contained 1x reaction buffer (100mM Tris), catalyst solution (1mM CuSO4), Bio-PCA(100μM Biotin picolyl azide), 1x buffer additive (100mM ascorbic acid) and water. For staining, streptavidin conjugated fluorophores were used.

2.3.12. Dual reporter enhancer analysis

For the analysis of enhancer activity, the dual luciferase assay kit (Promega) was used. Briefly, HEK293 cells were transfected with plasmids, and subsequently cultured for 24 hour. pRL-TK plasmid was used to control for transfection efficiency. The ratio of pRL-TK and pGL4.23 (pGL4.23-enhancer) used was 1:10. The cells were washed with cold PBS for once, and incubated with 1x Passive Lysis Buffer (PLB- did you define what this is) on a shaker for 20 mins at room temperature. The lysed samples were transferred to a white plate (OptiPlate-96, PerkinElmer). The assay was performed with a luminescence microplate reader (Berthold). The measurement was done as described in the manual. The activity was calculated as the ratio of firefly luciferase activity to renilla luciferase activity.

2.3.13. Flow cytometry

For isolation of muscle stem cells from postnatal mice, skeletal muscles was minced with scissors and digested at 37°C for about 45 min with digest medium containing 14mU/ml Collagenase and 2.5U/ml Dispase II; during the digestion, the sample was gently shaked at 110rpm in a shaker. The digestion was stopped by the addition of 2mM EDTA and 5% FCS. The samples were filtered throught 100 μm strainer once and 20 μm strainer twice, then centrifuged at 300g to collect the cells. The cells were incubated with PE-ScaI, PE-CD31, PE-CD45 (all in 1:200), and goat-Vcam1(1:100) for 15 min at 4°C. After incubation, the cells were washed three times, and subsequently incubated with a Cy5-conjugated secondary antibody for 15 min at 4°C. After three washes, the cells were analyzed and sorted by a BD Aria sorter. Propidium Iodide (PI) was used to exclude dead cells. Vcam1+/CD31-/CD45-/ScaI-/PI- cells were considered to correspond to live muscle stem cells.

For the isolation of muscle progenitor cells from E12.5 Pax7-nGFP transgenic embryos, the limbs were minced with 14mU/ml Collagenase and 2.5U/ml Diapase II at 37°C for 15 mins. Every 5 min, the samples were gently pipetted several times. The digestion was stopped with 2 mM EDTA and 5% FCS. After three washes, the cells were analyzed and sorted. Propidium Iodide (PI) was used to control dead cells. GFP+/PI- cells were considered to correspond to muscle progenitors.

For the analysis of cells in myosphere using FACS, spheres containing GFP+ cells were picked. After digestion with 0.05% Trypsin for 10 min at 37°C, the samples were pipetted several times to dissociate them into single cells. Then the cells were fixed with 4% PFA for 10 min at room temperature. Subsequently, the cells were washed three times with PBS, incubated with IF staining buffer for 1 hour at room temperature. Subsequently, the primary antibodies solution (in IF staining buffer) was added overnight at 4°C. After three washes with PBX , the secondary antibodies (in IF staining buffer) were

added for 1 hour at room temperature. After three washes with PBX, one additional wash with FACS sorting buffer was performed. Subsequently, the cells were analyzed by BD Aria sorter or LSR II analyzer.

2.3.14. Time lapses imaging analysis

Imaging analysis was performed using Fiji software (ImageJ, v.2.1) and Blob tracker plugin. The semi-automated tracking approach allows to determine cell locations and the intensity of the signal over time. Cells were identified using differences of Gaussian detection. Because of the muscle stem cells move quickly, the nearest neighbor searching approach was used in successive frames. This process can be corrected manually, taking the bright-field images into account. After the cell size parameter was set, the mean intensity values of the signal of different single cells over time were recorded. After subtraction of background, a 7th order Savitzky-Golay polynominal fitting was used to smooth the image. The oscillation periods were measured as the length of time between two peaks of bioluminescence signals. To define the stability of the oscillations, FFT with Hanning window was used by Origin software (OriginLab, Massachusetts, USA) or Matlab (R2016a, MathWorks, Massachusetts, USA), which transfers a time-dependent function into its corresponding frequency-domain function. The dominant frequency can be identified as a peak. The powers of the frequency bands corresponding to periods between 1.5 and 3.75 h were quantified as area under the FFT curve. Data from randomly chosen cells that could be followed over at least 10 h were analyzed. Matlab software (R2016a, MathWorks, Massachusetts, USA) was used to determine the phase relationship of oscillations in two coupled cells. To derive accurate phase differences, we performed the following signal processing steps: (i) detrending (by moving average with a window of 3 h); (ii) normalization (by dividing by a sliding standard deviation with a window of 3 h); (iii) Hilbert transformation analysis. The time at which the oscillatory signal in one cell corresponds to a peak was marked, and time intervals to the next peaks in oscillation of neighboring cells were determined.

2.3.15. Statistics

Statistical analysis (Student's t-test) was performed using Excel software (Microsoft). P values < 0.05 were considered as significant and are shown in the figures.

3. Results

3.1. Dll1 produced by muscle progenitor and activated muscle stem cells controls the self-renewal of neighboring cells

3.1.1. Dll1 is expressed in activated and differentiating muscle stem cells, but not quiescent muscle stem cells or myofibers

Mouse embryos with null mutations of *Dll1* die around E11, whereas mice that are heteroallelic for a null and a hypomorphic *Dll1* allele survive until birth (Schuster-Gossler et al., 2007). In these heteroallelic embryos, the size of the limb and trunk muscles is tiny because muscle progenitors differentiate prematurely (Brohl et al., 2012; Schuster-Gossler et al., 2007). Similarly, myogenic cells are depleted in cranial muscles of heteroallelic embryos, indicating that Notch signals suppress differentiation of muscle progenitor cells in all skeletal muscles (Czajkowski et al., 2014). However, the cell type that expresses Dll1 in the developing limb had not been identified. I therefore defined Dll1 expression in E11.5 embryos and tested whether Dll1 is expressed in muscle progenitor cells. For this, I used RNAscope on sections of embryos. RNAscope allows to detect expression in single cells through four steps of hybridization and TSA amplification, and can even be used for the detection of single RNA molecules. I observed that *Dll1* was expressed in *MyoD*+ and *MyoG*+ cells of E11.5 mouse embryos (Fig 3.1).

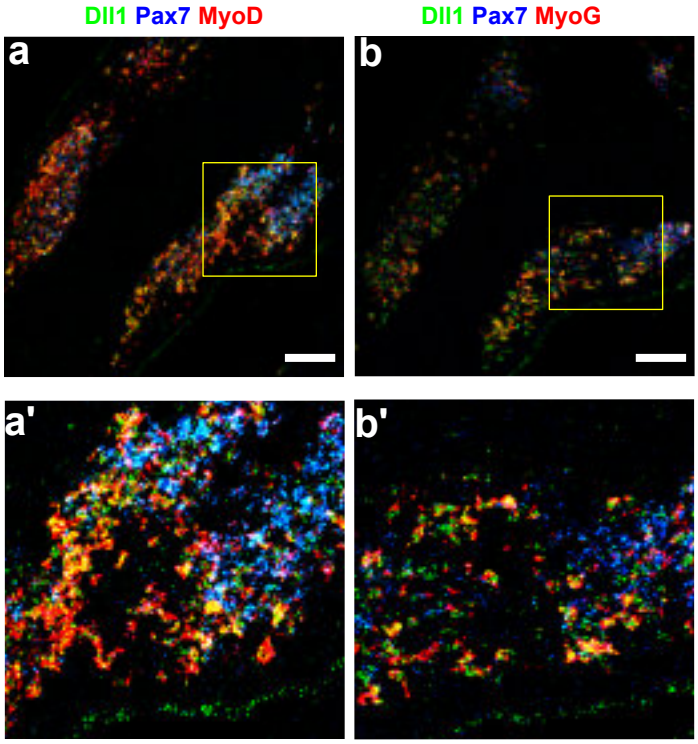

Fig. 3.1. *Dll1* expression in embryonic limbs (E11.5).

RNAscope analysis of E11.5 developing limb muscles at E11.5, using the following probes: Dll1(Green), Pax7(Blue) and MyoD(Red) (a), and Dll1(Green), Pax7(Blue) and MyoG(Red) (b). (a',b') Magnified pictures of the region labeled with yellow boxes in (a, b). n=2. Scale bars, 100 μm.

Previous RNAseq and microarray data had indicated that *Dll1* is expressed in adult muscle stem cells (Machado et al., 2017; van Velthoven et al., 2017; Yartseva et al., 2020). To verify the expression of *Dll1* in the adult muscle, RNAscope on tibiatlis anterior (TA) muscle sections was performed. Since most of the muscle stem cells are quiescent in the uninjured adult muscle, I also used regenerating muscle in which muscle stem cells are activated and known to proliferate and differentiate. The injury was introduced by cardiotoxin (CTX) injection into the muscle, and the muscle was analyzed at 7 days post injury (dpi), a stage at which muscle regeneration has proceeded and new muscle fibers are already present. Thus, I was able to test the *Dll1* expression in quiescent, activated and differentiating muscle stem cells. In quiescent muscle stem cells, I detected *Pax7* but neither *MyoD* nor *Dll1*. In the regenerating muscle, I detected *Dll1* in activated (*Pax7*+/*MyoD*+) or differentiating (*MyoG*+) cells. In myofibers, however, *Dll1* was not expressed (Fig 3.2).

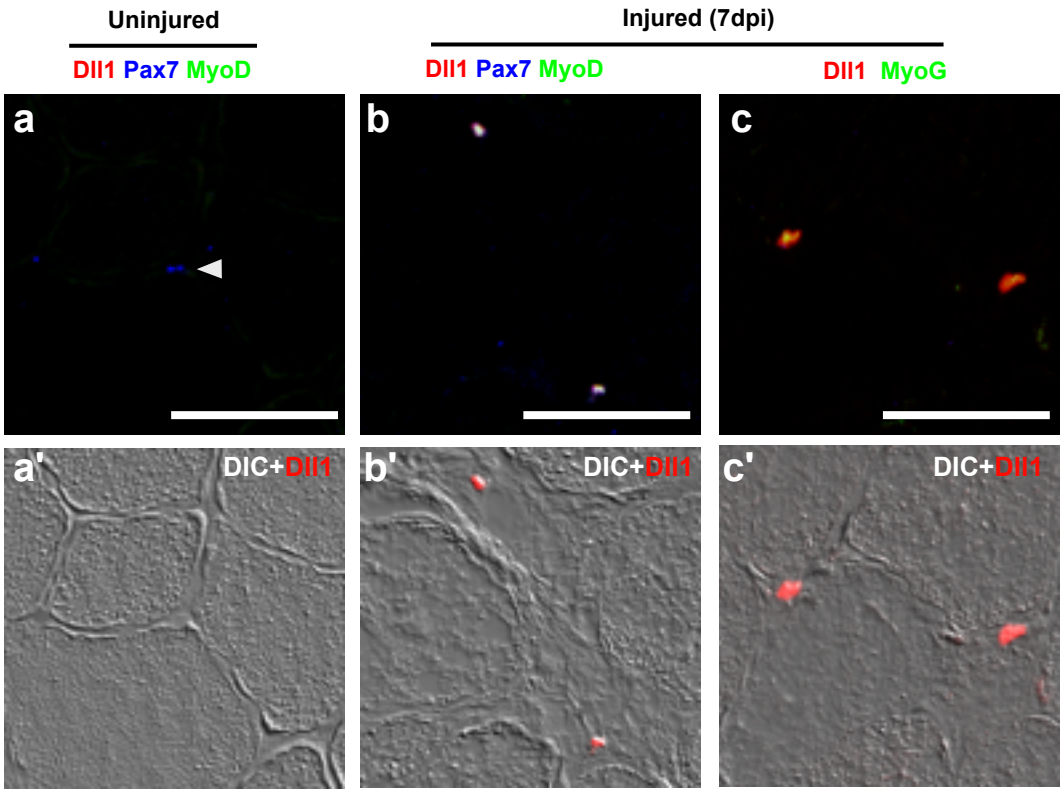

Fig 3.2. *Dll1* expression in single cells of adult muscle.

RNAscope analysis of the uninjured or regenerating TA muscle at 7dpi, using the following probes: Dll1 (Red), Pax7 (Blue) and MyoD (Green) (a,b) and Dll1 (Red) and MyoG (Green) (c). Overlay of the differential interference contrast (DIC) (a',b',c') picture and of the *Dll1* signal. n=3. Scale bars, 50 µm.

Because Dll1 is an important ligand of Notch and signals to neighboring cells that directly contact Dll1-expressing cells, I also analyzed Dll1 expression in cells that contact each other. In the later stages of muscle regeneration, the muscle stem cells are well separated and do not contact each other. Instead, they contact the muscle fiber. However, at early stages of regeneration (4dpi) they frequently contact each other. Therefore, I also tested *Dll1* expression in the regenerating muscle at 4 dpi. In activated muscle stem cells (*Pax7*+/*MyoD*+) that contact each other (also called coupled cells hereafter), I detected *Dll1* expression in both cells. When the cells were differentiating and

started to express *MyoG*, *Dll1* was expressed at higher levels in these cells than in activated cells (*Pax7*+/*MyoD*+) (Fig 3.3).

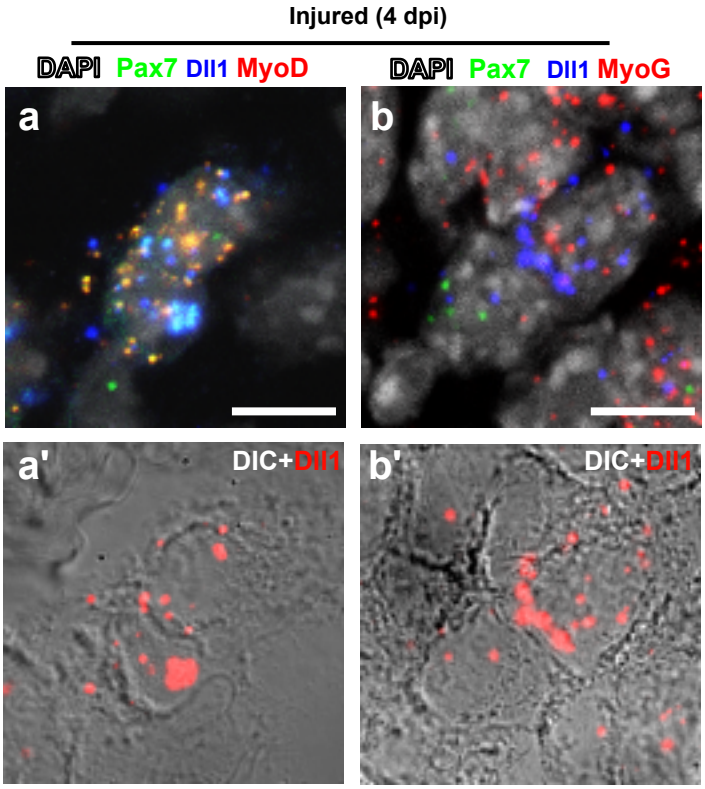

Fig 3.3. *Dll1* expression in coupled cells of adult muscle.

RNAscope analysis of injured TA muscles at 4dpi. Using the following probes for Dll1 (Blue), Pax7 (Green) and MyoD (Red) (a) and Dll1 (Blue), Pax7 (Green) and MyoG (Red) (b). DAPI (Gray) is used for nuclear counterstain. (a',b') Differential interference contrast (DIC; Gray) and *Dll1* (Red) signal pictures of (a, b). n=3. Scale bars, 10 μm.

A lack of appropriate antibodies impedes Dll1 immunostaining in tissues. Muscle stem cells are attached to myofibers *in vivo*, thus researchers speculated that muscle fibers expressed Dll1 in order to explain the high Notch activity in muscle stem cells. However, no direct proof supports this hypothesis. To analyze the Dll1 protein expression, I used a different approach.

I used *Dll1-luc* mice, which expressed a fusion protein of Dll1 and luciferase (Shimojo et al., 2016). Heterozygous mice derived from the knock-in allele displayed normal muscle. In contrast, homozygous *Dll1-luc* knock-in mice had

small segmentation defects that manifested in a shortened tail but displayed no obvious abnormality in the body. I analyzed the muscle of homozygous *Dll1-luc* mice to exclude that there were subtle effects on muscle formation or on muscle stem cells. I found that the body weight of homozygous *Dll1-luc* mice was unchanged compared to wild type mice, and there was also no significant difference between the weight of the TA muscle. Most importantly, the Pax7+ cell numbers in mutant and wild type animals were similar (Fig 3.4).

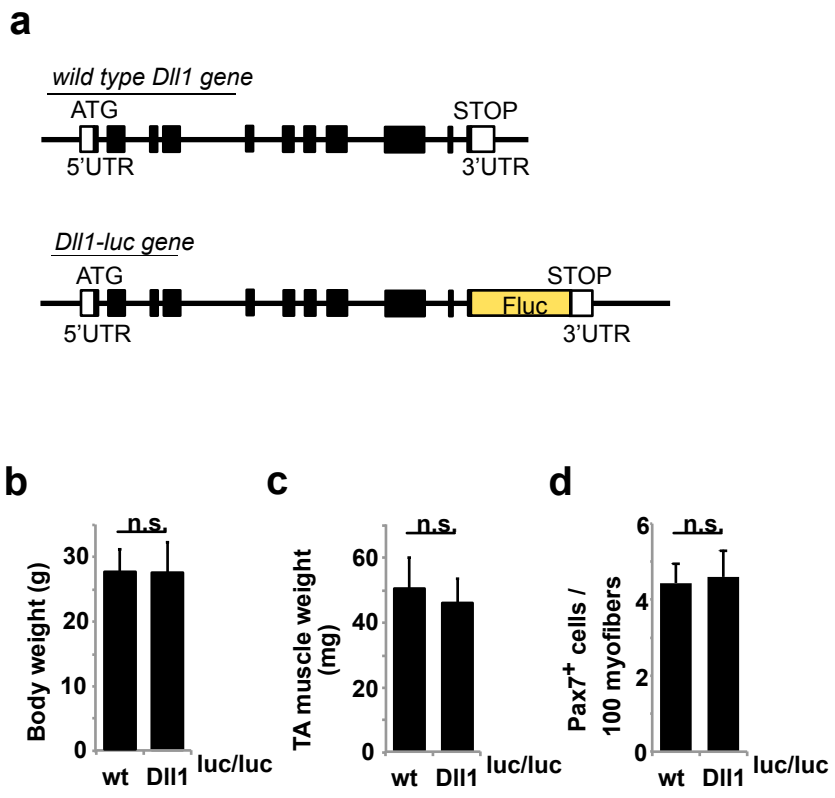

Fig 3.4. Analysis of homozygous Dll1-luc mice

(a) Schematic structures of the wildtype *Dll1* and *Dll1-luc* alleles; *Dll1-luc* encodes a protein in which Dll1 and firefly luciferase are fused. Indicated are the translation initiation (ATG) and stop codons (STOP), 5' and 3' UTRs, exons (Black boxes) and luciferase cDNA (Yellow box). (b) The homozygous *Dll1-luc* allele does not interfere with body weight. (c) The homozygous *Dll1-luc* allele does not interfere with TA muscle weight. (d) The homozygous *Dll1-luc* allele does not interfere with myogenesis, as assessed by quantification of Pax7+ muscle stem cells in adult animals. n=4. ns indicates $p>0.05$, unpaired two-sided t-test.

I used anti-luciferase antibodies to analyze the expression of the Dll1-luciferase fusion protein. I isolated myofibers with attached muscle stem cells from *Dll1-luc* mice, and fixed them either directly or cultured them for different times. Then, I used the anti-luciferase antibody to test for Dll1-luc protein expression in quiescent, activated and differentiating muscle stem cells and myofibers. When the fibers are freshly isolated, associated stem cells are quiescent. In the quiescent cells, I detected only Pax7 but not MyoD or Dll1-luc protein. When cultured as floating fibers, stem cells remain associated with myofibers. After around 42 hours of incubation, the first division occurs in the activated stem cells. In the activated cells, I detected MyoD, Pax7 and also Dll1-luc. After 72 hours of culture, the stem cells associated with myofibers formed small colonies containing activated cells that express Pax7 and MyoD, and differentiating cells that express MyoG. When the cells differentiate, I detected MyoG and Dll1-luc, but in myofibers I did not detect Dll1-luc protein (Fig 3.5).

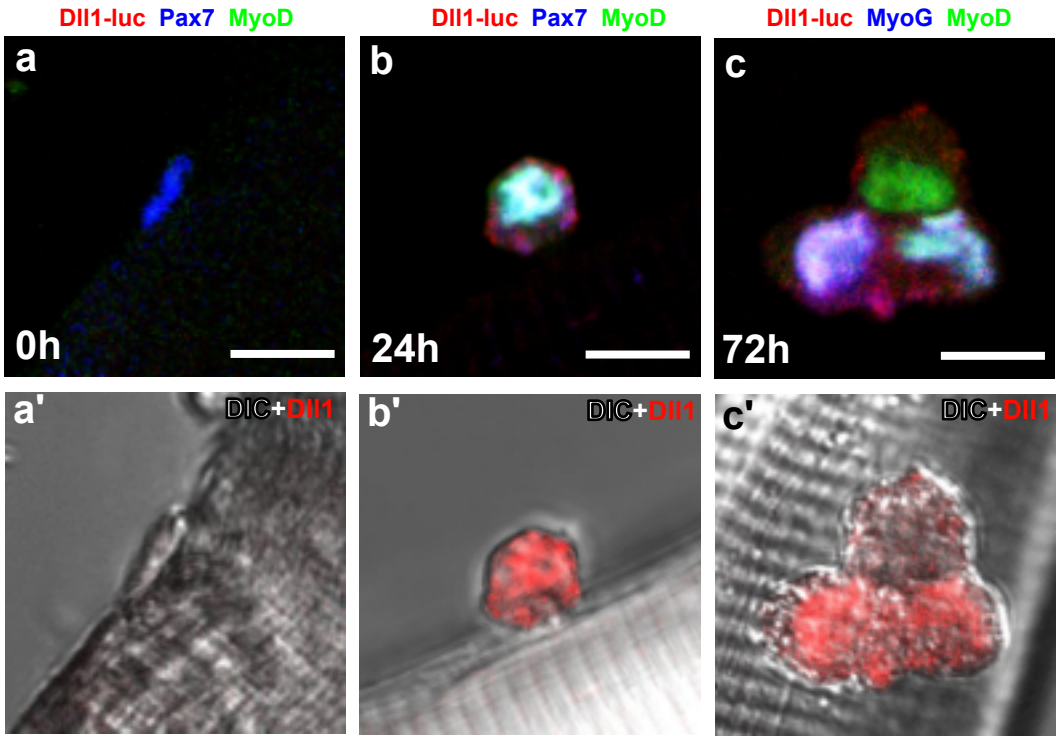

Fig 3.5. Dll1-luc protein in muscle stem cells associated with myofibers.

(a,b,c) Immunofluorescence analysis of muscle stem cells associated with fibers from mice carrying the Dll1-luc allele; myofibers were freshly

isolated (a), or cultured for 24 h (b) and 72 h (c) as indicated. (a',b',c') Differential interference contrast (DIC; Gray) and Dll1-luc protein (anti-luciferase; Red) pictures (a,b,c). The antibody against Pax7 (Blue), MyoD (Green) and luciferase (Red) were used in (a,b and a',b'). The antibody against MyoG (Blue), MyoD (Green) and luciferase (Red) were used in (c and c'). n=5. Scale bars, 10 µm

Taken together, Dll1 transcripts and protein are expressed in activated and differentiating muscle stem cells, but not in quiescent stem cells or myofibers.

3.1.2. Dll1 controls the self-renewal of neighboring cells

I asked whether Dll1 produced by activated muscle stem cells has an important function. I used RNA interference to knock down *Dll1* in cultured muscle stem cells associated with myofibers. First, I tested the efficiency of RNA interference by western blot using C2C12 myoblasts. Dll1 protein was strongly reduced at both 24 hours and 48 hours after siRNA transfection (Fig 3.6a). I then used siRNAs to knock down *Dll1* in muscle stem cells on floating fibers, and cultured them after the siRNA treatment for 72 hours. Compared to control siRNAs, I detected more differentiating cells (MyoG+) in the colonies. In parallel, the number of Pax7+ cells was reduced (Fig 3.6b).

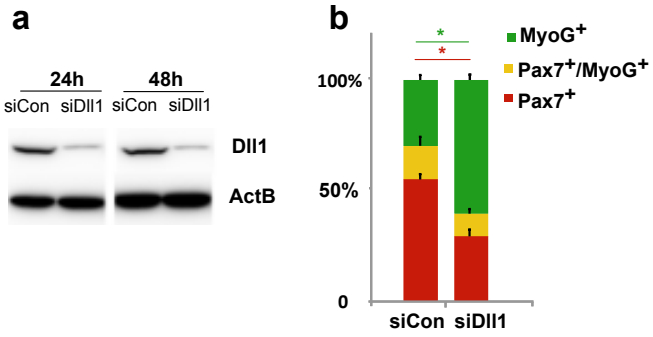

Fig 3.6. siDll1 function in muscle stem cells associated with myofibers

(a) Western blot analysis of Dll1 and β-actin levels in C2C12 myoblasts treated with control siRNA (siCon) and *Dll1* siRNA (siDll1) for 24 hours or 48 hours. β-actin was used for internal control. (b) Quantification of cells that express Pax7, Pax7 and MyoG, and MyoG in colonies associated with myofibers from siCon and siDll1 treated myofibers 72 hours after the

transfection of siRNA. n=3. Data are presented as mean values +/- SEM. * indicates p<0.05, unpaired two-sided t-test.

To verify the function of Dll1 in muscle stem cells, I used a genetic strategy to introduce a *Dll1* null mutation in adult muscle stem cells, i.e. *Pax7*^{CreERT2};*Dll1*$^{flox/flox}$ mice were treated with tamoxifen (called hereafter *TxDll1*$^{f/f}$). In such animals, a CreERT2 recombinase is expressed in Pax7+ muscle stem cells. Upon treatment with tamoxifen, the CreERT2 recombinase translocates to the nucleus where it recombines sequences that are surrounded by loxP sites. As control, I used *Pax7*^{CreERT2};*Dll1*$^{luc/flox}$ mice treated with tamoxifen (called hereafter *TxCon*). I isolated muscle stem cells from tamoxifen treated mice, and performed PCR to verify the recombination efficacy (Fig 3.7).

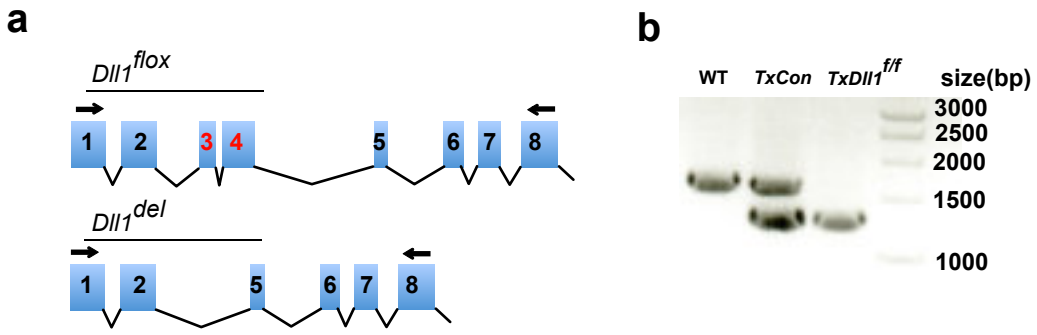

Fig 3.7. The recombination efficacy of *Pax7*^{CreERT2}*; Dll1*$^{flox/flox}$

(a) Schematic structures of the *Dll1flox* alleles; after recombination, the 3rd and 4th exon of *Dll1* gene, which are surrounded by loxP sites, were deleted. Black arrows showed the site of PCR primers used. (b) RT-PCR analysis of transcripts isolated from FAC-sorted muscle stem cells with the indicated genotypes. n=3.

First, I analyzed the effect of the mutation in an *in vitro* experiment. I cultured myofibers isolated from *TxDll1*$^{f/f}$ and *TxCon* animals with the associated muscle stem cells for 60 hours. The colonies on fibers from *TxDll1*$^{f/f}$ and *TxCon* mice were similar in size. When I cultured them for 72 hours, the *TxDll1*$^{f/f}$ colonies were smaller than the *TxCon* colonies. I also stained the colonies with Pax7 and MyoG antibodies, and observed that Pax7+ cell numbers were decreased and MyoG+ cell numbers were increased (Fig 3.8). This shows that muscle stem

cells in the *TxDll1*$^{f/f}$ colonies had a higher propensity to differentiate and express MyoG. Once the cells express MyoG, they are on the way to terminally differentiate, and they withdraw from the cell cycle. Thus, cells in *TxDll1*$^{f/f}$ colonies stopped dividing earlier and had formed smaller colonies after 72 hours of incubation. Since the genetic deletion of *Dll1* was specifically introduced in muscle stem cells, the results demonstrate that Dll1 produced by activated and differentiating muscle stem cells suppresses differentiation of neighboring stem cells.

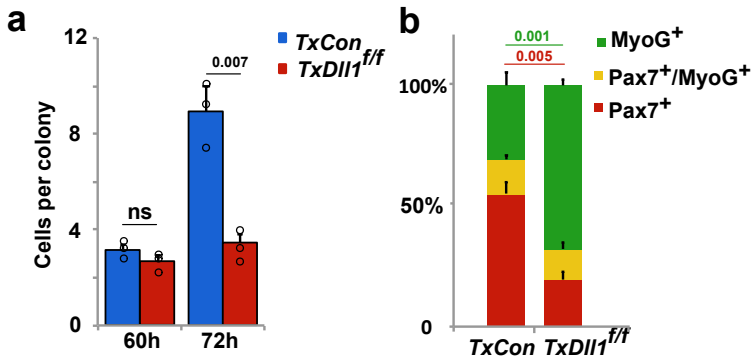

Fig 3.8. Genetic deletion of *Dll1* in muscle stem cells associated with myofibers

(a) Quantification of colony size of muscle stem cells on myofibers from *TxCon* and *TxDll1*$^{f/f}$ animals. Myofibers were cultured for 60 and 72 hours. (b) Quantification of cells that express Pax7, Pax7/MyoG and MyoG in colonies associated with myofibers from *TxCon* and *TxDll1*$^{f/f}$ animals. Myofibers were cultured for 72 hours. n=3. Data are presented as mean values +/- SEM. p values are indicated, unpaired two-sided t-test.

Next, I verified the function of Dll1 *in vivo*. Muscle stem cells in the adult are quiescent and become activated after muscle injury in order to regenerate the muscle. I investigated uninjured and regenerating TA muscle in adult animals. In the uninjured muscle, I detected similar numbers of Pax7+ cells in *TxDll1*$^{f/f}$ and *TxCon* mice. In the injured muscle, the activation of muscle stem cells occurred correctly, as assessed by the quantification of Pax7+ cells and of EdU incorporation in Pax7+ cells of *TxCon* and *TxDll1*$^{f/f}$ mice (Fig 3.9). However, at later stages of muscle regeneration, the cells differentiated prematurely *in vivo*. Compared to control animals, decreased numbers of Pax7+ cells and increased

numbers of MyoG+ cells were observed in the *TxDll1*$^{f/f}$ mice at 4 dpi. As a consequence of the premature differentiation, fewer Pax7+ cells were observed in the regenerated muscle of *TxDll1*$^{f/f}$ mice at 7 dpi and 21 dpi. The newly formed myofibers in *TxDll1*$^{f/f}$ mice contained fewer nuclei at 7 dpi and 21 dpi, and displayed smaller diameters at 21 dpi (Fig 3.10).

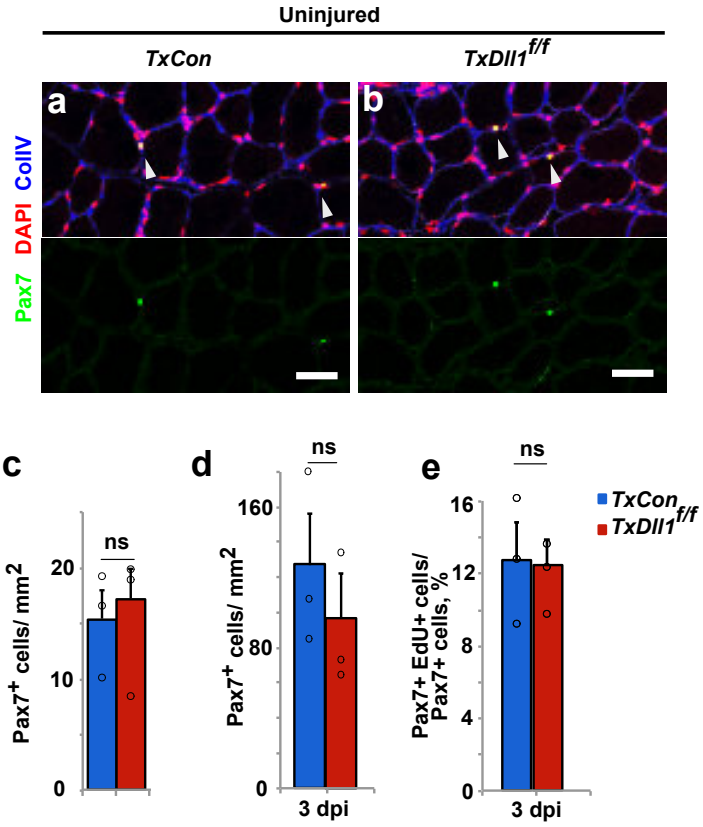

Fig 3.9. Effect of *Dll1* deletion on maintenance and activation of muscle stem cells.

(a,b) Histological analysis of the muscles from *TxCon* (a) and *TxDll1*$^{f/f}$ (b) mice using antibodies against Pax7 (Green) and Collagen IV (Blue). DAPI (Red) was used as a counterstain. (c) Quantification of the number of Pax7+ cells in the uninjured muscle of *TxCon* and *TxDll1*$^{f/f}$ mice. (d) Quantification of the number of Pax7+ cells in the regenerated muscle of *TxCon* and *TxDll1*$^{f/f}$ mice at 3 dpi. (e) Quantification of the proliferation of Pax7+ cells (assessed by EdU incorporation) in the regenerated muscle of *TxCon* and *TxDll1*$^{f/f}$ mice at 3 dpi. n=3. Scale bars, 50 µm. Data are presented as mean values +/- SEM. ns indicates $p>0.05$, unpaired two sided t-test.

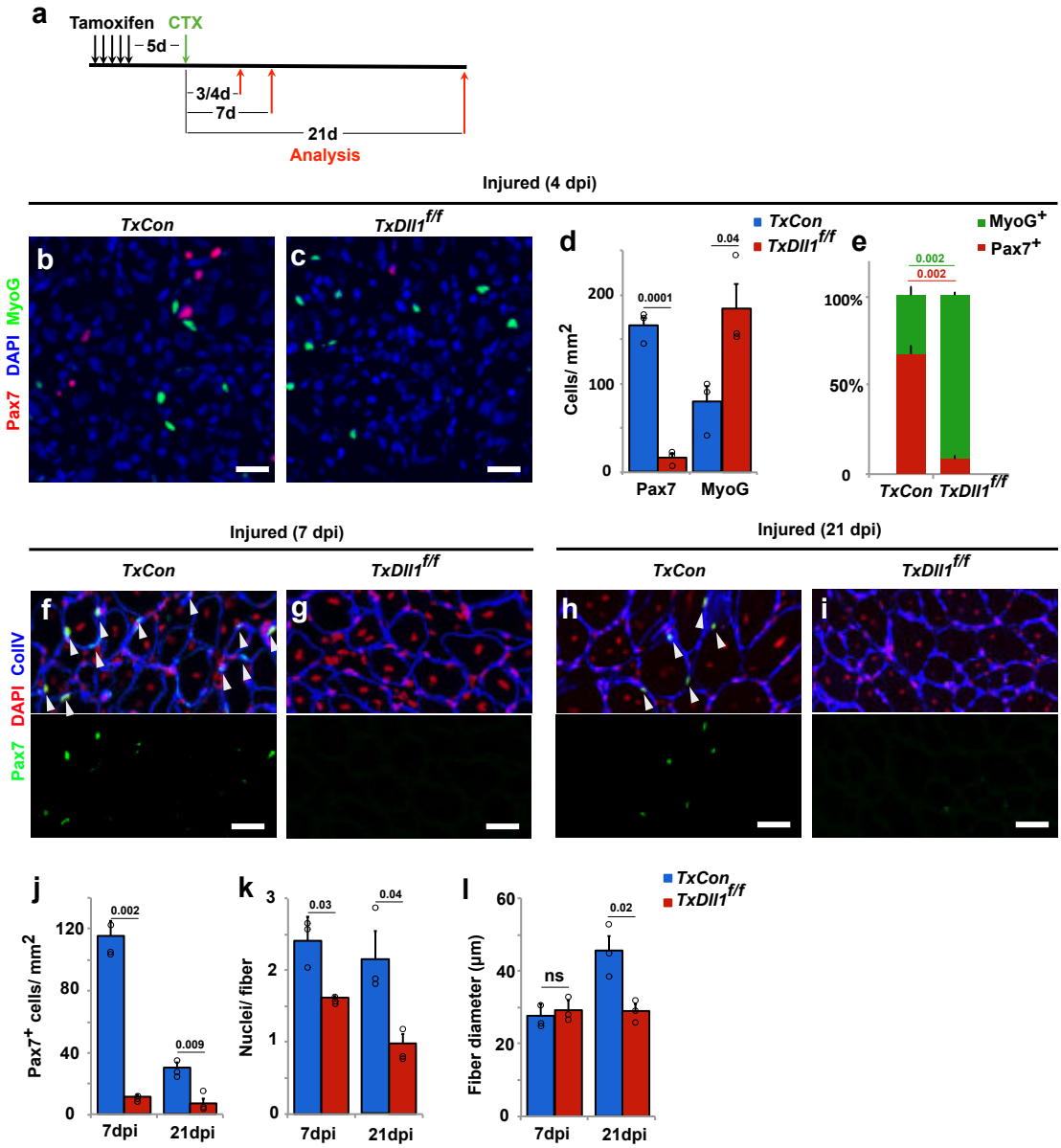

Fig 3.10. The effect of *Dll1* deletion in regenerated muscle at 4dpi, 7dpi and 21dpi.

(a) Schematic outline of the regeneration experiment. Muscle injury was induced by intramuscular CTX injections. Black arrows: tamoxifen injections; green arrow: cardiotoxin (CTX) treatment; red arrows: analysis of muscle regeneration. (b,c) Immunohistological analysis of cells expressing Pax7 (Red) and MyoG (Green) in the injured muscle of *TxCon* (b) and *TxDll1$^{f/f}$* (c) mice. (d) Quantification of Pax7+ cells and MyoG+ cells. (e) Quantification of the proportion of Pax7+ and MyoG+ cells. (f, g, h, i). Immunohistological analysis of cells expressing Pax7 (Green) in the injured muscle of *TxCon* (f) and *TxDll1$^{f/f}$* (g) mice at 7 dpi and *TxCon* (h) and *TxDll1$^{f/f}$* (i) mice at 21 dpi. (j) Quantification of Pax7+ cells in the regenerated muscle at 7 dpi and 21 dpi. (k) Quantification of nuclei per fiber in the regenerated muscle at 7 dpi and 21 dpi. (l) Quantification of

myofiber diameters in the regenerated muscle at 7 dpi and 21 dpi. n=3. Scale bars, 50 μm. Data are presented as mean values +/- SEM. P values are indicated, unpaired two sided t-test.

Taken together, muscle regeneration was severely impaired by *Dll1* deletion in muscle stem cells due to their premature differentiation. Thus, Dll1 expressed in regenerating cells functions to suppress differentiation of neighboring cells.

3.2. Oscillation of Dll1 expression in activated muscle stem cells

3.2.1. Dll1 expression oscillates in muscle progenitors

Bioluminescence imaging does not require external excitation and can be used to monitor the expression of luciferase fusion proteins over long periods without photo-damage. Moreover, bioluminescence imaging does not impair the survival or differentiation of myogenic cells. To check the dynamics of Dll1 protein in muscle progenitors, I used *Pax7-nGFP* transgenic mice crossed with *Dll1-luc* mice. I produced slices from embryonic limbs containing muscle progenitor cells of such animals, and cultured them under the microscope in order to follow bioluminescence in the cells. I detected oscillatory expression of Dll1 in GFP+ (i.e. Pax7+) muscle progenitors, and the oscillatory period was 2-3 hours (Fig 3.11).

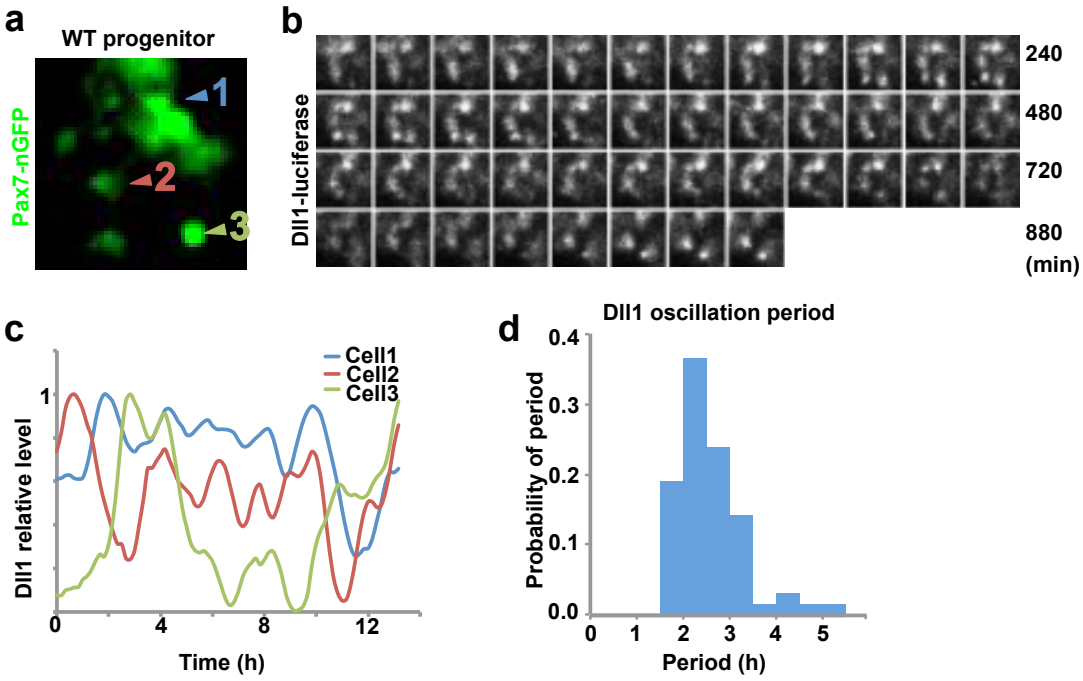

Fig 3.11. Dll1 protein expression dynamics in muscle progenitors

(a) The GFP signal identified myogenic cells in the slice. (b) The bioluminescence signals observed in the region shown in (a). (c) Quantification of the bioluminescence signals in the three cells indicated in (a). (d) Quantification of the Dll1 oscillatory period in embryonic muscle progenitor cells observed in slices. n=3.

3.2.2. Dll1 expression oscillates in activated muscle stem cells associated with myofibers

Since muscle stem cells *in vivo* are directly attached to myofibers, myofibers were thought to be the main source of Notch ligand. Recent results showed that Dll4 from myofibers maintained muscle stem cells (Eliazer et al., 2020). To maintain the proximity between muscle stem cells and myofibers, I isolated myofibers with associated muscle stem cells from mice carrying the *Dll1-luc* allele. Dll1-luciferase bioluminescence was neither detected in myofibers nor in the associated quiescent muscle stem cells. After culture overnight, the muscle stem cells were activated and I detected bioluminescence signals in such cells. In single muscle stem cells, Dll1 protein showed oscillatory expression. The oscillatory period was 2-3 hours (Fig 3.12).

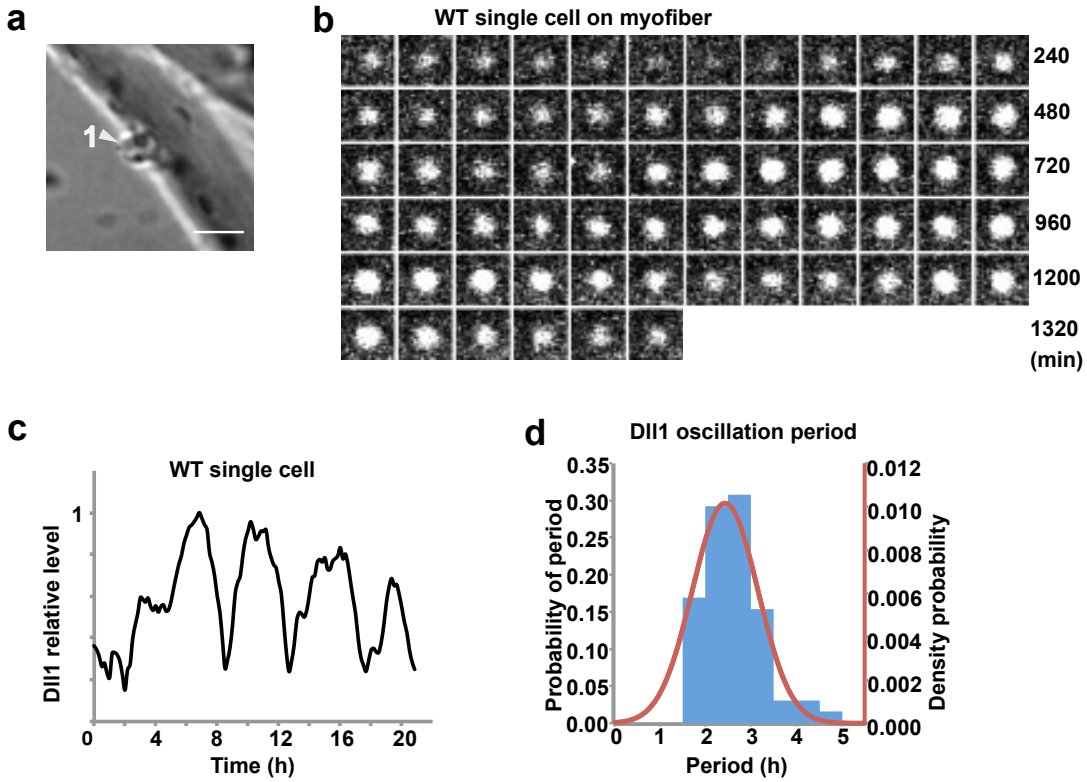

Fig 3.12. Dll1 expression dynamics in activated single muscle stem cells associated with myofibers

(a) The bright field image identified myogenic cells. (b) The bioluminescence signals observed in the cell which is shown in (a). (c) Quantification of the bioluminescence signals in the cell shown in (a). (d) Quantification of the Dll1 oscillatory period in muscle stem cells associated with myofibers. n=12. Scale bars, 15 μm.

When I cultured the myofiber with associated muscle stem cells over more than 42 hours, small colonies had formed in which the cells were contacting each other. I monitored the Dll1 expression dynamics in coupled cells, and detected Dll1 oscillation in both cells. The period was 2-3 hours in both cells. Interestingly, the oscillations of Dll1 protein in the coupled two cells are out of phase (Fig 3.13). When the myofibers were cultured for longer periods, the colonies became larger and contained more cells, which were impossible to track with bioluminescence imaging because cells constantly changed their relative positions.

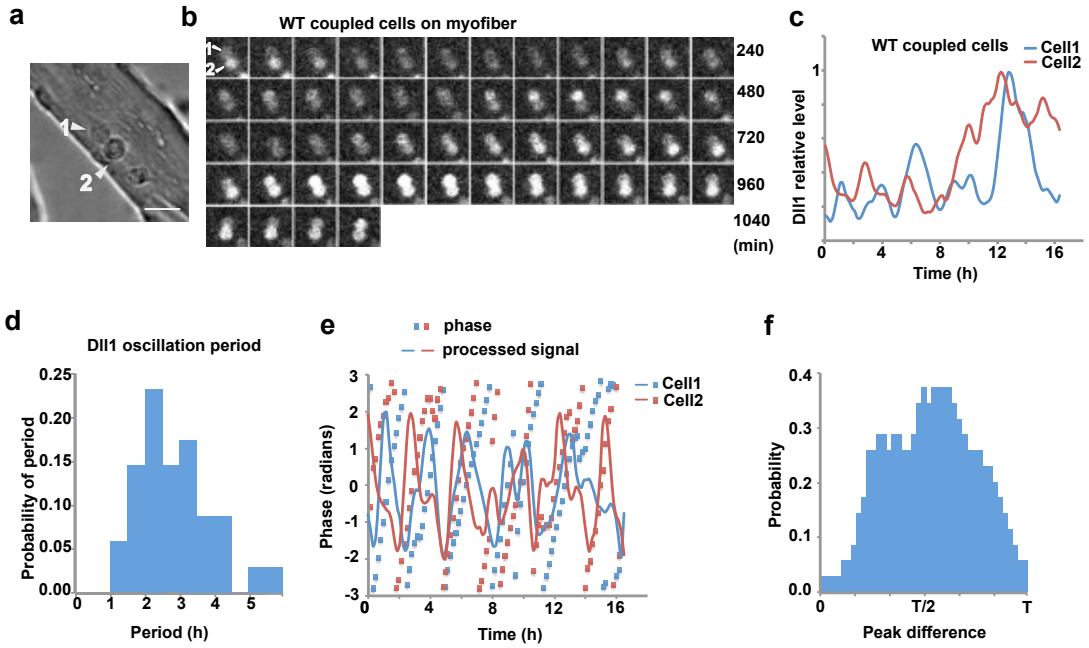

Fig 3.13. Dll1 expression dynamics in activated coupled muscle stem cells associated with myofibers

(a) The bright field image was used to identify myogenic cells. (b) The bioluminescence signals observed in the cells which are shown in (a). (c) Quantification of the bioluminescence signals in the two cells. (d) Quantification of Dll1 oscillatory period in these coupled muscle stem cells. (e) Hilbert transformation of phase time series in the coupled cells. (f) Relationship of Dll1 oscillation periods in two coupled cells on myofibers. n=6. Scale bars, 15 μm.

3.2.3. Dll1 expression oscillates in cultured muscle stem cells

To verify the Dll1 oscillation, I also isolated muscle stem cells by FAC sorting from mice carrying the *Dll1-luc* allele, and cultured them in proliferation medium containing FBS. I detected Dll1 oscillation with period of 2-3 hours in cultured muscle stem cells (Fig 3.14).

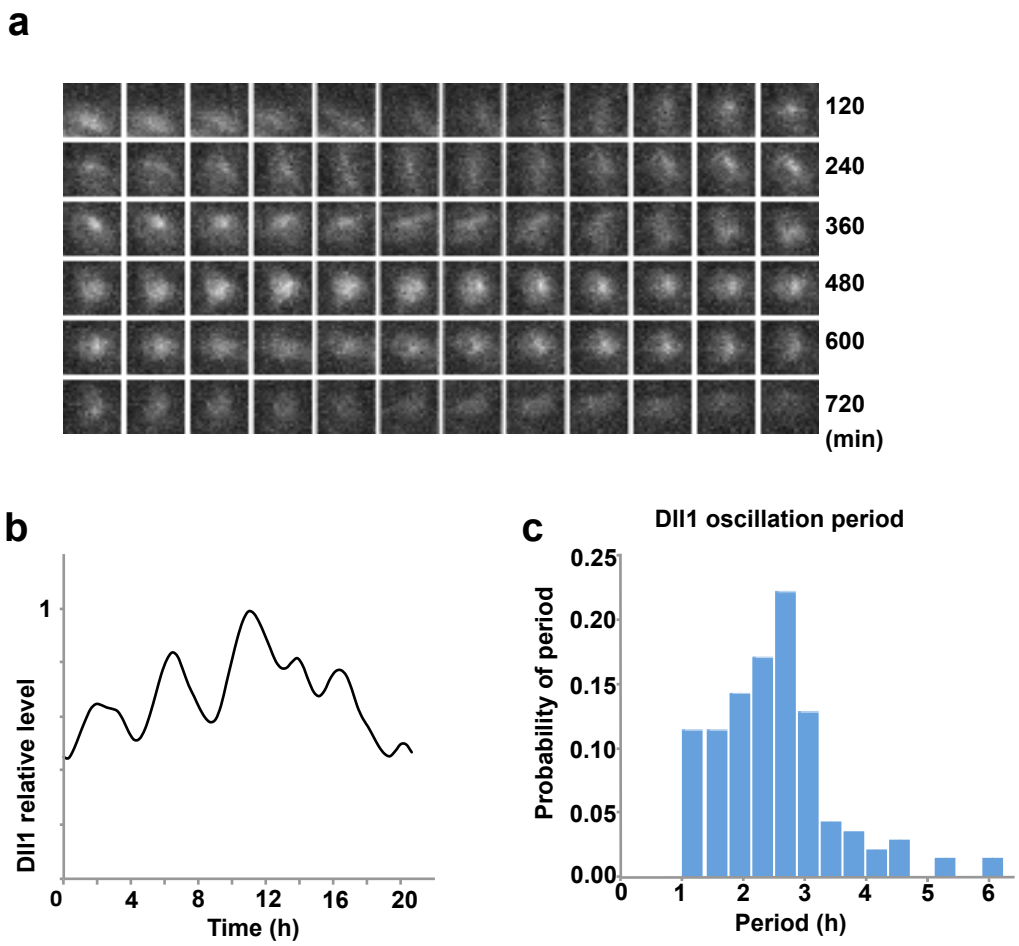

Fig 3.14. Dll1 expression dynamics in cultured muscle stem cells

(a) The bioluminescence signals in cultured muscle stem cell. (b) Quantification of the bioluminescence signals in the cell. (c) Quantification of Dll1 oscillatory period in cultured muscle stem cells. n=8.

3.2.4. Dll1 expression oscillates in muscle stem cells cultured as myospheres

To simulate the *in vivo* situation, I cultured muscle stem cells as clusters in free floating myospheres. In this situation, cells maintain their contact to neighboring cells. This cannot be achieved when the cells are plated on adhesive substrates, because they constantly move, making frequently new contacts and then again breaking the contacts. To verify the Dll1 oscillation in such cells, I co-transfected two plasmids. In the first plasmid, a *Dll1* promoter and enhancer drive a destabilized Nanoluc. The second plasmid encodes an

EGFP with a nuclear localization signal (nGFP), which allowed identifying and tracking transfected cells. Transfected and not transfected cells were mixed, and I identified spheres containing 1 or 2 transfected cells to follow their bioluminescence signals. Bioluminescence imaging demonstrated that Nanoluc was expressed in an oscillatory manner in the transfected cells of the spheres. The oscillatory period was 2-3 hours (Fig 3.15).

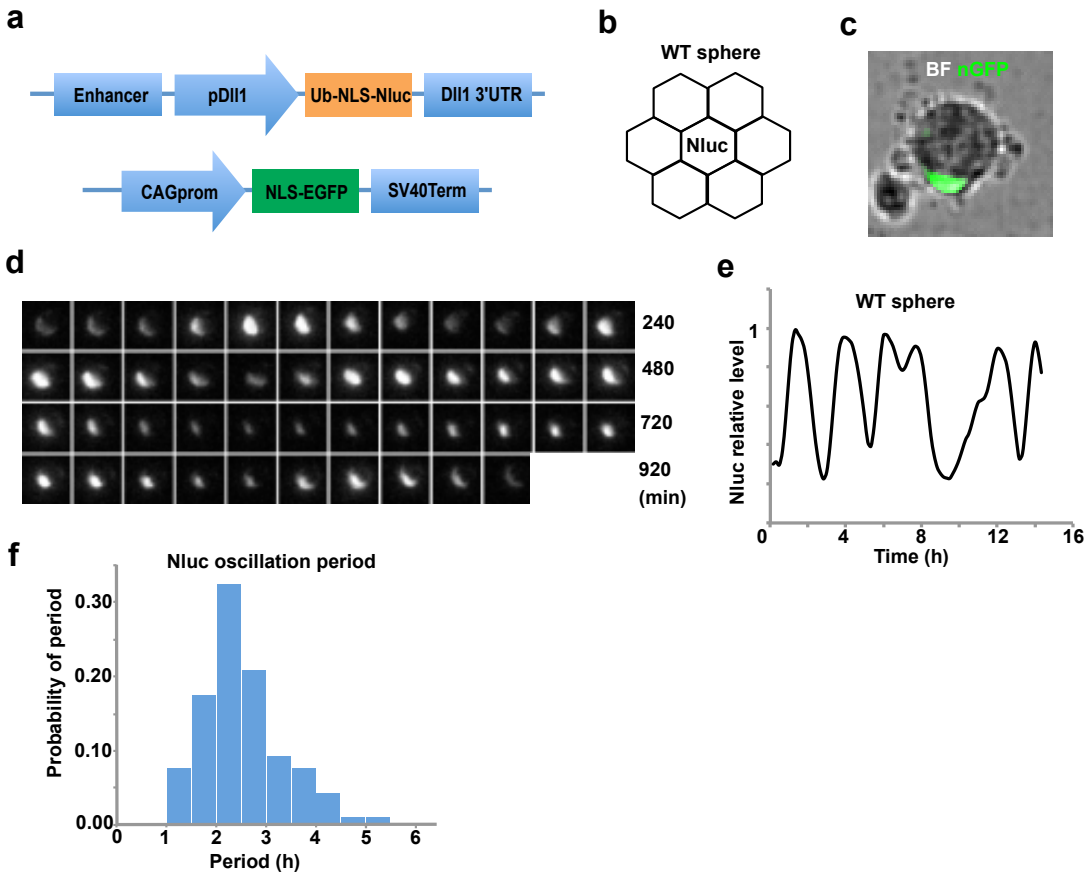

Fig 3.15. Dll1 expression dynamics in culture myospheres

(a) Schematic structure of plasmids used to monitor dynamic Dll1 expression in cells cultured as spheres. The EpDll1-NanoLuc plasmid (top) encodes a destabilized NanoLuc protein fused to a nuclear localization signal (Ub-NLS-Nluc), whose expression is controlled by the Dll1 enhancer and promoter. In addition, the 3' UTR of Dll1 is included. The plasmid encoding nGFP is also shown (bottom). (b) Schematic drawing of cells grown in a sphere; a co-transfected single cell is surrounded by many untransfected cells. (c) The bright field identified the myogenic sphere, nGFP the transfected cell. (d) The bioluminescence signals were detected in one cell of the sphere. (e) Quantification of the

bioluminescence signals in this cell. (f) Quantification of Dll1 oscillatory period in muscle stem cells cultured as spheres. n=4.

Taken together, Dll1 expression oscillates in developing and adult muscle stem cells kept under different conditions: in slice cultures, when the cells were cultured on fibers, when they were plated on culture dishes, or when they were cultured as myospheres.

3.3. Hes1 is a pacemaker of Dll1 oscillation, while MyoD increases Dll1 expression but does not affect Dll1 oscillation

The oscillatory period of Dll1 is similar to the one of MyoD and Hes1 protein described previously (Lahmann et al., 2019). I therefore asked whether the two oscillatory factors could drive oscillatory Dll1 expression.

3.3.1. Hes1 decreases Dll1 transcription and MyoD increases Dll1 transcription

To define a possible Dll1 regulation through MyoD, I used ChIP-seq data of a previous data set in which MyoD binding sites were defined in a genome-wide manner (Cao et al., 2010). I identified a region in the 4th intron of the *Dll1* gene which is bound by MyoD. In this fragment, there are three E-boxes (MyoD binding sites) and one N-box (Hes1 binding site). To test whether this fragment can act as an enhancer, I cloned the fragment (called EF fragment) into the pGL4.23 reporter plasmid, which contains a minimal promoter that drives luciferase. I transfected plasmids into HEK293 cells and measured the enhancer activity using a dual luciferase reporter system. The experiments demonstrated 48-fold and 16-fold increase in expression when the reporter plasmid was co-transfected with MyoD and MyoG expression plasmids, respectively. Thus, the EF fragment possesses enhancer activity when MyoD and MyoG are present. Co-transfection of a Hes1 expression plasmid suppressed the enhanced expression induced by MyoD. Moreover, I used two mutant EF fragments for dual reporter luciferase assays in HEK293 cells: one

that was lacking all E-boxes (EF-E), and the other that was lacking the N-box (EF-N). Expression driven by EF-E no longer responded to MyoD. Expression driven by EF-N no longer responded to Hes1, but MyoD still activated transcription (Fig 3.16). Together, these data indicate that Hes1 and MyoD function independently of each other to control gene expression through the EF fragment which acts as an enhancer.

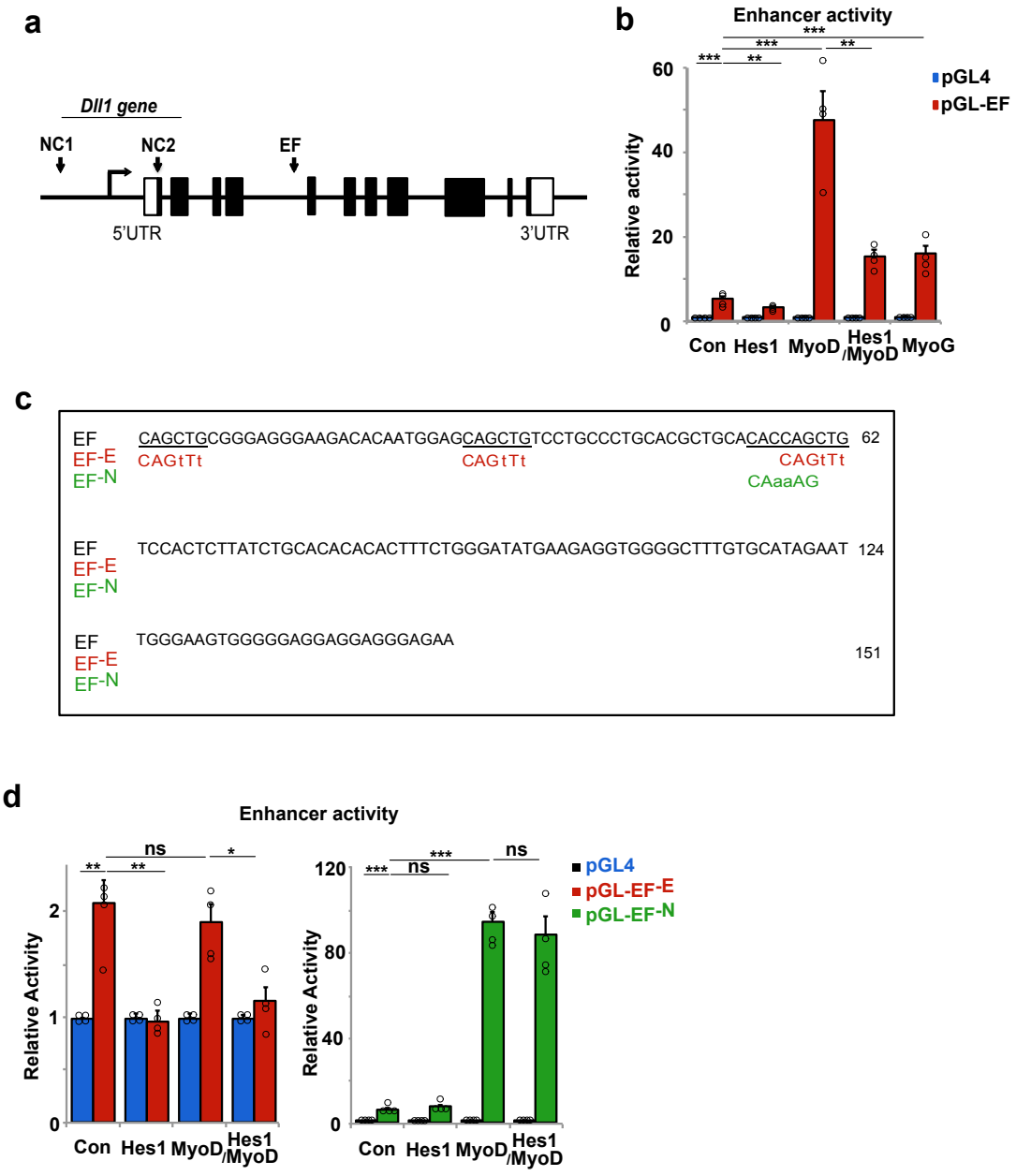

Fig 3.16. Enhancer activity analysis of EF, EF-E and EF-N fragments in response to Hes1 and MyoD

(a) Schematic display of the *Dll1* gene; the enhancer fragment (EF) corresponds to sequences located in the fourth intron. Two additional fragments were used as negative controls (NC1, NC2). (b) Test of the enhancer activity of the EF fragment using the dual-luciferase reporter system (pGL4 luciferase plasmid without an enhancer, blue bars; pGL-EF luciferase plasmid containing EF enhancer, red bars). Cells co-transfected with pCAG-nGFP (control, con), Hes1, MyoD, Hes1/MyoD and MyoG expression plasmids were analyzed; n = 4 experiments. (c) DNA sequence of the EF fragment that possesses enhancer activity; the sequences of mutant variants lacking all E-boxes (EF-E) or the N-box (EF-N) are shown below. (d) Comparison of the enhancer activity using the dual-luciferase reporter system; pGL4 luciferase plasmid without an enhancer (blue bars); pGL4-EF-E luciferase plasmid containing enhancer lacking E-box sequences (red bars); pGL4-EF-N luciferase plasmid containing enhancer lacking N-box sequences. Control (con) cells co-transfected with pCAG-nGFP, and cells co-transfected with Hes1, MyoD and Hes1/MyoD expression plasmids were analyzed; n = 4 experiments. Data are presented as mean values ± SEM. * $p<0.05$, ** $p<0.01$, *** $p<0.001$, unpaired two-sided t-test.

To test whether MyoD and Hes1 directly bind the EF enhancer in cells, I performed ChIP-PCR with anti-MyoD and anti-Hes1 antibodies using primers that amplify the EF fragment. This experiment demonstrated in myogenic C2C12 cells the binding of endogenous Hes1 and MyoD to the EF fragment from the *Dll1* locus. A previously characterized MyoD binding site in the Myomaker (*Mymk*) gene, and Hes1 binding sites from *MyoD* and *Hes1* loci were used as positive controls (Lahmann et al., 2019; Millay et al., 2014; Takebayashi et al., 1994). NC1 and NC2 from the *Dll1* gene were used as negative controls. Interestingly, the NC1 containing E-box site can be bound by the other bHLH factor Ascl1 in neural stem cells (Shimojo et al., 2008). However, the NC1 site was not bound by the bHLH factor MyoD in myogenic cells. Further, I also performed ChIP-PCR on the EF mutant fragments. This showed that MyoD bound the wild-type and EF−N fragments, but not EF−E, whereas Hes1 bound the wild-type and EF−E fragments, but not EF−N (Fig 3.17).

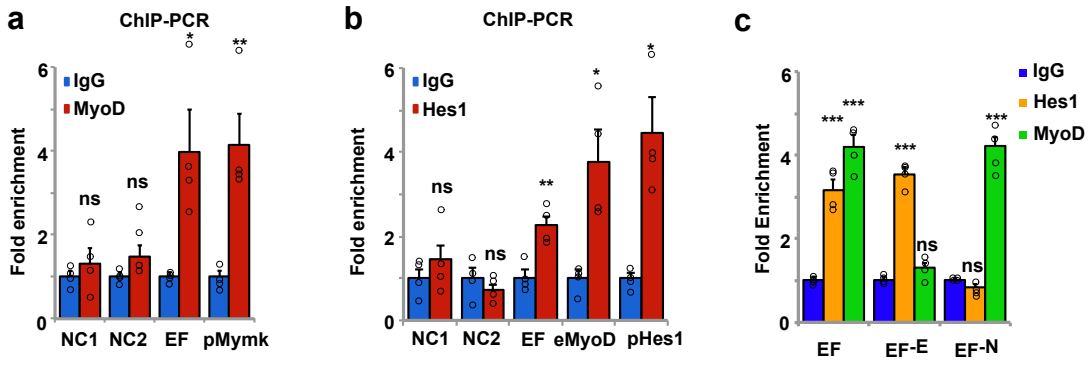

Fig 3.17. ChIP-PCR analysis for MyoD and Hes1 binding to the EF enhancer

(a) ChIP-PCR experiment analyzing MyoD binding to EF and NC1/NC2. The known binding site in the Myomaker (pMymk) gene was used as a positive control; n = 4. (b) ChIP-PCR experiment analyzing Hes1 binding to EF and to NC1/NC2. Known binding sites for Hes1 in the *MyoD* locus (eMyoD 23 kb upstream the MyoD transcript initiation site) and the *Hes1* promoter (pHes1) were used as positive controls; n = 4. (c) ChIP-PCR analysis of Hes1 and MyoD binding to EF, EF-E and EF-N sequences; shown are the fold changes of enrichment observed using anti-Hes1 (yellow bars) and anti-MyoD antibodies (green bars) compared to control IgG (blue bars); n=4. Data are presented as mean values +/- SEM. * p<0.05, ** p<0.01, *** p<0.001, ns indicates p>0.05, unpaired two-sided t-test.

To test the regulation of Dll1 in myogenic cells, I performed RT-PCR with muscle stem cells from wildtype and *MyoD*-/- mice. In *MyoD*-/- cells, *Myf5* was up-regulated, which confirms previous findings (Rudnicki et al., 1992). In contrast, *Dll1* expression was still decreased about 4-fold. Next, I used siRNA to knock down Hes1 expression in primary muscle stem cells. In these cells, *Dll1* transcript levels were increased around 2.5-fold in the presence of MyoD compared to the cells treated with control siRNA (siCon) (Fig 3.18). Thus, MyoD and Hes1 enhance and repress *Dll1* transcription, respectively, and directly bind to enhancer sequences in the *Dll1* gene.

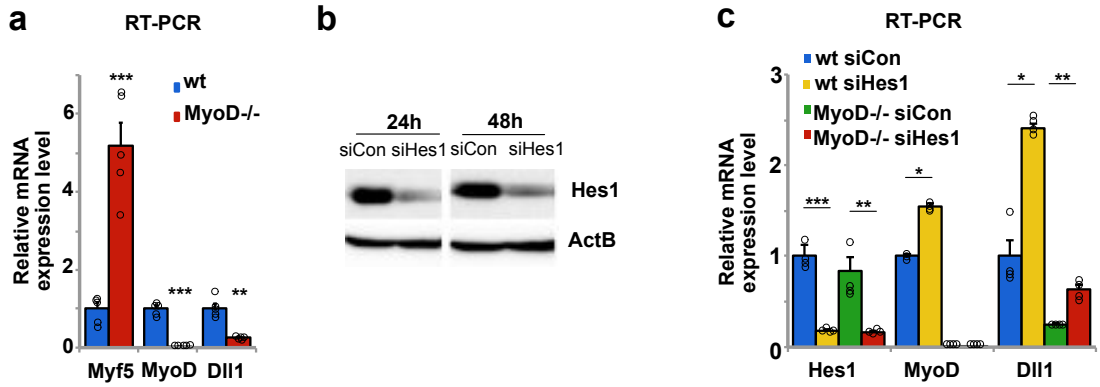

Fig 3.18. Expression of *Dll1* is regulated by MyoD and Hes1 in muscle stem cells

(a) qPCR analysis of *Dll1*, MyoD and *Myf5* transcripts in wild-type (wt) and *MyoD-/-* mutant muscle stem cells, demonstrating MyoD-dependent *Dll1* expression; n = 5. (b) Western blot analysis of Hes1 and β-actin levels in myoblasts treated with control siRNA (siCon) and Hes1 siRNA (siHes1) for 24 hours or 48 hours. β-actin was used as internal control. (c) qPCR analysis of *Hes1*, *MyoD* and *Dll1* in muscle stem cells isolated from wild-type and *MyoD−/−* mice; cells were further treated with siCon or siHes1; n = 4. Data are presented as mean values ± SEM.* p<0.05, ** p<0.01, *** p<0.001, unpaired two-sided t-test.

3.3.2. Dll1 oscillation is regulated by Hes1, but not MyoD

Since MyoD increased and Hes1 decreased Dll1 expression, I asked if the oscillation of Dll1 was regulated by these transcription factors. I isolated myofibers with associated muscle stem cells from *Dll1-luc*;*MyoD-/-* mice, and investigated Dll1 expressions dynamics by monitoring bioluminescence. Expression of the Dll1-luciferase protein oscillated in *MyoD-/-* cells. Quantifications using Fast Fourier transformation (power of FFT) showed that neither the stability nor the period of Dll1 oscillation was changed. However, the bioluminescence signals were weaker due to the lack of MyoD (Fig 3.19).

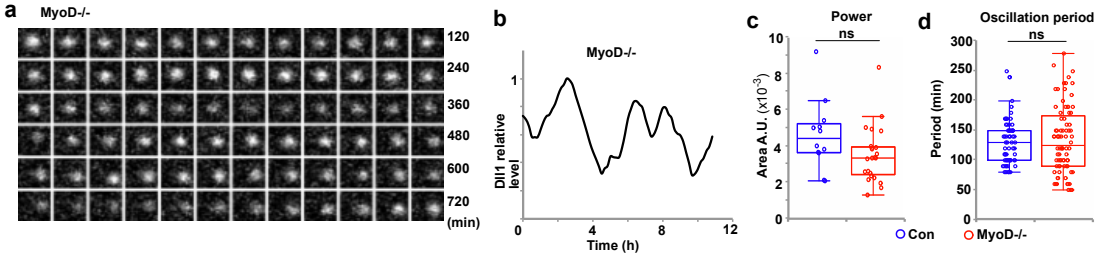

Fig 3.19. Dll1 expression dynamics in *MyoD*-/- muscle stem cells associated with myofibers

(a) Bioluminescence signals from Dll1-luciferase observed in a single *MyoD*−/− mutant muscle stem cells associated with a myofiber; the myofiber and associated stem cell were isolated from a *MyoD*−/−;*Dll1-luc* animal. (b) Quantification of the bioluminescence signals in the cell. (c) Quantification of the oscillatory stability (power of the Fast Fourier transformation). (d) The oscillatory period in control and *MyoD*−/− cells (right); each point represents data obtained from a single imaged cell; n = 23.

To investigate the function of Hes1 in the Dll1 oscillation, I used conditional mutagenesis and siRNA knockdown to test the effect of Hes1. To mutate *Hes1*, I used Pax7creERT2 and a conditional allele (*Hes1*$^{f/f}$), and treated the animals with tamoxifen. Myofibers were isolated from tamoxifen-treated *Pax7*^{creERT2};*Hes1*$^{f/f}$ mice (called *TxHes1*) that carried in addition the *Dll1-luc* allele. Dll1-luciferase protein produced by the *Dll1-luc* allele no longer oscillated in activated stem cells associated with myofibers that had been isolated from *TxHes1* mice. Instead, a sustained expression of the bioluminescence signal interrupted by small, irregular fluctuations were observed (Fig 3.20 a-c). Similar to the *Hes1* mutation, treatment with siHes1 interfered with Dll1-luciferase oscillations in stem cells associated with myofibers, whereas control siRNA had no effect (Fig 3.20 d-h). Previous data showed that Hes1 directly repressed MyoD expression (Lahmann et al., 2019). To test the gene regulatory network among Hes1, MyoD and Dll1, I knocked down Hes1 in *MyoD*-/- muscle stem cells, and tested Dll1 expression dynamics. The presence of the *MyoD* mutation rescued muscle stem cell numbers but not the oscillatory Dll1-luciferase expression after Hes1 siRNA treatment (Fig 3.20 i-l). Thus, the Dll1 oscillation is driven by Hes1 independently of the presence or absence of MyoD.

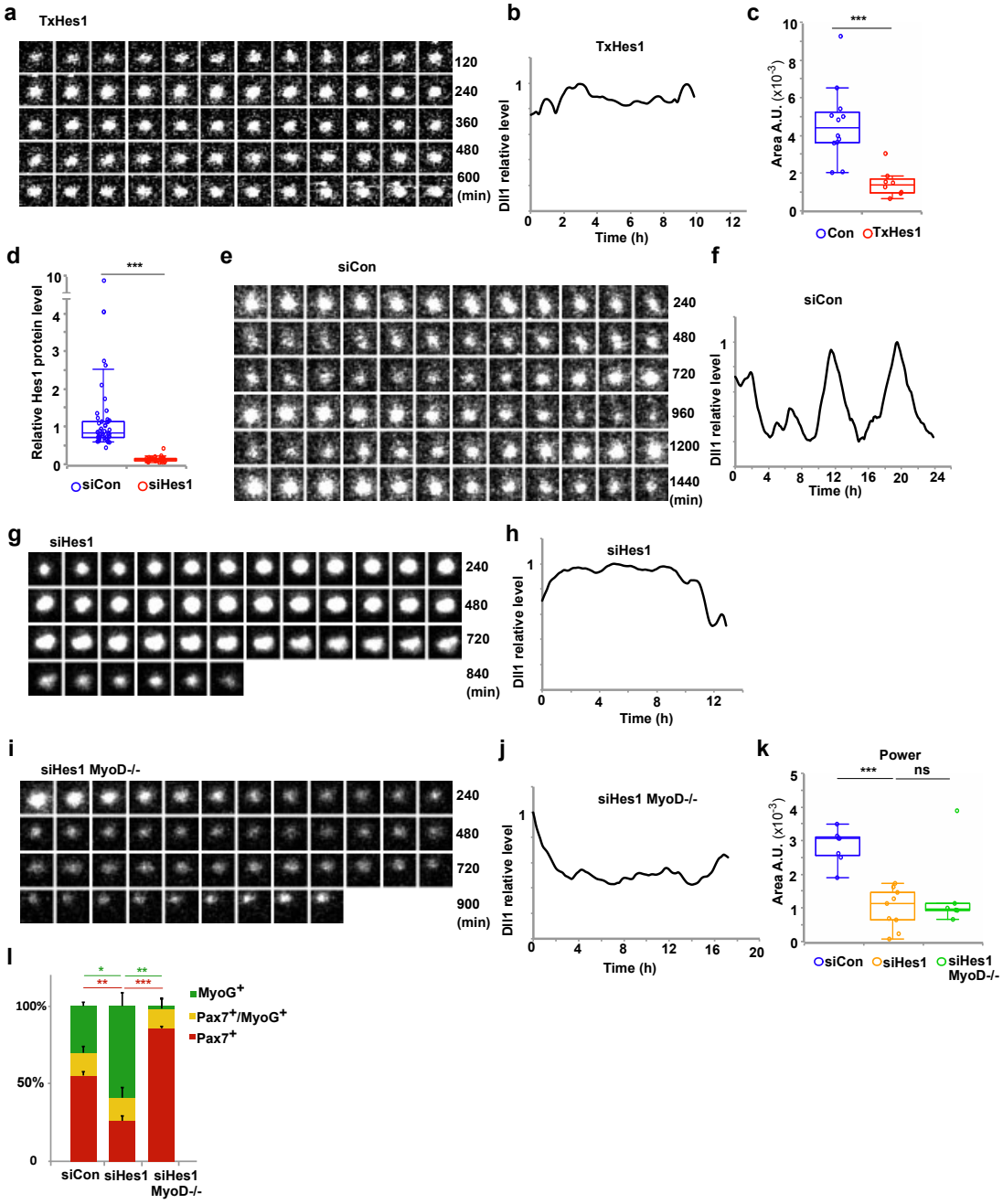

Fig 3.20. The effect of Hes1 on Dll1 oscillation in muscle stem cells associated with myofibers

(a) Bioluminescence signals from Dll1-luciferase observed in a single *TxHes1* mutant muscle stem cell associated with a myofiber; the myofiber and associated stem cell were isolated from a *TxHes1;Dll1$^{f/luc}$* animal. (b) Quantification of the bioluminescence signals in the cell. (c) Quantification of the oscillatory stability (power of the Fast Fourier transformation). (d) Assessment of Hes1 siRNA efficacy. Relative Hes1 protein levels compared to Pax7 levels in muscle stem cells associated with myofibers treated with control (siCon) and Hes1 (siHes1) siRNAs. (e) Bioluminescence signals from Dll1-luciferase observed in a single

siCon treated muscle stem cell associated with a myofiber; the myofiber and associated stem cell were isolated from a *Dll1-luc* animal. (f) Quantification of the bioluminescence signals in the cell. (g) Bioluminescence signals from Dll1-luciferase observed in a single siHes1 treated muscle stem cell associated with a myofiber; the myofiber and associated stem cell were isolated from a *Dll1-luc* animal. (h) Quantification of the bioluminescence signals in the cell. (i) Bioluminescence signals from Dll1-luciferase observed in a single muscle stem cell associated with a fiber; the fiber and associated stem cell were derived from a *MyoD−/−;Dll1-luc* animal and treated with siHes1. (j) Quantification of this bioluminescence signal. (k) Quantification of the oscillatory stability (power of the Fast Fourier transformation) in siRNA control (n = 5) and siHes1 RNA (n = 9) treated wild-type cells, and siHes1 RNA treated *MyoD−/−* (n = 6) mutant cells. (l) Consequences of Hes1 siRNA treatment on differentiation of control and *MyoD-/-* muscle stem cells associated with myofibers; the fibers were analyzed after 72hrs of culture and the relative proportions of MyoG+ (green), Pax7+ (red), Pax7+ and MyoG+ (yellow) cells in colonies on the fibers were determined; n=3. In the box plot, center lines show the medians; box limits indicate the 25th and 75th percentiles; whiskers extend 1.5 times the interquartile range. ***P<0.001, ns indicates P > 0.05, unpaired two-sided t-test.

Taken all together, Hes1 drives Dll1 oscillations and decreases Dll1 expression levels, while MyoD enhances Dll1 expression but has no role in the Dll1 oscillation.

3.4. *Dll1type2* muscle stem cells show dampened oscillations but similar expression level of Dll1

To test whether the Dll1 oscillations are of functional importance in muscle stem cells, I used a previously generated *Dll1* allele, *Dll1type2*. In this allele, the length of the *Dll1* transcript was increased by insertion of *Dll1-luc* cDNA into the first exon. However, protein generated from this allele is identical to the one produced by the *Dll1-luc* allele that does not impair myogenesis (See Fig 3.4). The time needed for production of luciferase from the *Dll1type2* and *Dll1-luc* genes had been previously compared (Shimojo et al., 2016). This had indicated that the transcription of *Dll1type2* takes longer, around 6 minutes or 0.1h. This change in the transcription time impairs Dll1 oscillations in the

presomitic mesoderm (PSM) and in neuronal stem cells (Shimojo et al., 2016). I tested the effect of the *Dll1type2* mutation on myogenesis and on the oscillatory network in muscle stem cells (For details, see Appendix: Delay modeling).

First, I analyzed the expression levels of Dll1 and Notch target genes like Hes1, Hes5 and Hey1 using qPCR. The results showed similar expression levels in *Dll1*$^{type2/type2}$ mutant and wildtype muscle progenitor and stem cells (Fig 3.21).

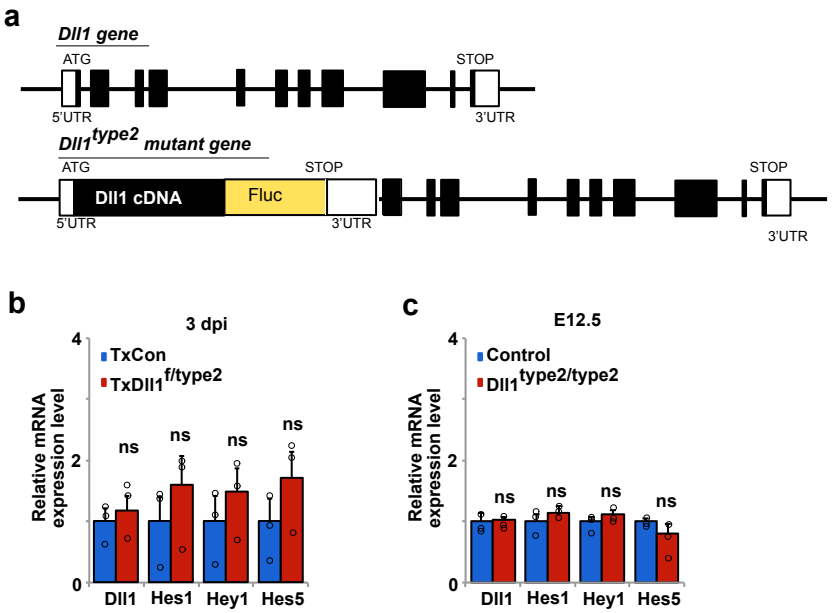

Fig 3.21. qPCR analysis of the expression of Dll1 and Notch target genes in control and *Dll1type2* cells

(a) Schematic display of *Dll1* gene and the *Dll1type2* mutant allele; in the *Dll1type2* allele, a cDNA encoding *Dll1* (black) and firefly luciferase (luc, yellow) were inserted into the *Dll1* locus; the 5′ and 3′ UTR, a translational stop codon (Stop), and the initiation codon (ATG) are indicated. (b) Expression of *Dll1*, *Hes1*, *Hey* and *Hes5* in muscle stem cells isolated from control (*TxCon*, blue bars) and *Dll1type2* (*TxDll1*$^{f/type2}$, red bars) regenerating (3 dpi) muscle. n=3. (c) Expression of *Dll1*, *Hes1*, *Hey* and *Hes5* in muscle progenitor cells isolated from control (blue bars) and *Dll1type2* (*Dll1*$^{type2/type2}$, red bars) embryos (E12.5). n=3. Data are presented as mean values +/- SEM. ns indicates P>0.05, unpaired two-sided t-test.

Next, I investigated Dll1 protein dynamics in muscle progenitors or the limb of E11.5 *Dll1*$^{type2/type2}$ mice in slice cultures. Luciferase expression no longer oscillated in such slices, and instead I observed sustained expression interrupted by small and irregular luciferase fluctuations. FFT was used to quantify the luciferase expression dynamics in cultured slices from *Dll1*$^{type2/type2}$ embryos, which also demonstrated that stable oscillations were no longer observable. However, in single adult muscle stem cells associated with myofibers from *TxDll1*$^{f/type2}$ mice, I found that Dll1 oscillates normally, and that neither the oscillatory stability nor the period was changed. The delay induced by the mutation of *Dll1* should affect the production of the ligand that transmits a signal, and I speculated if the change in delay affects oscillations; this might only occur in coupled cells, in which cells provide and receive Dll1 signals. I cultured myofibers with associated muscle stem cells over 42 hours, a time point at which small colonies had formed. Interestingly, Dll1 oscillations were indeed no longer observed in coupled cells from *TxDll1*$^{f/type2}$ mice. Moreover, oscillation of the Dll1 reporter disappeared in myospheres formed by *TxDll1*$^{f/type2}$ cells (Fig 3.22). I conclude that the *Dll1*type2 mutation in muscle stem cells disrupts Dll1 oscillations in coupled but not in single activated muscle stem cells.

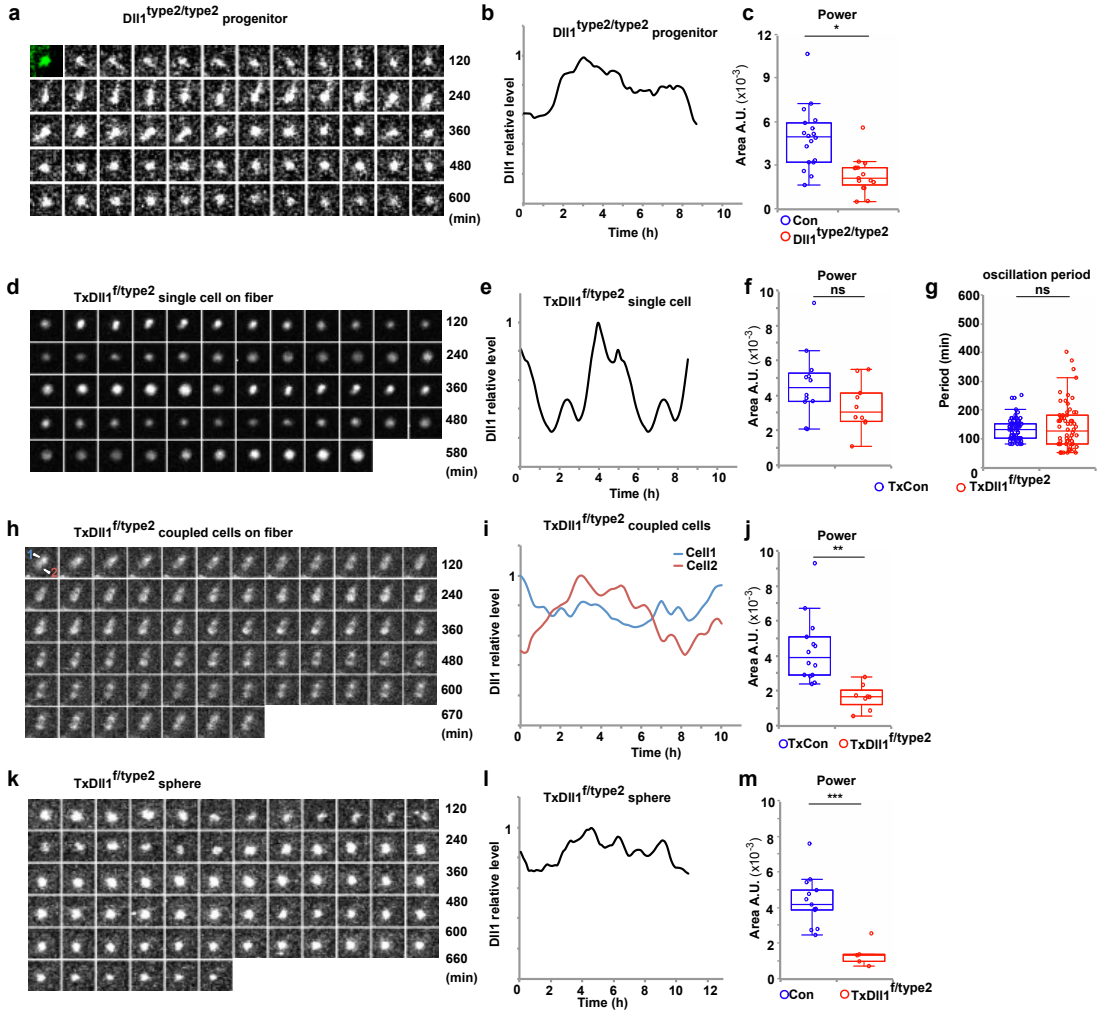

Fig 3.22. Dll1 expression dynamics in *Dll1*$^{type2/type2}$ muscle progenitors and *Dll1*$^{f/type2}$ muscle stem cells

(a) Dynamic luciferase signals in muscle stem cells of a cultured slice from a *Dll1*$^{type2/type2}$ embryo (E11.5). (b) Quantification of the signal. (c) Quantification of the oscillatory stability (power of FFT) in cells from control (Con, blue) and *Dll1*$^{type2/type2}$ (red) animals; n=3. (d) Bioluminescence images observed in a single *Dll1*type2 mutant muscle stem cell associated with a myofiber. (e) Quantification of this bioluminescence signal; the fiber and associated stem cell were obtained from a *TxDll1*$^{f/type2}$ animal. (f) Quantification of the oscillatory stability (power of the Fast Fourier transformation). (g) Quantification of the oscillatory period of luciferase bioluminescence in control and *Dll1type2* mutant cells; n = 10. (h) Bioluminescence images observed in two *Dll1type2* mutant muscle stem cells contacting each other on a cultured myofiber. (i) Quantification of the bioluminescence signals in each of the two cells (signals from cell 1 and 2 in (h) are shown in blue and red, respectively). (j) Quantification of the oscillatory stability (power of the Fast Fourier transformation) of luciferase bioluminescence in coupled control and *Dll1type2* mutant cells (right); n = 4. (k) NanoLuc

bioluminescence signals in a cell located in a sphere of *Dll1type2* mutant cells; one cell co-transfected with an nGFP and EpDll1-NanoLuc expression plasmid was monitored. (l) Quantification of the Nanoluc signals in the transfected cells in a sphere of *Dll1type2* mutant cells. (m) Quantification of the oscillatory stability (power of the Fast Fourier transformation) in sphere cultures of *Dll1type2* mutant cells (right); n = 5 animals. In the box plot, center lines show the medians; box limits indicate the 25th and 75th percentiles; whiskers extend 1.5 times the interquartile range. * P<0.05, ** P<0.01, *** P<0.001, ns indicates P > 0.05, unpaired two-sided t-test.

To further investigate the role of the transcription delay time in cell-cell coupling mediated by Notch signaling, I directly assessed how oscillations are affected in mixed cultures of wild type and *TxDll1$^{f/type2}$* cells. For this I generated chimeric spheres containing wildtype and *TxDll1$^{f/type2}$* mutant cells. When a small ratio (1:50) of wild type cells that had been transfected with the EpDll1-NanoLuc and nGFP expression plasmids were mixed into the *TxDll1$^{f/type2}$* cell population, the wild-type cells showed normal oscillation of the Nanoluc reporter. Neither the oscillatory stability nor the period was changed. Moreover, when a small ratio (1:50) of transfected *TxDll1$^{f/type2}$* cells were mixed into a wild type population, the Nanoluc reporter oscillates with normal stability and period (Fig 3.23).

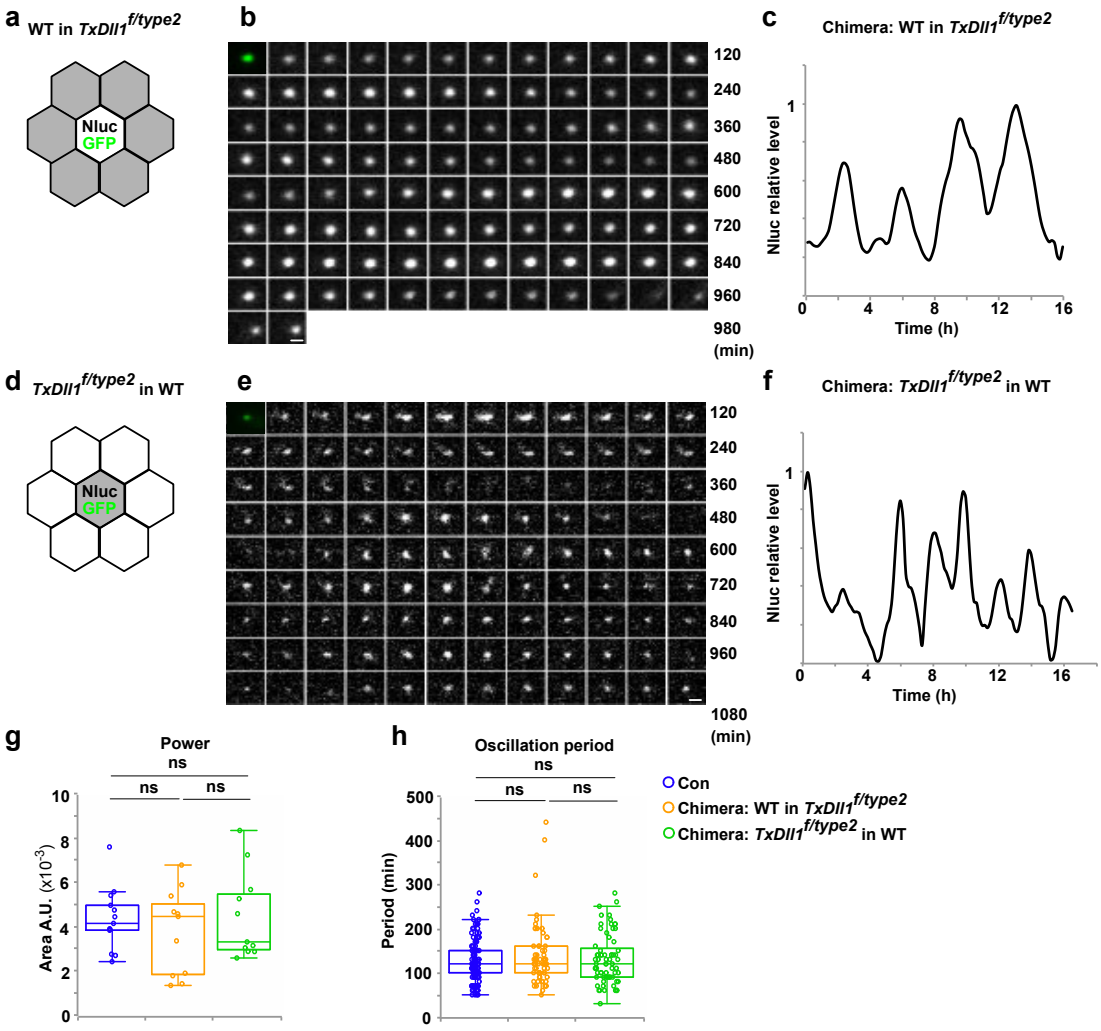

Fig 3.23. Effect of *Dll1type2* mutation on oscillatory expression dynamics in chimeric myospheres

(a) Schematic picture of a chimeric sphere showing one wild type cell (white hexagon) surrounded by *TxDll1*$^{f/type2}$ cells (grey hexagons). Nluc/GFP indicates the wildtype cell transfected with EpDll1-NanoLuc and nGFP expression plasmids. (b) Dynamic Nanoluc signals in a wildtype cell surrounded by *TxDll1*$^{f/type2}$ cells. (c) Quantification of these signals. (d) Schematic picture of a chimeric sphere showing one *TxDll1*$^{f/type2}$ cell (grey hexagon) that is transfected with EpDll1-NanoLuc and nGFP plasmids (Nluc/GFP) and that is surrounded by wildtype cells (white hexagons). (e) Example of dynamic Nanoluc signals in a *TxDll1*$^{f/type2}$ cell surrounded by wildtype cells. (f) Quantification of these signals. (g) Quantification of the oscillatory stability. (h) Quantification of the oscillatory period in sphere cultures. Compared are spheres containing only wildtype cells (Con: blue) and two chimeric situations, a wildtype cell surrounded by *Dll1*type2 cells (wt in *TxDll1*$^{f/type2}$: yellow), and a *Dll1*type2 cell surrounded by wildtype cells (*TxDll1*$^{f/type2}$ in wt: green); n=11. In the box plot, center lines show the medians; box limits indicate 25th and 75th

percentiles; whiskers extend 1.5 times the interquartile range. ns indicates P>0.05, unpaired two-sided t-test.

Taken together, the *Dll1type2* mutation interferes with stable oscillations in coupled cells, but does not affect the expression level of Dll1 or Notch target genes. In contrast, when *Dll1type2* mutant cells are mixed with wild type cells, they still express Dll1 in an oscillatory manner.

3.5. Dampened oscillations in muscle progenitors and stem cells impair muscle development and regeneration

3.5.1. Dampened oscillations affect muscle development

To investigate the function of Dll1 oscillation in muscle development, I used homozygous *Dll1type2* mutant embryos. The mutant embryos are not born because of severe deficits. Obviously, they have a shorter tail. Muscle progenitor and stem cells originate from somites. Since *Dll1type2* mutant mice have a severe defect in somite formation, it was necessary to test whether muscle progenitor cells are correctly generated and migrate to the limbs. I detected Pax3 and Pax7 positive cells using immunohistochemistry in the myotomes and limbs of E11.5 wild-type embryos. Similarly, Pax3 and Pax7 positive cells were also present in the myotomes and limb of *Dll1type2* mutant embryos, indicating that these skeletal muscle progenitors can migrate and are properly generated (Fig 3.24).

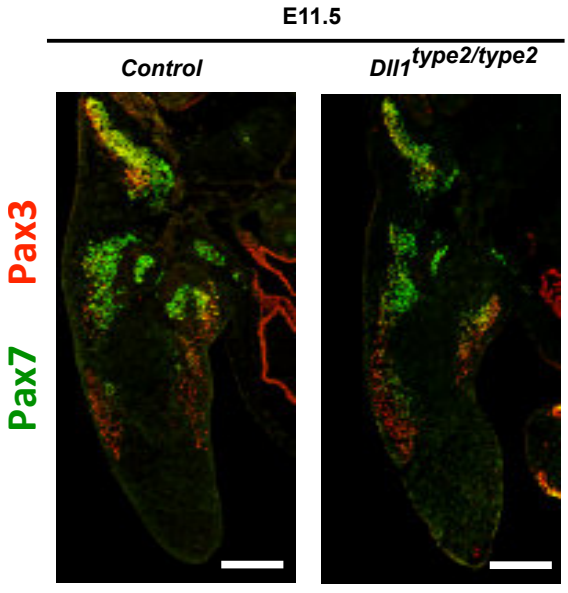

Fig 3.24. The effects of Dll1 oscillations on early limb development

Immunohistological analysis of the limb muscles of control and *Dll1*$^{type2/type2}$ mutant mice at E11.5 using the indicated antibodies. Myogenic progenitor cells were stained with Pax3 (Red) and Pax7 (Green) antibodies. Scale bars, 200 μm

However, less Pax7 expressing cells were detected in developing mutant skeletal muscles at E14.5. Interestingly, I found no evidence for decreased proliferation (EdU incorporation) in mutant muscle progenitor cells (Pax7+ cells) at this stage. However, the ratio of MyoG+ to Pax7+ cells in the mutant limbs was increased. Thus, myogenic progenitor cells differentiated in an uncontrolled and premature manner, indicating that this caused the reduction in the number of muscle progenitor cells. Eventually, this resulted in a very severe reduction of muscle progenitor cell numbers, and the formation of small muscles at E17.5 (Fig 3.25).

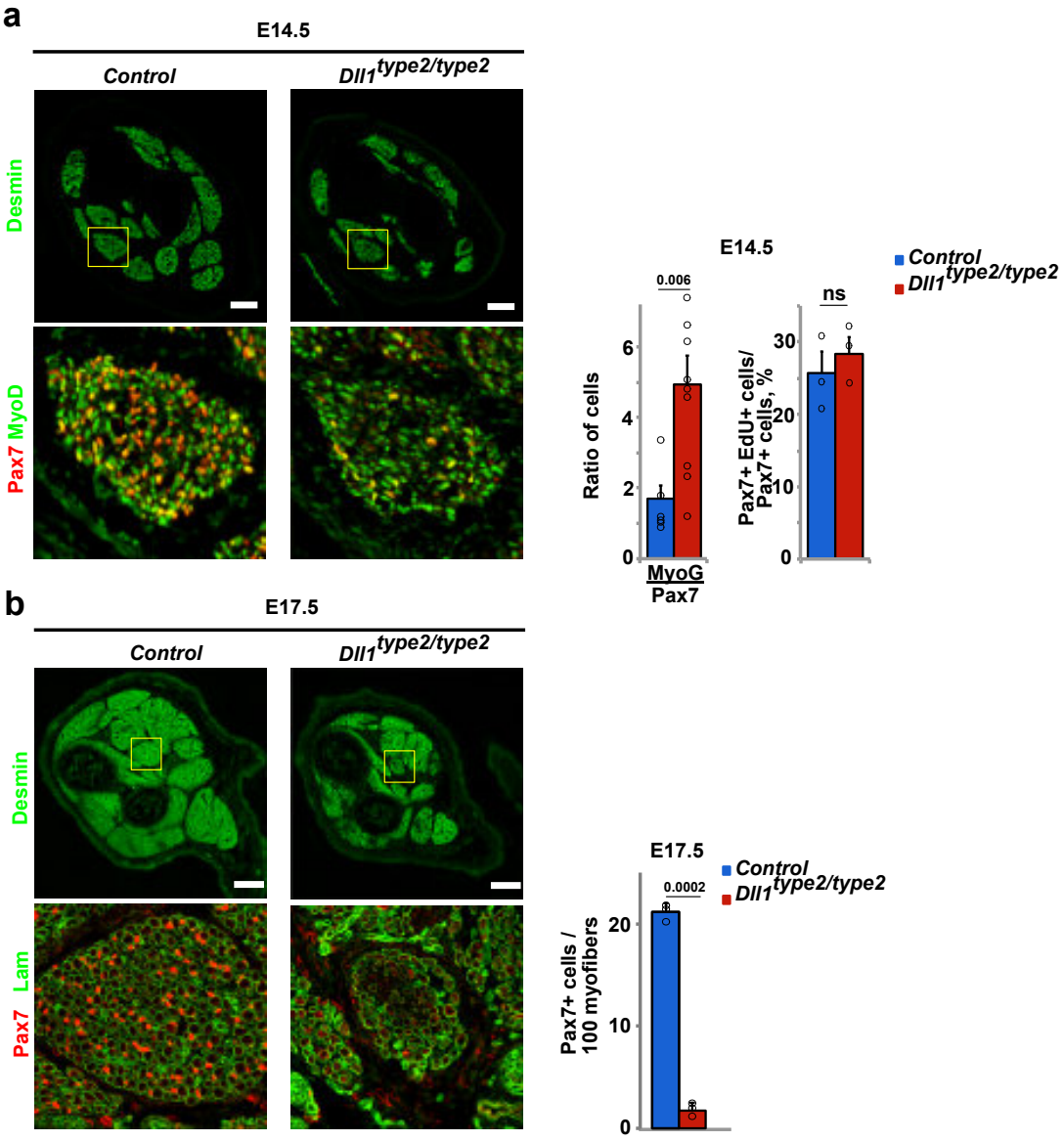

Fig 3.25. The effects of the loss of Dll1 oscillation on muscle growth in fetal development

(a) Immunohistological analysis of the limb muscles of control and *Dll1*$^{type2/type2}$ mutant mice at E14.5 using the indicated antibodies: Pax7 (Red), Desmin (Green) and MyoD (Green). The ratio of MyoG+/Pax7+ cells and the quantification of the proliferation of Pax7+ cells (EdU incorporation into Pax7+ cells) is shown to the right (n = 3). (b) Immunohistological analysis of limb muscles from control and *Dll1*$^{type2/type2}$ mutant mice at E17.5 using the indicated antibodies: Pax7 (Red), Desmin (Green) and Laminin (Green). Quantification of the number of Pax7+ cells in the muscle is shown at the right (n = 3). Scale bars, 100 µm (a) and 200 µm (b). Data are presented as mean values ± SEM. Exact p values are indicated, ns indicates P > 0.05, unpaired two-sided t-test.

3.5.2. Loss of oscillations in muscle stem cells affects muscle regeneration

Next, I assessed the functional consequences of the loss of Dll1 oscillations in cultured floating myofibers and in myospheres *in vitro*. In floating myofibers from *TxCon* and *TxDll1*$^{f/type2}$ animals that were cultured for 60h, the stem cell colonies associated with the myofibers contained similar numbers of cells. However, after 72h of culture, the number of cells in colonies was smaller on *TxDll1*$^{f/type2}$ fibers. A higher percentage of MyoG+ cells and lower percentage of Pax7+ cells were observed in the colonies (Fig. 3.26 a,b). Thus, the cells differentiated prematurely and expressed MyoG, which is associated with a cell cycle exit.

Also in sphere cultures, *TxDll1*$^{f/type2}$ mutant cells showed higher propensity to differentiation than wild-type cells, as assessed by the percentage of MyoG+ and Pax7+ cells present (Fig. 3.26 c). However, the differentiation of *TxDll1*$^{f/type2}$ mutant cells was suppressed by the presence of wild type cells in chimeric spheres, which correlated with the rescue of oscillatory behavior observed in these chimeric conditions (Fig 3.26 d). Thus, not only the presence of Dll1 but also its expression dynamics determines the balance between self-renewal and differentiation of coupled muscle stem cells in culture.

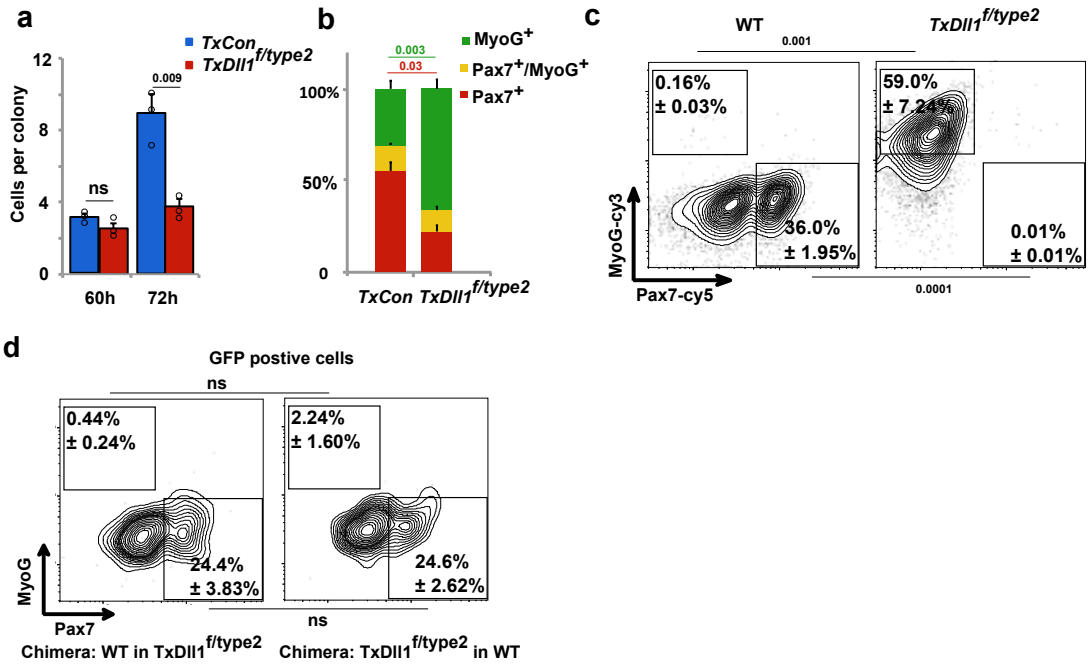

Fig. 3.26. The effects of the *Dll1*type2 mutation on differentiation of cells in cultured muscle stem cells associated with myofibers and cultured muscle stem cells in spheres

(a) Quantification of the number of cells in colonies formed on myofibers; myofibers were isolated from *TxCon* (blue bars) and *TxDll1*$^{f/type2}$ mice (red bars) and cultured for 60 and 72 h; n = 3. (b) Quantification of cells that express MyoG+ only (green), MyoG+ and Pax7+ (yellow), and Pax7+ only (red) in colonies associated with myofibers after 72 h of culture; fibers were isolated from *TxCon* and *TxDll1*$^{f/type2}$ mice; n = 3. (c) Gating strategy and representative FACS plot used to define MyoG+ (MyoG-cy3) and Pax7+ (Pax7-cy5) cells in cultured spheres containing wild-type (WT) and *Dll1*type2 mutant cells; n = 3. (d) FACS gating used for the quantification of MyoG+ and Pax7+ cells in cultured chimeric spheres containing either (left) GFP-positive wildtype cells surrounded by GFP-negative *Dll1*type2 mutant cells or (right) GFP+ *Dll1*type2 mutant cells surrounded by GFP-negative wildtype cells. n=3. Data are presented as mean values ± SEM. Exact p values are indicated, ns indicates P > 0.05, unpaired two-sided t-test.

Next, I assessed the consequences of the *Dll1type2* mutation in the regenerating muscle *in vivo*. The ratio of MyoG+ to Pax7+ cells in the early regenerating muscle of *TxDll1*$^{f/type2}$ mice was increased compared to control mice. However, the proliferative capacities of Pax7+ muscle stem cells were unchanged. Moreover, while average Hes1 protein levels were similar in Pax7+

cells of control and mutant muscle, the Hes1 variance was larger in coupled control than coupled *Dll1type2* mutant cells, suggesting that the Hes1 oscillation was affected because of impaired cell-cell communication in the mutant mice (Fig 3.27 a). At later stages of regeneration, a severe depletion of Pax7+ cells was observed in *TxDll1$^{f/type2}$* mutants. Newly formed myofibers contain fewer nuclei at 7 dpi and 21 dpi, and the fiber diameters were significantly smaller at 21 dpi (Fig 3.27 b).

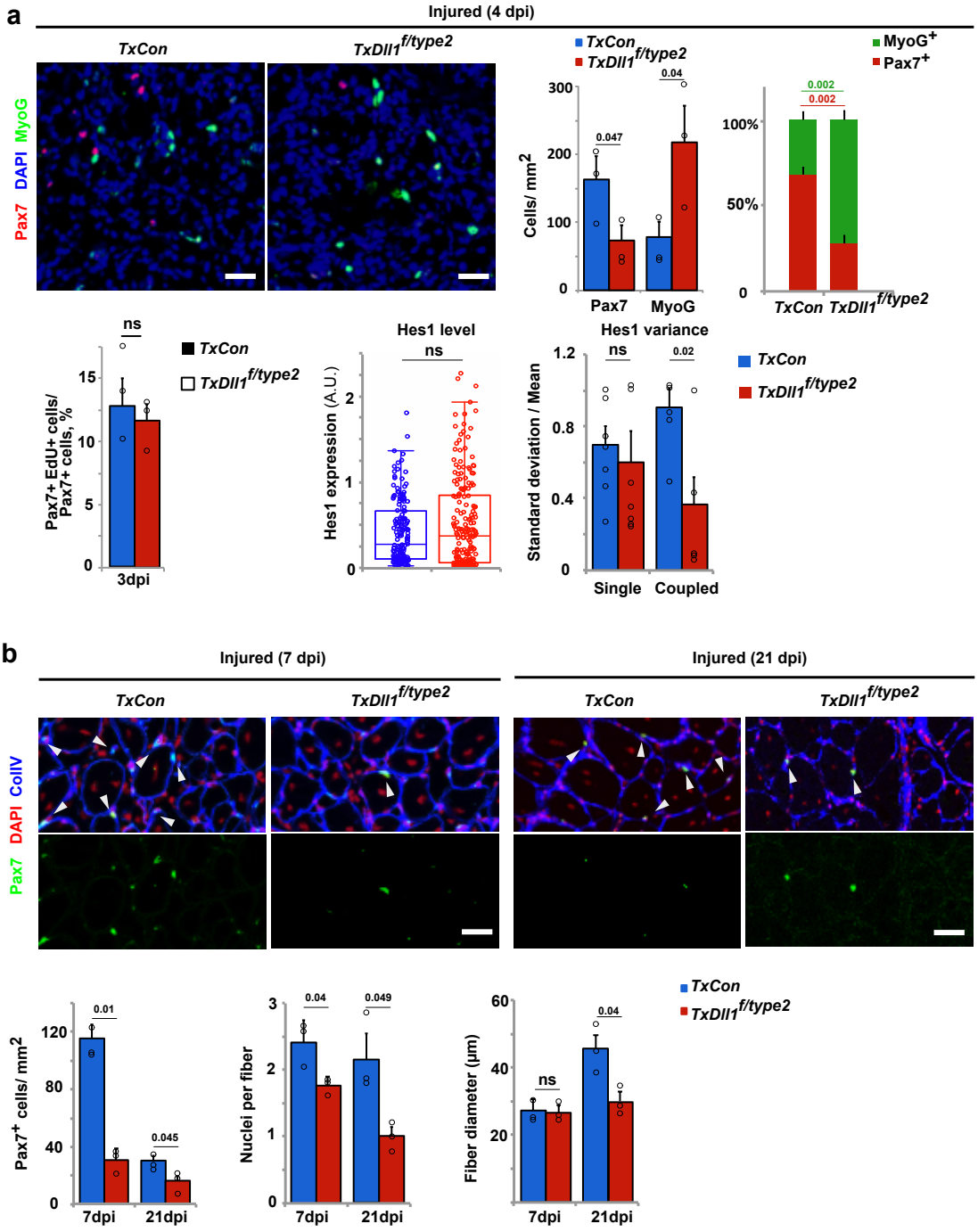

Fig 3.27. The effects of dampened Dll1 oscillation on muscle regeneration

(a) Immunohistological analysis of the regenerating muscle of *TxCon* and *TxDll1f/type2* mutant mice at 4 dpi using anti-Pax7 (red) and anti-MyoG (green) antibodies; DAPI (blue) was used as counterstain (upper left). Quantifications of the number of Pax7+ and MyoG+ cells in *TxCon* (blue bars) and *TxDll1f/type2* (red bars) muscle, and relative proportion of MyoG+ (green) and Pax7+ (red) cells in *TxCon* and *TxDll1f/type2* muscle (upper right). Quantification of the proliferation of Pax7+ cells (assessed by EdU incorporation) at an early stage of muscle injury (3 dpi) in control (*TxCon*, blue bar) and *TxDll1f/type2* (red bar) mice; n=3. Quantification of Hes1 expression levels in Pax7+ cells and variance of Hes1 protein levels in single and coupled Pax7+ cells of the regenerating muscle (4 dpi) of *TxCon* (blue bars) and *TxDll1f/type2* (red bars) animals (lower panels); n = 3. (b) Immunofluorescence analysis of *TxCon* and *TxDll1f/type2* mutant mice at 7 and 21 dpi using anti-Pax7 (green) and anti-collagen IV (ColIV; blue) antibodies; DAPI (red) was used as counterstain (upper panels). Quantification of the number of Pax7+ cells, number of nuclei/fiber and fiber diameter in the regenerating muscle of *TxCon* (blue bars) and *TxDll1f/type2* (red bars) mice at 7 and 21 dpi (lower panels); n = 3. Scale bars, 50 μm. Data are presented as mean ± SEM. Exact p values are indicated, ns indicates $P > 0.05$, unpaired two-sided t-test.

Taken all together, the balance between self-renewal and differentiation of coupled muscle stem cells during muscle regeneration depends on the oscillatory input of the Dll1 signal, and the mere presence of Dll1 does not suffice to ensure the correct balance.

4. Discussion

In muscle development and regeneration, the balance between differentiation and self-renewal of stem cells is important to maintain muscle stem cell numbers. The Notch pathway is recognized to control this balance and therefore the maintenance of muscle stem cells. Ablation of *Rbpj* or *Hes1* in adult muscle stem cells of mice impaired muscle regeneration, and resulted in smaller muscle as well as a pronounced loss of Pax7+ muscle stem cells, suggesting that Notch signaling is active during regeneration (Lahmann et al., 2019; Vasyutina et al., 2007). However, which of the Notch ligands plays a role during the process, and whether the dynamics of Notch signaling is important was unclear when I started this study.

In my work, I showed that Dll1 is expressed in activated and differentiating muscle stem cells, but not quiescent stem cells and myofibers. I observed that Dll1 expressed by muscle stem cells has an important role in muscle regeneration. Moreover, I found that Dll1 oscillates in muscle progenitors and activated stem cells. Hes1 and MyoD are also expressed in an oscillatory manner in such cells, and I analyzed whether one of these factors drives the Dll1 oscillations. My results showed that the Dll1 oscillations are mainly regulated by Hes1 which acts as an oscillatory pacemaker. The other oscillatory factor, MyoD, controls Dll1 expression levels but has no effect on the oscillatory stability or period of Dll1. Finally, I found that dampening of Dll1 oscillations impairs muscle development and regeneration. Thus, Hes1, MyoD and Dll1 form an oscillatory network that functions in the maintenance of the muscle progenitor and stem cell pool, and has thus very important roles in normal muscle growth and regeneration.

4.1. Tools for the analysis of Dll1 oscillations

Methods like in situ hybridization and immunostaining can supply a snapshot of transcripts and protein expression in fixed tissues and cells. For the analysis

of gene expression dynamics, live imaging is necessary. Because of the short period (2-3 hours) of Dll1 oscillations, the reporter requires the following characteristics: a fast maturation rate, a fast degradation rate and sufficient sensitivity. Some fluorescent proteins were used to analyze oscillations (Elowitz and Leibler, 2000; Sonnen et al., 2018; Yoshioka-Kobayashi et al., 2020). However, the dynamic range of fluorescent proteins is small, which results in less detail when the expression dynamics is analyzed. Moreover, muscle fibers have a relatively high autofluorescence, which makes the use of fluorescent proteins in the muscle problematic.

Here, I used a luciferase, Nanoluc, to analyze Dll1 expression in cultured primary cells. To destabilize the Nanoluc protein, I fused it with a mutant form of ubiquitin (UbG76V), which accelerates proteolysis of the reporter (Dantuma et al., 2000). Moreover, to destabilize *Nanoluc* mRNA, I used the *Dll1* 3'UTR which regulates the half-life of the *Dll1* mRNA (Isomura et al., 2017). The whole construct was driven by the *Dll1* promoter and enhancer. Bioluminescence signals showed oscillations, indicating that *Dll1* expression oscillates in muscle stem cells.

To analyse Dll1 protein dynamics, I used the Dll1-luc knock-in allele. In this allele, the firefly luciferase cDNA was inserted into the *Dll1* gene so that a Dll1-luc fusion protein was expressed. The homozygous *Dll1-luc* mice displayed slight segmentation deficits that manifest in a short tail but no apparent abnormality in body vertebrae or ribs. I tested whether this allele impairs myogenesis. In homozygous *Dll1-luc* and wildtype mice, I found similar numbers of muscle stem cells, indicating that the allele does not affect myogenesis. Thus, I was able to use muscle stem cells from heterozygous *Dll1-luc* mice to track the oscillatory bioluminescence signal in muscle stem cells over prolonged time periods.

Several methods allow the quantification of oscillatory stability. A commonly used one is Fast Fourier transformation (FFT). It allows to transform the periodical information from time domains to frequency domains. I used FFT to

analyze luciferase tracks of cells that had been followed for at least 10 hours with 1/600 Hz of sampling frequency. The dominant frequency can be identified as a peak. The area under the peak corresponding to periods between 1.5 and 3.75h were calculated as power. With statistical analyses, I was able to distinguish normal oscillations and random fluctuations. Because of the low resolution of FFT in the frequency domain, I determined the period as the average of time between two oscillatory peaks. This allowed me to compare the oscillatory period observed under different conditions (e.g. developing and adult MuSC, different culture conditions).

4.2. The oscillatory network identified in myogenic cells

Hes1 can bind its own promoter and suppress its own expression (Sakagami et al., 1994). This negative feedback allows the generation of an oscillator. Hes1 can form homo- or heterodimers with other bHLH proteins such as Hey1 (Iso et al., 2001), and monomers are less stable than homodimers. Such a nonlinear regulation is also necessary for a gene oscillator. Both of Hes1 mRNA and protein are unstable and possess short half-lives. Previous reports demonstrated that instability of Hes1 is critical for its oscillation (Hirata et al., 2002; Kobayashi et al., 2015). Indeed, Hes1 oscillates in a stable manner in myogenic cells and other cell types (Imayoshi et al., 2013; Lahmann et al., 2019). Previous data showed that a null mutation of *Hes1* abolished MyoD oscillations (Lahmann et al., 2019). I showed that ablation or siRNA knock-down of *Hes1* abolished Dll1 oscillations, and instead I observed only random Dll1 fluctuations. Thus, I conclude that Hes1 is the pacemaker for the oscillation of Dll1 and of other genes in activated muscle stem cells.

MyoD is a myogenic determination factor. Its oscillatory expression in activated muscle stem cells allows a balance between self-renewal and differentiation (Lahmann et al., 2019). MyoD can orchestrate the expression of a broad set of genes to regulate myogenesis. In the frog, MyoD is a direct and positive regulator of *Delta-1* (Wittenberger et al., 1999). *MyoD*-/-;*Myf5*-/- mouse embryo fibroblasts transfected with MyoD-ER (a MyoD protein fused to

the estrogen receptor, ER) and treated with beta-estradiol display increased *Dll1* expression, suggesting that differentiating muscle stem cells, which express higher MyoD, might inhibit adjacent cells from differentiation by activating the Notch pathway in neighboring cells via up-regulating *Dll1* (Bergstrom et al., 2002). In my work, I identified an enhancer in the fourth intron of the *Dll1* gene which can be directly bound by MyoD. *MyoD* ablation in isolated primary muscle stem cells resulted in increased *Myf5* and decreased *Dll1* transcription. Although it was suggested that Myf5 may up-regulate Dll1 (Kuang et al., 2007), the increased *Myf5* expression did not suffice to rescue *MyoD* ablation. Thus, MyoD regulates the expression level of Dll1 in muscle stem cells. However, neither the stability nor the period of Dll1 oscillations were significantly different in *MyoD*-/- muscle stem cells. The only small difference was in the distribution of time between two peaks of Dll1 expression, which was more variable in *MyoD*-/- muscle stem cells than in control cells, suggesting that the noise in the oscillations increases when *MyoD* is lacking. Therefore, the most obvious function of MyoD was the positive control of Dll1 expression levels, but MyoD has also a role related to noise resistance. In general, gene expression can fluctuate, and such noise is more prone to affect genes expressed at low levels than strongly expressed genes (Vilar et al., 2002). Thus, the positive regulation results in a fast transcriptional switch, which allows transcription rate to change very fast from low to high levels and that allows a robust expression. In this way, the time in which low expression is prone to fluctuations is largely reduced.

Taken together, my work shows that Hes1 acts as a pacemaker for Dll1 oscillations, while MyoD does not affect Dll1 oscillations but up-regulates Dll1 to allow robust expression.

4.3. Transcriptional delays and their role in oscillatory gene expression

Oscillatory expression driven by negative feedback was first predicted to exist by a mathematical model, the Goodwin model (Goodwin, 1965). In this model, in addition to the oscillating mRNA and protein, at least one oscillatory intermediate component exists (Griffith, 1968). The single-cell ordinary differential equation models for Hes1 and MyoD also required an unidentified intermediate in the feedback loop (Lahmann et al., 2019). In these models, transcription and translation were assumed to occur at the same time, and the time needed for these processes was not considered. However, considerable time is needed for transcription, splicing and other processing steps, for protein production, modifications (e.g. glycosylation), and transfer to the plasma membrane or other subcellular compartments. In the delay time model, oscillations occur if the delay between transcription and protein production pass a critical value (Smolen et al., 2000a, b). For instance, intron deletion of *Hes1* and *Hes7* shortens the transcription delay time because less time is needed to complete transcription of the genes; this abolished the oscillations of Hes1 and Hes7 (Ochi et al., 2020; Takashima et al., 2011). Longer delays in the feedback loop result in an increased oscillatory period (Swinburne et al., 2008). One example for this is the Hes7 oscillation in cells of the human presomitic mesoderm that display a 5 hour period, which is longer than the one in the presomitic mesoderm of the mouse (2-3 hours). A reason for this is the longer delay time in human cells due to the generally slower biochemical reaction speed (Matsuda et al., 2020a). Thus, the delay time is an important determinant for oscillatory stability and period.

In coupled cells, the one cell with higher Dll1 levels is thought to signal to the neighboring cell expressing Dll1 at lower levels (Sprinzak et al., 2010). Since Dll1 oscillates in muscle stem cells, the dynamics of Dll1 in a coupled receiver and sender switch periodically. The proper delay in such coupled cells has been analyzed in cells with asynchronous, synchronous and dampened oscillations that were generated using optogenetic methods (Shimojo et al., 2016; Yoshioka-Kobayashi et al., 2020). I observed an anti-phase oscillation of Dll1 in coupled muscle stem cells. This differs from the in-phase oscillation of Dll1 in the presomitic mesoderm (Aulehla, 2017; Aulehla and Pourquie, 2006, 2008).

One possible explanation for the different modes of oscillation of neighboring cells is a difference in the time needed for the signal transmission of Dll1-Notch in the two cell types. Lfng, a glycosylase, modifies Dll1 and Notch and regulates their activities (Panin et al., 2002). Lfng is essential for the synchronized oscillation in coupled presomitic mesoderm cells (Okubo et al., 2012; Yoshioka-Kobayashi et al., 2020). However, Lfng is expressed at low levels in the muscle. The presence/absence of Lfng-modifications in the two cell types may change coupling delays in Dll1-Notch signal transmission and result in different oscillation phase states in the two cell types.

In my experiments I used the *Dll1type2* allele that increases the coupling delay due to an increased time needed for transcription (Shimojo et al., 2016). The *Dll1type2* mutation abolished Dll1 oscillations. Mathematical modeling performed by Katarina Baum and Jana Wolf at the MDC using a the coupled-cell delay differential equation model predicted that this increases the coupling delay between the oscillators in chimeric situations in which one wildtype and one *Dll1type2* cell are coupled and communicate with each other, and that this will dampen the oscillatory amplitude but not abolish oscillations. Indeed, I still observed oscillations in such chimeric situations, which demonstrates that oscillations are only abolished when the changes in the delays surpass a critical value.

It was previously reported that elongation of *Dll1* transcription time in the *Dll1ki* allele led to segmentation defects and impaired myogenesis (Schuster-Gossler et al., 2007). In the *Dll1type2* allele, *Dll1* and *luciferase* cDNAs were inserted into the first exon, whereas in the *Dll1ki* allele only *Dll1* cDNA (and a sequence that allows polyadenylation) was inserted into the first exon. This led to a shorter transcription time of the *Dll1ki* than the *Dll1type2* allele. The amplitude of Dll1 oscillation can therefore be expected to be less quenched in *Dll1ki*. Of note, the phenotype in $Dll1^{ki/lacZ}$ mice is stronger than that the one in *Dll1type2* mice, not only because of the quenched amplitude but also because of low Dll1 expression levels (Schuster-Gossler et al., 2007).

4.4. Notch signaling in the muscle stem cell niche

Notch signals prevent differentiation of muscle progenitor and stem cells, which was first studied in cultured C2C12 cells and primary muscle stem cells (Delfini et al., 2000; Kopan et al., 1994; Kuroda et al., 1999; Mourikis et al., 2012; Shawber et al., 1996). Experiments that relied on mouse genetics also revealed that Notch signaling suppresses myogenic differentiation and controls self-renewal of muscle progenitor and stem cells (Brohl et al., 2012; Vasyutina et al., 2007). Mechanistically, this is mediated by the induction of the well-known target genes, the members of the Hes/Hey family. Hes/Hey in turn suppress myogenic differentiation factors, e.g. Hey1 suppresses *MyoG* and Hes1 suppresses *MyoD* (Buas et al., 2010; Lahmann et al., 2019; Shawber et al., 1996). Moreover, Hes1 was shown to compete with MyoD binding to regulatory sequences, thereby repressing p57 and p21 induction which is required for cell cycle exit and terminal myogenic differentiation (Reynaud et al., 2000; Zalc et al., 2014). The Notch-dependent suppression of differentiation is observed in myogenesis during development and in adult muscle regeneration. However, Notch has a second function in the adult where it also controls the quiescence of muscle stem cells. Thus, when Notch signaling is ablated in quiescent muscle stem cells, they quickly become activated and enter the cell cycle (Mourikis et al., 2012; van Velthoven et al., 2017). In the adult, the two functions of Notch in quiescence and differentiation are elicited by distinct Notch ligands.

The ligand that allows quiescence of the muscle stem cells appears to be produced by myofibers. Thus, Dll4 produced by myofibers plays an important role in the quiescence of muscle stem cells (Eliazer et al., 2020). Single cell RNA sequencing had shown that differentiating muscle stem cells express *Dll1* (Yartseva et al., 2020). In my study, I observed that Dll1 is expressed not only by differentiating but also by activated muscle stem cells. However, in myofiber and quiescent muscle stem cells, I could not detect Dll1. Moreover, I showed that this ligand allows the self-renewal of the muscle stem cells. Thus, when I ablated *Dll1* specifically in adult muscle stem cells, the cells were unable to self-

renew during regeneration because Dll1 provided by activated and differentiating muscle stem cells suppressed differentiation of neighboring muscle stem cells. However in the uninjured muscle, the stem cells do not contact each other. In such a situation *Dll1* ablation had no effect on muscle stem cells. Thus, Dll1 from muscle stem cells is an important source of Notch ligands that is needed in a regenerative situation or during muscle development where muscle stem cells contact each other.

I showed in this study that the mere presence of Dll1 in muscle stem cells does not suffice to correctly regulate myogenesis in development and regeneration. Instead, the Dll1 expression dynamics is also important. For this I used the *Dll1type2* mutation in which the transcription delay is lengthened. The mutation interferes with Dll1 oscillations in situations where muscle stem cells contact each other, e.g. in communities of muscle stem cells in culture or during developmental and regenerative myogenesis *in vivo*. I suggest that incorrect timing of Dll1-mediated input quenches the Hes1 amplitude in such cell communities, and thus interferes with the stable oscillations of the entire network. This is supported by the fact that the variance of Hes1 expression levels was larger in control than in mutant cell communities, but similar in isolated cells of both genotypes. Despite the fact that the *Dll1type2* mutation has pronounced effects on developmental and regenerative myogenesis, a null mutation of *Dll1* results in even more severe phenotypes. Thus, the sustained Dll1 produced in *Dll1type2* mutants retains a partial function.

4.5. Factors regulating oscillations

Several pathways are known to cooperate with Notch to regulate oscillations related to the Notch pathway. For example, Notch oscillations need enough Notch signaling to trigger the oscillation. Weak Notch signaling induces oscillations only when Yap signaling is low, indicating that Yap signaling controls the excitability threshold of Notch (Hubaud et al., 2017). Also, serum factors can regulate Hes1 expression (Masamizu et al., 2006). Here, I used low serum medium for the culture of muscle stem cells associated with myofibers.

Higher serum concentration increased the migratory behavior of muscle stem cells and increased proliferation, which made it more difficult to follow the cells and their expression dynamics. Moreover, higher serum concentrations (20%) in slice culture resulted in more noise in Dll1-luc oscillations (data not shown).

The FGF pathway is important for muscle stem cell growth, and is also known to regulate oscillations of Hes1 and Hes7 in the presomitic mesoderm (Diaz-Cuadros et al., 2020; Nakayama et al., 2008). In my experiments, I added bFGF to the culture medium for isolated muscle stem cells culture, with the goal to promote proliferation of the muscle stem cells and to prevent differentiation. A number of distinct signaling pathways are activated by FGF, including p38, ERK/MAPK, PI3K, and Akt (Brewer et al., 2016). Activation of p38 and ERK/MAPK are required for satellite cell activation, MyoD induction and terminal differentiation (Jones et al., 2005; Perdiguero et al., 2007a; Perdiguero et al., 2007b). Whether the FGF pathway regulates Hes1/Dll1/MyoD oscillations in muscle stem cells might be the subject of future research.

4.6. Outlook

Expression dynamics such as oscillations, pulses and fluctuations, encode information in various cell types and result in different biological outcomes (Li and Elowitz, 2019). For example, oscillatory or sustained Ascl1 expression determines whether neural progenitors will retain their proliferative capacity or differentiate (Imayoshi et al., 2013). However, how the cells decode these differences of the signals is not well known. The yeast transcription factor Msn2 exhibits oscillatory translocations to the nucleus under glucose starvation (Hao and O'Shea, 2012). Individual promoters can serve as discrete signal-processing modules and decode the dynamics of the transcription factor. According to their reactions to the Msn2 input, the promoters can be classified as HS promoters (high amplitude threshold and slow promoter activation) and LF promoters (low amplitude threshold and fast promoter activation) (Hansen and O'Shea, 2013). In myogenic cells, MyoD oscillates in activated muscle stem

cells and the cells can proliferate. In contrast, sustained MyoD induces exit from cell cycle and differentiation of muscle stem cells. MyoD can bind to the promoters of cell cycle genes, such as the *Ccnd1* gene encoding Cyclin D1, and to the promoter of *MyoG* that controls terminal differentiation (Cao et al., 2010). Interestingly, without the chromatin remodeling enzymes SWI/SNF, MyoD can not induce terminal muscle differentiation (de la Serna et al., 2001). It is possible that nucleosome remodeling participates in decoding the expression dynamics of transcription factors and allows the different cellular reaction in response to oscillatory or sustained MyoD.

5. Summary/ Zusammenfassung

5.1. Summary

Dll1 is a ligand that mediates Notch signals and is provided by sender cells, such as muscle stem cells. The experiments performed in this study revealed an important role of Dll1 expression dynamics in muscle development and regeneration. Dll1 protein oscillates and its oscillations are important for maintaining the balance between self-renewal and differentiation of muscle stem and progenitor cells. The function of Dll1 oscillation cannot be replaced by sustained Dll1 expression.

I found that Dll1 was expressed in activated and differentiating muscle stem cells, but that Dll1 is not present in quiescent stem cells or myofibers. To analyze the function of Dll1, I introduced a conditional Dll1 mutation with tamoxifen dependent Pax7creERT2 line. When Dll1 was ablated in adult muscle stem cells, changes in differentiation were only observed in regenerating muscle, i.e. when muscle stem cells were activated and contacted each other.

To observe Dll1 expression dynamics, I used cultures of Dll1-luc muscle progenitor and stem cells. This demonstrated that the expression of Dll1 protein oscillated. Previous data that had shown that also Hes1 and MyoD expression oscillate in activated muscle stem cells. Therefore I investigated whether Hes1 and MyoD regulated Dll1 and Dll1 oscillations. I demonstrated that Hes1 suppressed Dll1 transcription and served as an oscillatory pacemaker for Dll1. In the absence of Hes1, Dll1 no longer oscillated. In contrast, MyoD induced Dll1 transcription, but did not affect Dll1 oscillation.

Finally, I investigated the role of Dll1 expression dynamics. A mutation named Dll1-type2 increased the transcription time because it lengthened the Dll1 gene, but didn't affect the overall Dll1 mRNA levels. Dll1 oscillations were abolished when Dll1-type2 muscle stem cells contacted each other, and instead Dll1 was

expressed in a sustained manner. This resulted in premature differentiation of muscle progenitor and stem cells. Thus, oscillations of Dll1 are important for a correct balance between self-renewal and differentiation of muscle stem cells.

5.2. Zusammenfassung

Dll1 ist ein Ligand, der Notch-Signale vermittelt, der von Senderzellen wie Muskelstammzellen bereitgestellt wird. Die in dieser Studie durchgeführten Experimente zeigten eine wichtige Rolle der Dll1 Expressionsdynamik in der Muskelentwicklung und -regeneration. Die Expression des Dll1-Protein oszilliert in aktivierten Muskelstammzellen, und diese Oszillation ist wichtig für die Aufrechterhaltung des Gleichgewichts zwischen Selbsterneuerung und Differenzierung. Oszillierendes Dll1 kann also nicht durch eine anhaltende Dll1-Expression ersetzt werden.

Ich fand heraus, dass das Dll1-Protein in aktivierten und differenzierenden Muskelstammzellen exprimiert wird, jedoch nicht in ruhenden Stammzellen oder Muskelfasern. Um die Funktion des Dll1-Proteins zu analysieren, führe ich eine induzierbare Dll1-Mutation mit der Tamoxifen-abhängigen Pax7-creERT2-Linie ein. Wurde Dll1 im adulten Muskelstammzellen ablatiert, wurde eine Veränderung der Differenzierungsveränderungen im regenerierten Muskel beobachte. Unter diesen Umständen sind die Muskelstammzellen aktiviert und kontaktieren sich gegenseitig.

Ausserdem untersuchte ich die Expressionsdynamik von Dll1. In Kulturen von Dll1-luc-Muskelvorläufer- und -stammzellen konnte ich zeigen, dass die Expression des Dll1-Proteins oszilliert. Vorarbeiten von anderen hatten auch gezeigt, dass die Expression von MyoD und Hes1 in Muskelvorläufer- und -stammzellen ebenfalls oszilliert. Ich untersuchte deshalb, ob die oszillatorische Expression von Dll1 durch MyoD und Hes1 kontrolliert wird. Ich konnte beobachten, dass Hes1 die Dll1-Transkription reprimiert und als Schrittmacher für die Dll1-Oszillation funktioniert. Im Gegensatz dazu aktivierte MyoD die Dll1-Transkription, beeinflusste jedoch nicht die Dll1-Oszillation. Um die Rolle der Dll1 Expressionsdynamik zu untersuchen, setzte ich eine Mutation namens Dll1-Typ2 ein. Diese Mutation verlängerte die Transkriptionszeit aufgrund der Verlängerung des Gens, hatte jedoch keinen Einfluss auf die Menge der Dll1-mRNA. In Dll1-Typ2-Muskelstammzellen die

sich gegenseitig kontaktieren, konnte ich keine Dll1-Oszillationen beobachten. Stattdessen wurde Dll1 konstant exprimiert. Dies führte zu einer vorzeitigen Differenzierung von Muskelvorläufer- und Stammzellen. Daher ist die Oszillation des Dll1-Ergebnisses wichtig für das Gleichgewicht zwischen Selbsterneuerung und Differenzierung für Muskelstammzellen.

6. References

Ables, J.L., DeCarolis, N.A., Johnson, M.A., Rivera, P.D., Gao, Z.L., Cooper, D.C., Radtke, F., Hsieh, J., and Eisch, A.J. (2010). Notch1 Is Required for Maintenance of the Reservoir of Adult Hippocampal Stem Cells. J Neurosci *30*, 10484-10492.

Andersson, E.R., Sandberg, R., and Lendahl, U. (2011). Notch signaling: simplicity in design, versatility in function. Development *138*, 3593-3612.

Arnold, L., Henry, A., Poron, F., Baba-Amer, Y., van Rooijen, N., Plonquet, A., Gherardi, R.K., and Chazaud, B. (2007). Inflammatory monocytes recruited after skeletal muscle injury switch into antiinflammatory macrophages to support myogenesis. J Exp Med *204*, 1057-1069.

Artavanis-Tsakonas, S., Rand, M.D., and Lake, R.J. (1999). Notch signaling: Cell fate control and signal integration in development. Science *284*, 770-776.

Aulehla, A. (2017). Oscillatory signals controlling mesoderm patterning in vertebrate embryos. Mech Develop *145*, S7-S7.

Aulehla, A., and Pourquie, O. (2006). On periodicity and directionality of somitogenesis. Anat Embryol *211*, S3-S8.

Aulehla, A., and Pourquie, O. (2008). Oscillating signaling pathways during embryonic development. Current Opinion in Cell Biology *20*, 632-637.

Baird, M.F., Graham, S.M., Baker, J.S., and Bickerstaff, G.F. (2012). Creatine-kinase- and exercise-related muscle damage implications for muscle performance and recovery. J Nutr Metab *2012*, 960363.

Basak, O., Giachino, C., Fiorini, E., MacDonald, H.R., and Taylor, V. (2012). Neurogenic Subventricular Zone Stem/Progenitor Cells Are Notch1-Dependent in Their Active But Not Quiescent State. J Neurosci *32*, 5654-5666.

Benedito, R., Roca, C., Sorensen, I., Adams, S., Gossler, A., Fruttiger, M., and Adams, R.H. (2009). The Notch Ligands Dll4 and Jagged1 Have Opposing Effects on Angiogenesis. Cell *137*, 1124-1135.

Bergstrom, D.A., Penn, B.H., Strand, A., Perry, R.L.S., Rudnicki, M.A., and Tapscott, S.J. (2002). Promoter-specific regulation of MyoD binding and signal transduction cooperate to pattern gene expression. Mol Cell *9*, 587-600.

Bessho, Y., Hirata, H., Masamizu, Y., and Kageyama, R. (2003). Periodic repression by the bHLH factor Hes7 is an essential mechanism for the somite segmentation clock. Gene Dev *17*, 1451-1456.

Bessho, Y., Sakata, R., Komatsu, S., Shiota, K., Yamada, S., and Kageyama, R. (2001). Dynamic expression and essential functions of Hes7 in somite segmentation. Gene Dev *15*, 2642-2647.

Bi, P.P., Yue, F., Sato, Y., Wirbisky, S., Liu, W.Y., Shan, T.Z., Wen, Y.F., Zhou, D.G., Freeman, J., and Kuang, S.H. (2016). Stage-specific effects of Notch activation during skeletal myogenesis. Elife *5*.

Biressi, S., Tagliafico, E., Lamorte, G., Monteverde, S., Tenedini, E., Roncaglia, E., Ferrari, S., Ferrari, S., Angelis, M.G.C.D., Tajbakhsh, S.*, et al.* (2007). Intrinsic phenotypic diversity of embryonic and fetal myoblasts is revealed by genome-wide gene expression analysis on purified cells. Dev Biol *304*, 633-651.

Bjornson, C.R.R., Cheung, T.H., Liu, L., Tripathi, P.V., Steeper, K.M., and Rando, T.A. (2012). Notch Signaling Is Necessary to Maintain Quiescence in Adult Muscle Stem Cells. Stem Cells *30*, 232-242.

Bladt, F., Riethmacher, D., Isenmann, S., Aguzzi, A., and Birchmeier, C. (1995). Essential Role for the C-Met Receptor in the Migration of Myogenic Precursor Cells into the Limb Bud. Nature *376*, 768-771.

Blaumueller, C.M., Qi, H.L., Zagouras, P., and ArtavanisTsakonas, S. (1997). Intracellular cleavage of notch leads to a heterodimeric receptor on the plasma membrane. Cell *90*, 281-291.

Bocci, F., Onuchic, J.N., and Jolly, M.K. (2020). Understanding the Principles of Pattern Formation Driven by Notch Signaling by Integrating Experiments and Theoretical Models. Front Physiol *11*.

Brack, A.S., Conboy, I.M., Conboy, M.J., Shen, J., and Rando, T.A. (2008). A temporal switch from Notch to Wnt signaling in muscle stem cells is necessary for normal adult myogenesis. Cell Stem Cell *2*, 50-59.

Braun, T., Rudnicki, M.A., Arnold, H.H., and Jaenisch, R. (1992). Targeted Inactivation of the Muscle Regulatory Gene Myf-5 Results in Abnormal Rib Development and Perinatal Death. Cell *71*, 369-382.

Bray, S., and Bernard, F. (2010). Notch Targets and Their Regulation. Notch Signaling *92*, 253-275.

Bray, S.J. (2006). Notch signalling: a simple pathway becomes complex. Nat Rev Mol Cell Bio *7*, 678-689.

Bray, S.J. (2016). Notch signalling in context. Nat Rev Mol Cell Bio *17*, 722-735.

Brewer, J.R., Mazot, P., and Soriano, P. (2016). Genetic insights into the mechanisms of Fgf signaling. Gene Dev *30*, 751-771.

Bridges, C.B. (1916). Non-Disjunction as Proof of the Chromosome Theory of Heredity (Concluded). Genetics *1*, 107-163.

Brohl, D., Vasyutina, E., Czajkowski, M.T., Griger, J., Rassek, C., Rahn, H.P., Purfurst, B., Wende, H., and Birchmeier, C. (2012). Colonization of the Satellite Cell Niche by Skeletal Muscle Progenitor Cells Depends on Notch Signals. Dev Cell *23*, 469-481.

Brohmann, H., Jagla, K., and Birchmeier, C. (2000). The role of Lbx1 in migration of muscle precursor cells. Development *127*, 437-445.

Brou, C., Logeat, F., Gupta, N., Bessia, C., LeBail, O., Doedens, J.R., Cumano, A., Roux, P., Black, R.A., and Israel, A. (2000). A novel proteolytic cleavage involved in Notch signaling: The role of the disintegrin-metalloprotease TACE. Mol Cell *5*, 207-216.

Buas, M.F., Kabak, S., and Kadesch, T. (2010). The Notch Effector Hey1 Associates with Myogenic Target Genes to Repress Myogenesis. J Biol Chem *285*, 1249-1258.

Cao, Y., Yao, Z.Z., Sarkar, D., Lawrence, M., Sanchez, G.J., Parker, M.H., MacQuarrie, K.L., Davison, J., Morgan, M.T., Ruzzo, W.L.*, et al.* (2010). Genome-wide MyoD Binding in Skeletal Muscle Cells: A Potential for Broad Cellular Reprogramming. Dev Cell *18*, 662-674.

Chedotal, A. (2020). The human segmentation clock rings every five hours. Cr Biol *343*, 7-8.

Christ, B., Brandsaberi, B., Grim, M., and Wilting, J. (1992). Local Signaling in Dermomyotomal Cell Type Specification. Anat Embryol *186*, 505-510.

Christ, B., Jacob, H.J., and Jacob, M. (1977). Experimental-Analysis of Origin of Wing Musculature in Avian Embryos. Anat Embryol *150*, 171-186.

Christ, B., and Ordahl, C.P. (1995). Early Stages of Chick Somite Development. Anat Embryol *191*, 381-396.

Coller, H.A., Sang, L.Y., and Roberts, J.M. (2006). A new description of cellular quiescence. Plos Biol *4*, 329-349.

Conboy, I.M., Conboy, M.J., Smythe, G.M., and Rando, T.A. (2003). Notch-mediated restoration of regenerative potential to aged muscle. Science *302*, 1575-1577.

Conboy, I.M., and Rando, T.A. (2002). The regulation of notch signaling controls satellite cell activation and cell fate determination in postnatal myogenesis. Dev Cell *3*, 397-409.

Cravchik, A., Subramanian, G., Broder, S., and Venter, J.C. (2001). Sequence analysis of the human genome - Implications for the understanding of nervous system function and disease. Arch Neurol-Chicago *58*, 1772-1778.

Czajkowski, M.T., Rassek, C., Lenhard, D.C., Brohl, D., and Birchmeier, C. (2014). Divergent and conserved roles of Dll1 signaling in development of craniofacial and trunk muscle. Dev Biol *395*, 307-316.

D'Souza, B., Meloty-Kapella, L., and Weinmaster, G. (2010). Canonical and Non-Canonical Notch Ligands. Notch Signaling *92*, 73-129.

Dantuma, N.P., Lindsten, K., Glas, R., Jellne, M., and Masucci, M.G. (2000). Short-lived green fluorescent proteins for quantifying ubiquitin/proteasome-dependent proteolysis in living cells. Nat Biotechnol *18*, 538-543.

Darr, K.C., and Schultz, E. (1987). Exercise-Induced Satellite Cell Activation in Growing and Mature Skeletal-Muscle. J Appl Physiol *63*, 1816-1821.

Daston, G., Lamar, E., Olivier, M., and Goulding, M. (1996). Pax-3 is necessary for migration but not differentiation of limb muscle precursors in the mouse. Development *122*, 1017-1027.

Davis, T.A., and Fiorotto, M.L. (2009). Regulation of muscle growth in neonates. Curr Opin Clin Nutr *12*, 78-85.

Davis, T.A., Fiorotto, M.L., Nguyen, H.V., and Reeds, P.J. (1989). Protein-Turnover in Skeletal-Muscle of Suckling Rats. Am J Physiol *257*, R1141-R1146.

de la Serna, I.L., Roy, K., Carlson, K.A., and Imbalzano, A.N. (2001). MyoD can induce cell cycle arrest but not muscle differentiation in the presence of dominant negative SWI/SNF chromatin remodeling enzymes. J Biol Chem *276*, 41486-41491.

De Strooper, B., Annaert, W., Cupers, P., Saftig, P., Craessaerts, K., Mumm, J.S., Schroeter, E.H., Schrijvers, V., Wolfe, M.S., Ray, W.J.*, et al.* (1999). A presenilin-1-dependent gamma-secretase-like protease mediates release of Notch intracellular domain. Nature *398*, 518-522.

Delaune, E.A., Francois, P., Shih, N.P., and Amacher, S.L. (2012). Single-Cell-Resolution Imaging of the Impact of Notch Signaling and Mitosis on Segmentation Clock Dynamics. Dev Cell *23*, 995-1005.

Delfini, M.C., Hirsinger, E., Pourquie, O., and Duprez, D. (2000). Delta 1-activated Notch inhibits muscle differentiation without affecting Myf5 and Pax3 expression in chick limb myogenesis. Development *127*, 5213-5224.

Dell'Orso, S., Juan, A.H., Ko, K.D., Naz, F., Perovanovic, J., Gutierrez-Cruz, G., Feng, X.S., and Sartorelli, V. (2019). Single cell analysis of adult mouse skeletal

muscle stem cells in homeostatic and regenerative conditions (vol 146, dev174177, 2019). Development *146*.

Denetclaw, W.F., and Ordahl, C.P. (2000). The growth of the dermomyotome and formation of early myotome lineages in thoracolumbar somites of chicken embryos. Development *127*, 893-905.

Dequeant, M.L., Glynn, E., Gaudenz, K., Wahl, M., Chen, J., Mushegian, A., and Pourquie, O. (2006). A complex oscillating network of signaling genes underlies the mouse segmentation clock. Science *314*, 1595-1598.

Diaz-Cuadros, M., Wagner, D.E., Budjan, C., Hubaud, A., Tarazona, O.A., Donelly, S., Michaut, A., Al Tanoury, Z., Yoshioka-Kobayashi, K., Niino, Y.*, et al.* (2020). In vitro characterization of the human segmentation clock. Nature.

Eliazer, S., Sun, X., and Brack, A.S. (2020). Spatial heterogeneity of Delta-like 4 within a multinucleated niche cell maintains muscle stem cell diversity. bioRxiv.

Elowitz, M.B., and Leibler, S. (2000). A synthetic oscillatory network of transcriptional regulators. Nature *403*, 335-338.

Epstein, J.A., Shapiro, D.N., Cheng, J., Lam, P.Y.P., and Maas, R.L. (1996). Pax3 modulates expression of the c-Met receptor during limb muscle development. P Natl Acad Sci USA *93*, 4213-4218.

Fisher, A.L., Ohsako, S., and Caudy, M. (1996). The WRPW motif of the hairy-related basic helix-loop-helix repressor proteins acts as a 4-amino-acid transcription repression and protein-protein interaction domain. Mol Cell Biol *16*, 2670-2677.

Fiuza, U.M., Klein, T., Arias, A.M., and Hayward, P. (2010). Mechanisms of Ligand-Mediated Inhibition in Notch Signaling Activity in Drosophila. Dev Dynam *239*, 798-805.

Fukada, S., Ma, Y.R., Ohtani, T., Watanabe, Y., Murakami, S., and Yamaguchi, M. (2013). Isolation, characterization, and molecular regulation of muscle stem cells. Front Physiol *4*.

Fukada, S., Yamaguchi, M., Kokubo, H., Ogawa, R., Uezumi, A., Yoneda, T., Matev, M.M., Motohashi, N., Ito, T., Zolkiewska, A.*, et al.* (2011). Hesr1 and Hesr3 are essential to generate undifferentiated quiescent satellite cells and to maintain satellite cell numbers. Development *138*, 4609-4619.

Gazave, E., Lapebie, P., Richards, G.S., Brunet, F., Ereskovsky, A.V., Degnan, B.M., Borchiellini, C., Vervoort, M., and Renard, E. (2009). Origin and evolution of the Notch signalling pathway: an overview from eukaryotic genomes. Bmc Evol Biol *9*.

Giachino, C., Basak, O., Lugert, S., Knuckles, P., Obernier, K., Fiorelli, R., Frank, S., Raineteau, O., Alvarez-Buylla, A., and Taylor, V. (2014). Molecular Diversity Subdivides the Adult Forebrain Neural Stem Cell Population. Stem Cells *32*, 70-84.

Golson, M.L., Le Lay, J., Gao, N., Bramswig, N., Loomes, K.M., Oakey, R., May, C.L., White, P., and Kaestner, K.H. (2009). Jagged1 is a competitive inhibitor of Notch signaling in the embryonic pancreas. Mech Develop *126*, 687-699.

Goodwin, B.C. (1965). Oscillatory behavior in enzymatic control processes. Adv Enzyme Regul *3*, 425-438.

Goulding, M., Lumsden, A., and Paquette, A.J. (1994). Regulation of Pax-3 Expression in the Dermomyotome and Its Role in Muscle Development. Development *120*, 957-971.

Griffith, J.S. (1968). Mathematics of Cellular Control Processes .I. Negative Feedback to 1 Gene. J Theor Biol *20*, 202-&.

Griger, J.C., Schneider, R.B., Lahmann, L., Schowel, V., Keller, C., Spuler, S., Nazare, M., and Birchmeier, C. (2017). Loss of Ptpn11 (Shp2) drives satellite cells into quiescence. Elife *6*.

Gross, M.K., Moran-Rivard, L., Velasquez, T., Nakatsu, M.N., Jagla, K., and Goulding, M. (2000). Lbx1 is required for muscle precursor migration along a lateral pathway into the limb. Development *127*, 413-424.

Hansen, A.S., and O'Shea, E.K. (2013). Promoter decoding of transcription factor dynamics involves a trade-off between noise and control of gene expression. Mol Syst Biol *9*.

Hao, N., and O'Shea, E.K. (2012). Signal-dependent dynamics of transcription factor translocation controls gene expression. Nat Struct Mol Biol *19*, 31-U47.

Harima, Y., Takashima, Y., Ueda, Y., Ohtsuka, T., and Kageyama, R. (2013). Accelerating the Tempo of the Segmentation Clock by Reducing the Number of Introns in the Hes7 Gene. Cell Rep *3*, 1-7.

Hasty, P., Bradley, A., Morris, J.H., Edmondson, D.G., Venuti, J.M., Olson, E.N., and Klein, W.H. (1993). Muscle Deficiency and Neonatal Death in Mice with a Targeted Mutation in the Myogenin Gene. Nature *364*, 501-506.

Hirata, H., Yoshiura, S., Ohtsuka, T., Bessho, Y., Harada, T., Yoshikawa, K., and Kageyama, R. (2002). Oscillatory expression of the bHLH factor Hes1 regulated by a negative feedback loop. Science *298*, 840-843.

Huard, J., Li, Y., and Fu, F.H. (2002). Current concepts review - Muscle injuries and repair: Current trends in research. J Bone Joint Surg Am *84a*, 822-832.

Hubaud, A., Regev, I., Mahadevan, L., and Pourquie, O. (2017). Excitable Dynamics and Yap-Dependent Mechanical Cues Drive the Segmentation Clock. Cell *171*, 668-+.

Imayoshi, I., Isomura, A., Harima, Y., Kawaguchi, K., Kori, H., Miyachi, H., Fujiwara, T., Ishidate, F., and Kageyama, R. (2013). Oscillatory Control of Factors Determining Multipotency and Fate in Mouse Neural Progenitors. Science *342*, 1203-1208.

Imayoshi, I., Shimogori, T., Ohtsuka, T., and Kageyama, R. (2008). Hes genes and neurogenin regulate non-neural versus neural fate specification in the dorsal telencephalic midline. Development *135*, 2531-2541.

Ishii, K., Suzuki, N., Mabuchi, Y., Ito, N., Kikura, N., Fukada, S., Okano, H., Takeda, S., and Akazawa, C. (2015). Muscle Satellite Cell Protein Teneurin-4 Regulates Differentiation During Muscle Regeneration. Stem Cells *33*, 3017-3027.

Iso, T., Sartorelli, V., Poizat, C., Iezzi, S., Wu, H.Y., Chung, G., Kedes, L., and Hamamori, Y. (2001). HERP, a novel heterodimer partner of HES/E(spl) in notch signaling. Mol Cell Biol *21*, 6080-6089.

Isomura, A., Ogushi, F., Kori, H., and Kageyama, R. (2017). Optogenetic perturbation and bioluminescence imaging to analyze cell-to-cell transfer of oscillatory information. Gene Dev *31*, 524-535.

Jacobsen, T.L., Brennan, K., Arias, A.M., and Muskavitch, M.A.T. (1998). Cis-interactions between Delta and Notch modulate neurogenic signalling in Drosophila. Development *125*, 4531-4540.

Janssen, I., Heymsfield, S.B., Wang, Z.M., and Ross, R. (2000). Skeletal muscle mass and distribution in 468 men and women aged 18-88 yr. J Appl Physiol *89*, 81-88.

Jones, N.C., Tyner, K.J., Nibarger, L., Stanley, H.M., Cornelison, D.D.W., Fedorov, Y.V., and Olwin, B.B. (2005). The p38 alpha/beta MAPK functions as a molecular switch to activate the quiescent satellite cell. J Cell Biol *169*, 105-116.

Kann, A.P., and Krauss, R.S. (2019). Multiplexed RNAscope and immunofluorescence on whole-mount skeletal myofibers and their associated stem cells. Development *146*.

Kassar-Duchossoy, L., Gayraud-Morel, B., Gomes, D., Rocancourt, D., Buckingham, M., Shinin, V., and Tajbakhsh, S. (2004). Mrf4 determines skeletal muscle identity in Myf5 : Myod double-mutant mice. Nature *431*, 466-471.

Kassar-Duchossoy, L., Giacone, E., Gayraud-Morel, B., Jory, A., Gomes, D., and Tajbakhsh, S. (2005). Pax3/Pax7 mark a novel population of primitive myogenic cells during development. Gene Dev *19*, 1426-1431.

Keller, C., Hansen, M.S., Coffin, C.M., and Capecchi, M.R. (2004). Pax3 : Fkhr interferes with embryonic Pax3 and Pax7 function: implications for alveolar rhabdomyosarcoma cell of origin. Gene Dev *18*, 2608-2613.

Kitamoto, T., and Hanaoka, K. (2010). Notch3 Null Mutation in Mice Causes Muscle Hyperplasia by Repetitive Muscle Regeneration. Stem Cells *28*, 2205-2216.

Kobayashi, T., Iwamoto, Y., Takashima, K., Isomura, A., Kosodo, Y., Kawakami, K., Nishioka, T., Kaibuchi, K., and Kageyama, R. (2015). Deubiquitinating enzymes regulate Hes1 stability and neuronal differentiation. Febs J *282*, 2475-2487.

Kobayashi, T., and Kageyama, R. (2011). Hes1 Oscillations Contribute to Heterogeneous Differentiation Responses in Embryonic Stem Cells. Genes-Basel *2*, 219-228.

Kondoh, K., Sunadome, K., and Nishida, E. (2007). Notch signaling suppresses p38 MAPK activity via induction of MKP-1 in myogenesis. J Biol Chem *282*, 3058-3065.

Kopan, R., and Ilagan, M.X.G. (2009). The Canonical Notch Signaling Pathway: Unfolding the Activation Mechanism. Cell *137*, 216-233.

Kopan, R., Nye, J.S., and Weintraub, H. (1994). The Intracellular Domain of Mouse Notch - a Constitutively Activated Repressor of Myogenesis Directed at the Basic Helix-Loop-Helix Region of Myod. Development *120*, 2385-2396.

Kuang, S.H., Kuroda, K., Le Grand, F., and Rudnicki, M.A. (2007). Asymmetric self-renewal and commitment of satellite stem cells in muscle. Cell *129*, 999-1010.

Kuroda, K., Tani, S., Tamura, K., Minoguchi, S., Kurooka, H., and Honjo, T. (1999). Delta-induced notch signaling mediated by RBP-J inhibits MyoD expression and myogenesis. J Biol Chem *274*, 7238-7244.

Lahmann, I., Brohl, D., Zyrianova, T., Isomura, A., Czajkowski, M.T., Kapoor, V., Griger, J., Ruffault, P.L., Mademtzoglou, D., Zammit, P.S.*, et al.* (2019). Oscillations of MyoD and Hes1 proteins regulate the maintenance of activated muscle stem cells. Gene Dev *33*, 524-535.

Lee, J.Y., Qu-Petersen, Z., Cao, B.H., Kimura, S., Jankowski, R., Cummins, J., Usas, A., Gates, C., Robbins, P., Wernig, A.*, et al.* (2000). Clonal isolation of muscle-derived cells capable of enhancing muscle regeneration and bone healing. J Cell Biol *150*, 1085-1099.

Li, P.L., and Elowitz, M.B. (2019). Communication codes in developmental signaling pathways. Development *146*.

Liu, N., Garry, G.A., Li, S., Bezprozvannaya, S., Sanchez-Ortiz, E., Chen, B., Shelton, J.M., Jaichander, P., Bassel-Duby, R., and Olson, E.N. (2017). A Twist2-dependent progenitor cell contributes to adult skeletal muscle. Nat Cell Biol *19*, 202-213.

Lowell, S., Jones, P., Le Roux, I., Dunne, J., and Watt, F.M. (2000). Stimulation of human epidermal differentiation by Delta-Notch signalling at the boundaries of stem-cell clusters. Curr Biol *10*, 491-500.

Machado, L., de Lima, J.E., Fabre, O., Proux, C., Legendre, R., Szegedi, A., Varet, H., Ingerslev, L.R., Barres, R., Relaix, F.*, et al.* (2017). In Situ Fixation Redefines Quiescence and Early Activation of Skeletal Muscle Stem Cells. Cell Rep *21*, 1982-1993.

Machado, L., Geara, P., Camps, J., Dos Santos, M., Teixeira-Clerc, F., Van Herck, J., Varet, H., Legendre, R., Pawlotsky, J.M., Sampaolesi, M.*, et al.* (2021). Tissue damage induces a conserved stress response that initiates quiescent muscle stem cell activation. Cell Stem Cell *28*, 1125-+.

Masamizu, Y., Ohtsuka, T., Takashima, Y., Nagahara, H., Takenaka, Y., Yoshikawa, K., Okamura, H., and Kageyama, R. (2006). Real-time imaging of the somite segmentation clock: Revelation of unstable oscillators in the individual presomitic mesoderm cells. P Natl Acad Sci USA *103*, 1313-1318.

Matsuda, M., Hayashi, H., Garcia-Ojalvo, J., Yoshioka-Kobayashi, K., Kageyama, R., Yamanaka, Y., Ikeya, M., Toguchida, J., Alev, C., and Ebisuya, M. (2020a). Species-specific segmentation clock periods are due to differential biochemical reaction speeds. Science *369*, 1450-+.

Matsuda, M., Yamanaka, Y., Uemura, M., Osawa, M., Saito, M.K., Nagahashi, A., Nishio, M., Guo, L., Ikegawa, S., Sakurai, S.*, et al.* (2020b). Recapitulating the human segmentation clock with pluripotent stem cells. Nature *580*, 124-+.

Mennerich, D., Schafer, K., and Braun, T. (1998). Pax-3 is necessary but not sufficient for lbx1 expression in myogenic precursor cells of the limb. Mech Develop *73*, 147-158.

Merly, F., Lescaudron, L., Rouaud, T., Crossin, F., and Gardahaut, M.F. (1999). Macrophages enhance muscle satellite cell proliferation and delay their differentiation. Muscle Nerve *22*, 724-732.

Micchelli, C.A., Rulifson, E.J., and Blair, S.S. (1997). The function and regulation of cut expression on the wing margin of Drosophila: Notch, Wingless and a dominant negative role for Delta and Serrate. Development *124*, 1485-1495.

Millay, D.P., Sutherland, L.B., Bassel-Duby, R., and Olson, E.N. (2014). Myomaker is essential for muscle regeneration. Gene Dev *28*, 1641-1646.

Mizuno, H., Nakamura, A., Aoki, Y., Ito, N., Kishi, S., Yamamoto, K., Sekiguchi, M., Takeda, S., and Hashido, K. (2011). Identification of Muscle-Specific MicroRNAs in Serum of Muscular Dystrophy Animal Models: Promising Novel Blood-Based Markers for Muscular Dystrophy. Plos One *6*.

Moloney, D.J., Panin, V.M., Johnston, S.H., Chen, J.H., Shao, L., Wilson, R., Wang, Y., Stanley, P., Irvine, K.D., Haltiwanger, R.S.*, et al.* (2000). Fringe is a glycosyltransferase that modifies Notch. Nature *406*, 369-375.

Mourikis, P., Sambasivan, R., Castel, D., Rocheteau, P., Bizzarro, V., and Tajbakhsh, S. (2012). A Critical Requirement for Notch Signaling in Maintenance of the Quiescent Skeletal Muscle Stem Cell State. Stem Cells *30*, 243-252.

Murphy, M.M., Lawson, J.A., Mathew, S.J., Hutcheson, D.A., and Kardon, G. (2011). Satellite cells, connective tissue fibroblasts and their interactions are crucial for muscle regeneration. Development *138*, 3625-3637.

Nabeshima, Y., Hanaoka, K., Hayasaka, M., Esumi, E., Li, S.W., Nonaka, I., and Nabeshima, Y. (1993). Myogenin Gene Disruption Results in Perinatal Lethality Because of Severe Muscle Defect. Nature *364*, 532-535.

Nakayama, K., Satoh, T., Igari, A., Kageyama, R., and Nishida, E. (2008). FGF induces oscillations of Hes1 expression and Ras/ERK activation. Curr Biol *18*, R332-R334.

Nandagopal, N., Santat, L.A., and Elowitz, M.B. (2019). Cis-activation in the Notch signaling pathway. Elife *8*.

Nichols, J.T., Miyamoto, A., and Weinmaster, G. (2007). Notch signaling - constantly on the move. Traffic *8*, 959-969.

Ochi, S., Imaizura, Y., Shimojo, H., Miyachi, H., and Kageyama, R. (2020). Oscillatory expression of Hes1 regulates cell proliferation and neuronal differentiation in the embryonic brain. Development *147*.

Okubo, Y., Sugawara, T., Abe-Koduka, N., Kanno, J., Kimura, A., and Saga, Y. (2012). Lfng regulates the synchronized oscillation of the mouse segmentation clock via trans-repression of Notch signalling. Nat Commun *3*.

Ordahl, C.P., and Ledouarin, N.M. (1992). 2 Myogenic Lineages within the Developing Somite. Development *114*, 339-353.

Ozbudak, E.M., and Lewis, J. (2008). Notch signalling synchronizes the zebrafish segmentation clock but is not needed to create somite boundaries. Plos Genet *4*.

Panin, V.M., Shao, L., Lei, L., Moloney, D.J., Irvine, K.D., and Haltiwanger, R.S. (2002). Notch Ligands are substrates for protein O-fucosyltransferase-1 and fringe. J Biol Chem *277*, 29945-29952.

Paroush, Z., Finley, R.L., Kidd, T., Wainwright, S.M., Ingham, P.W., Brent, R., and Ishhorowicz, D. (1994). Groucho Is Required for Drosophila Neurogenesis, Segmentation, and Sex Determination and Interacts Directly with Hairy-Related Bhlh Proteins. Cell *79*, 805-815.

Peault, B., Rudnicki, M., Torrente, Y., Cossu, G., Tremblay, J.P., Partridge, T., Gussoni, E., Kunkel, L.M., and Huard, J. (2007). Stem and progenitor cells in skeletal muscle development, maintenance, and therapy. Mol Ther *15*, 867-877.

Peng, H.R., and Huard, J. (2004). Muscle-derived stem cells for musculoskeletal tissue regeneration and repair. Transpl Immunol *12*, 311-319.

Perdiguero, E., Ruiz-Bonilla, V., Gresh, L., Hui, L., Ballestar, E., Sousa-Victor, P., Baeza-Raja, B., Jardi, M., Bosch-Comas, A., Esteller, M.*, et al.* (2007a). Genetic analysis of p38 MAP kinases in myogenesis: fundamental role of p38 alpha in abrogating myoblast proliferation. Embo J *26*, 1245-1256.

Perdiguero, E., Ruiz-Bonilla, V., Serrano, A.L., and Munoz-Canoves, P. (2007b). Genetic deficiency of p38 alpha reveals its critical role in myoblast cell cycle exit - The p38 alpha-JNK connection. Cell Cycle *6*, 1298-1303.

Pfeuty, B. (2015). A computational model for the coordination of neural progenitor self-renewal and differentiation through Hes1 dynamics. Development *142*, 477-485.

Pizza, F.X., Peterson, J.M., Baas, J.H., and Koh, T.J. (2005). Neutrophils contribute to muscle injury and impair its resolution after lengthening contractions in mice. J Physiol-London *562*, 899-913.

Quinlan, J.G., Lyden, S.P., Cambier, D.M., Johnson, S.R., Michaels, S.E., and Denman, D.L. (1995). Radiation Inhibition of Mdx Mouse Muscle Regeneration - Dose and Age Factors. Muscle Nerve *18*, 201-206.

Ratnayake, D., Nguyen, P.D., Rossello, F.J., Wimmer, V.C., Tan, J.L., Galvis, L.A., Julier, Z., Wood, A.J., Boudier, T., Isiaku, A.I.*, et al.* (2021). Macrophages provide a transient muscle stem cell niche via NAMPT secretion. Nature *591*, 281-+.

Rayon, T., Stamataki, D., Perez-Carrasco, R., Garcia-Perez, L., Barrington, C., Melchionda, M., Exelby, K., Lazaro, J., Tybulewicz, V.L.J., Fisher, E.M.C.*, et al.* (2020). Species-specific pace of development is associated with differences in protein stability. Science *369*, 1449-+.

Relaix, F., Polimeni, M., Rocancourt, D., Ponzetto, C., Schafer, B.W., and Buckingham, M. (2003). The transcriptional activator PAX3-FKHR rescues the defects of Pax3 mutant mice but induces a myogenic gain-of-function phenotype with ligand-independent activation of Met signaling in vivo. Gene Dev *17*, 2950-2965.

Reynaud, E.G., Leibovitch, M.P., Tintignac, L.A.J., Pelpel, K., Guillier, M., and Leibovitch, S.A. (2000). Stabilization of MyoD by direct binding to p57(Kip2). J Biol Chem *275*, 18767-18776.

Riedel-Kruse, I.H., Muller, C., and Oates, A.C. (2007). Synchrony dynamics during initiation, failure, and rescue of the segmentation clock. Science *317*, 1911-1915.

Rooke, J., Pan, D., Xu, T., and Rubin, G.M. (1996). KUZ, a conserved metalloprotease-disintegrin protein with two roles in Drosophila neurogenesis. Science *273*, 1227-1231.

Rudnicki, M.A., Braun, T., Hinuma, S., and Jaenisch, R. (1992). Inactivation of Myod in Mice Leads to up-Regulation of the Myogenic Hlh Gene Myf-5 and Results in Apparently Normal Muscle Development. Cell *71*, 383-390.

Rudnicki, M.A., Schnegelsberg, P.N.J., Stead, R.H., Braun, T., Arnold, H.H., and Jaenisch, R. (1993). Myod or Myf-5 Is Required for the Formation of Skeletal-Muscle. Cell *75*, 1351-1359.

Sachs, M., Brohmann, H., Zechner, D., Muller, T., Hulsken, J., Walther, I., Schaeper, U., Birchmeier, C., and Birchmeier, W. (2000). Essential role of Gab1 for signaling by the c-Met receptor in vivo. J Cell Biol *150*, 1375-1384.

Sakagami, T., Sakurada, K., Sakai, Y., Watanabe, T., Nakanishi, S., and Kageyama, R. (1994). Structure and Chromosomal Locus of the Mouse Gene Encoding a Cerebellar Purkinje Cell-Specific Helix-Loop-Helix Factor Hes-3. Biochem Bioph Res Co *203*, 594-601.

Sakai, H., Fukuda, S., Nakamura, M., Uezumi, A., Noguchi, Y., Sato, T., Morita, M., Yamada, H., Tsuchida, K., Tajbakhsh, S.*, et al.* (2017). Notch ligands regulate the

muscle stem-like state ex vivo but are not sufficient for retaining regenerative capacity. Plos One *12*.

Sambasivan, R., Gayraud-Morel, B., Dumas, G., Cimper, C., Paisant, S., Kelly, R., and Tajbakhsh, S. (2009). Distinct Regulatory Cascades Govern Extraocular and Pharyngeal Arch Muscle Progenitor Cell Fates. Dev Cell *16*, 810-821.

Schmalbruch, H., and Lewis, D.M. (2000). Dynamics of nuclei of muscle fibers and connective tissue cells in normal and denervated rat muscles. Muscle Nerve *23*, 617-626.

Schmidt, C., Bladt, F., Goedecke, S., Brinkmann, V., Zschiesche, W., Sharpe, M., Gherardi, E., and Birchmeier, C. (1995). Scatter Factor/Hepatocyte Growth-Factor Is Essential for Liver Development. Nature *373*, 699-702.

Schneider, B.S., Brickson, S., Corr, D.T., and Best, T. (2002). CD11b(+) neutrophils predominate over RAM11(+) macrophages in stretch-injured muscle. Muscle Nerve *25*, 837-844.

Schuster-Gossler, K., Cordes, R., and Gossler, A. (2007). Premature myogenic differentiation and depletion of progenitor cells cause severe muscle hypotrophy in Delta1 mutants. P Natl Acad Sci USA *104*, 537-542.

Shawber, C., Nofziger, D., Hsieh, J.J.D., Lindsell, C., Bogler, O., Hayward, D., and Weinmaster, G. (1996). Notch signaling inhibits muscle cell differentiation through a CBF1-independent pathway. Development *122*, 3765-3773.

Shimojo, H., Isomura, A., Ohtsuka, T., Kori, H., Miyachi, H., and Kageyama, R. (2016). Oscillatory control of Delta-like1 in cell interactions regulates dynamic gene expression and tissue morphogenesis. Gene Dev *30*, 102-116.

Shimojo, H., Ohtsuka, T., and Kageyama, R. (2008). Oscillations in notch signaling regulate maintenance of neural progenitors. Neuron *58*, 52-64.

Smolen, P., Baxter, D.A., and Byrne, J.H. (2000a). Mathematical modeling of gene networks. Neuron *26*, 567-580.

Smolen, P., Baxter, D.A., and Byrne, J.H. (2000b). Modeling transcriptional control in gene networks - Methods, recent results, and future directions. B Math Biol *62*, 247-292.

Snow, M.H. (1978). Autoradiographic Study of Satellite Cell-Differentiation into Regenerating Myotubes Following Transplantation of Muscles in Young-Rats. Cell Tissue Res *186*, 535-540.

Sonnen, K.F., Lauschke, V.M., Uraji, J., Falk, H.J., Petersen, Y., Funk, M.C., Beaupeux, M., Francois, P., Merten, C.A., and Aulehla, A. (2018). Modulation of Phase Shift between Wnt and Notch Signaling Oscillations Controls Mesoderm Segmentation. Cell *172*, 1079-+.

Sprinzak, D., Lakhanpal, A., LeBon, L., Santat, L.A., Fontes, M.E., Anderson, G.A., Garcia-Ojalvo, J., and Elowitz, M.B. (2010). Cis-interactions between Notch and Delta generate mutually exclusive signalling states. Nature *465*, 86-U95.

Struhl, G., and Adachi, A. (2000). Requirements for presenilin-dependent cleavage of notch and other transmembrane proteins. Mol Cell *6*, 625-636.

Struhl, G., and Greenwald, I. (1999). Presenilin is required for activity and nuclear access of Notch in Drosophila. Nature *398*, 522-525.

Swinburne, I.A., Miguez, D.G., Landgraf, D., and Silver, P.A. (2008). Intron length increases oscillatory periods of gene expression in animal cells. Gene Dev *22*, 2342-2346.

Tajbakhsh, S., and Buckingham, M. (2000). The birth of muscle progenitor cells in the mouse: Spatiotemporal considerations. Curr Top Dev Biol *48*, 225-268.

Takashima, Y., Ohtsuka, T., Gonzalez, A., Miyachi, H., and Kageyama, R. (2011). Intronic delay is essential for oscillatory expression in the segmentation clock. P Natl Acad Sci USA *108*, 3300-3305.

Takebayashi, K., Sasai, Y., Sakai, Y., Watanabe, T., Nakanishi, S., and Kageyama, R. (1994). Structure, Chromosomal Locus, and Promoter Analysis of the Gene Encoding the Mouse Helix-Loop-Helix Factor Hes-1 - Negative Autoregulation through the Multiple N-Box Elements. J Biol Chem *269*, 5150-5156.

van Velthoven, C.T.J., de Morree, A., Egner, I.M., Brett, J.O., and Rando, T.A. (2017). Transcriptional Profiling of Quiescent Muscle Stem Cells In Vivo. Cell Rep *21*, 1994-2004.

Vasyutina, E., Lenhard, D.C., Wende, H., Erdmann, B., Epstein, J.A., and Birchmeier, C. (2007). RBP-J (Rbpsuh) is essential to maintain muscle progenitor cells and to generate satellite cells. P Natl Acad Sci USA *104*, 4443-4448.

Vasyutina, E., Stebler, J., Brand-Saberi, B., Schulz, S., Raz, E., and Birchmeier, C. (2005). CXCR4 and Gab1 cooperate to control the development of migrating muscle progenitor cells. Genes Dev *19*, 2187-2198.

Venter, J.C. (2001). The sequence of the human genome (vol 292, pg 1304, 2001). Science *292*, 1838-1838.

Vilar, J.M.G., Kueh, H.Y., Barkai, N., and Leibler, S. (2002). Mechanisms of noise-resistance in genetic oscillators. P Natl Acad Sci USA *99*, 5988-5992.

Wakeford, S., Watt, D.J., and Partridge, T.A. (1991). X-Irradiation Improves Mdx Mouse Muscle as a Model of Myofiber Loss in Dmd. Muscle Nerve *14*, 42-50.

Weller, B., Karpati, G., Lehnert, S., Carpenter, S., Ajdukovic, B., and Holland, P. (1991). Inhibition of Myosatellite Cell-Proliferation by Gamma-Irradiation Does Not Prevent the Age-Related Increase of the Number of Dystrophin-Positive Fibers in Soleus Muscles of Mdx Female Heterozygote Mice. Am J Pathol *138*, 1497-1502.

Wigmore, P.M., and Evans, D.J.R. (2002). Molecular and cellular mechanisms involved in the generation of fiber diversity during myogenesis. Int Rev Cytol *216*, 175-232.

Wittenberger, T., Steinbach, O.C., Authaler, A., Kopan, R., and Rupp, R.A.W. (1999). MyoD stimulates Delta-1 transcription and triggers Notch signaling in the Xenopus gastrula. Embo J *18*, 1915-1922.

Wooddell, C.I., Radley-Crabb, H.G., Griffin, J.B., and Zhang, G. (2011). Myofiber Damage Evaluation by Evans Blue Dye Injection. Curr Protoc Mouse Biol *1*, 463-488.

Yamaguchi, M., Ogawa, R., Watanabe, Y., Uezumi, A., Miyagoe-Suzuki, Y., Tsujikawa, K., Yamamoto, H., Takeda, S., and Fukada, S. (2012). Calcitonin receptor and Odz4 are differently expressed in Pax7-positive cells during skeletal muscle regeneration. J Mol Histol *43*, 581-587.

Yang, X.M., Vogan, K., Gros, P., and Park, M. (1996). Expression of the met receptor tyrosine kinase in muscle progenitor cells in somites and limbs is absent in Splotch mice. Development *122*, 2163-2171.

Yartseva, V., Goldstein, L.D., Rodman, J., Kates, L., Chen, M.Z., Chen, Y.J.J., Foreman, O., Siebel, C.W., Modrusan, Z., Peterson, A.S.*, et al.* (2020). Heterogeneity of Satellite Cells Implicates DELTA1/NOTCH2 Signaling in Self-Renewal. Cell Rep *30*, 1491-+.

Yoshioka-Kobayashi, K., Matsumiya, M., Niino, Y., Isomura, A., Kori, H., Miyawaki, A., and Kageyama, R. (2020). Coupling delay controls synchronized oscillation in the segmentation clock. Nature.

Yoshiura, S., Ohtsuka, T., Takenaka, Y., Nagahara, H., Yoshikawa, K., and Kageyama, R. (2007). Ultradian oscillations of Stat, Smad, and Hes1 expression in response to serum. P Natl Acad Sci USA *104*, 11292-11297.

Zaharieva, I.T., Calissano, M., Scoto, M., Preston, M., Cirak, S., Feng, L., Collins, J., Kole, R., Guglieri, M., Straub, V.*, et al.* (2013). Dystromirs as Serum Biomarkers for Monitoring the Disease Severity in Duchenne Muscular Dystrophy. Plos One *8*.

Zalc, A., Hayashi, S., Aurade, F., Brohl, D., Chang, T., Mademtzoglou, D., Mourikis, P., Yao, Z.Z., Cao, Y., Birchmeier, C.*, et al.* (2014). Antagonistic regulation of p57(kip2) by Hes/Hey downstream of Notch signaling and muscle regulatory factors regulates skeletal muscle growth arrest. Development *141*, 2780-2790.

Zismanov, V., Chichkov, V., Colangelo, V., Jamet, S., Wang, S., Syme, A., Koromilas, A.E., and Crist, C. (2016). Phosphorylation of eIF2 alpha Is a Translational Control Mechanism Regulating Muscle Stem Cell Quiescence and Self-Renewal. Cell Stem Cell *18*, 79-90.

7. Appendix

7.1. Supplementary figure

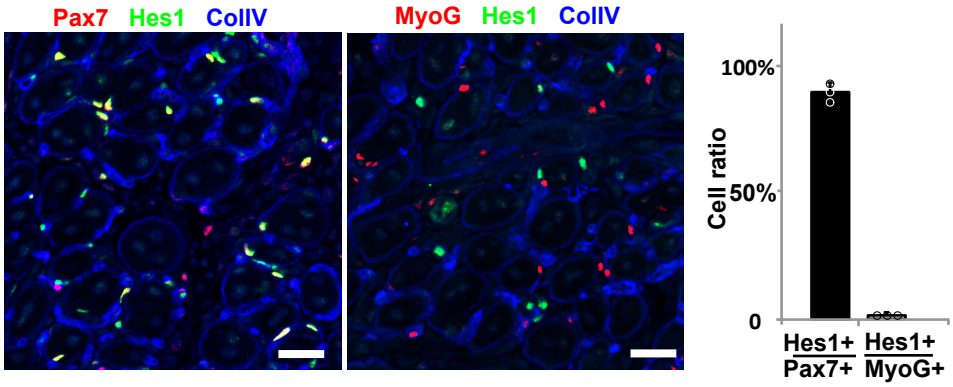

Supplementary figure 1. Hes1 is expressed in Pax7+ cells but not MyoG+ cells.
Immunohistological analysis of Hes1 (green), Pax7 or MyoG (red, as indicated) and collagen IV (ColIV, blue) of injured muscle (4 dpi); the quantification (right) demonstrates that MyoG+ cells do not express Hes1; n=3.

7.2. Delay modeling

To explain what happened in *Dll1tpye2* mutant muscle stem cells, I used the delay differential equation (DDE) model. This model is developed by Dr. Katharina Baum and Dr. Jana Wolf.

First, we constructed a single-cell DDE model according to the Hes1-Dll1 regulatory network (Supplementary figure 2).

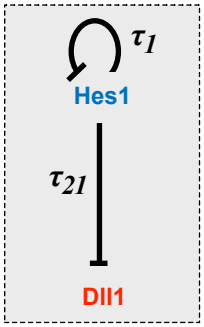

Supplementary figure 2. Scheme of the transcriptional regulation of Dll1 by Hes1 in a single cell.
Hes1 protein (Blue) and Dll1 protein (Red) are indicated. Here, *τ1* is the time required for Hes1 protein to affect its production through the negative feedback loop. *τ21* is the time that Hes1 protein needs to reduce Dll1 protein levels through reducing the transcription of the Dll1 gene.

This model consists of two variables *HP(t)* and *DP(t)*. Hes1 protein (HP) inhibits synthesis of its production with delay time *τ1*, as well as the inhibition of Dll1 protein (DP) production with delay time *τ21*. Both proteins are degraded at a constant rate. The DDE equations in a single cell are as follows,

$$\frac{\mathrm{d\,HP}}{\mathrm{dt}}(t) = k_1 \cdot \frac{k_2^2}{k_2^2 + (\mathrm{HP}(t-\tau_1))^2} - k_3 \cdot \mathrm{HP}(t) \quad (1)$$

$$\frac{\mathrm{d\,DP}}{\mathrm{dt}}(t) = k_4 \cdot \frac{k_5^2}{k_5^2 + (\mathrm{HP}(t-\tau_{21}))^2} - k_6 \cdot \mathrm{DP}(t) \quad (2)$$

Here, we use Hes1 protein synthesis rate constant *k1*=100 and Dll1 protein synthesis rate constant *k4*=11.2. The parameters *k2* and *k5* correspond to the typical amounts of Hes1 that account for the repression to itself (*k2*) or to Dll1 (*k5*). The degradation rates of Hes1 protein and Dll1 protein are linear; *k3*=2.6 corresponds to a half-live of Hes1 protein of about 16 min (ln2/half-live in hours), and *k6*=1.04 corresponds to a half-life of Dll1 protein of about 40 min (ln2/half-life in hours). Both are from experimental data. The delay times are *τ1*=0.725 h and *τ21*=0.35h. We mapped the dynamics of Hes1 and Dll1 protein with the model in a single cell. Both Hes1 and Dll1 protein expressions oscillate with the oscillatory period of 2 hours (Supplementary figure 3).

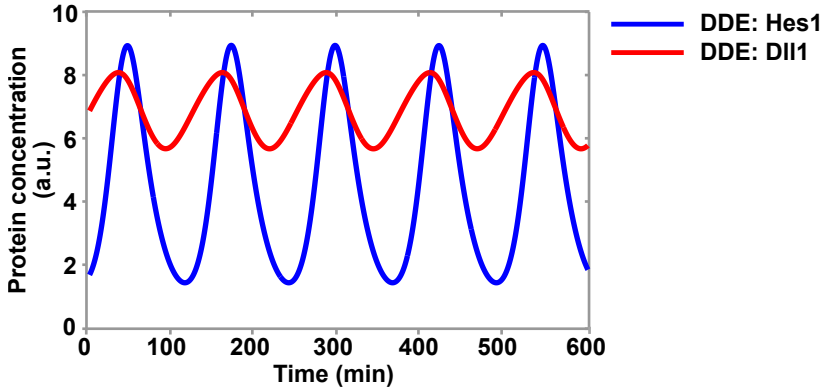

Supplementary figure 3. Expression dynamics in the single-cell DDE model
Hes1 protein (Blue) and Dll1 protein (Red) oscillate. Equations (1-2) are used.

Next, we adjusted the parameter $\tau 21$ to 0.45h (increased by 0.1h) to mimic the protein dynamics in *Dll1type2* mutant muscle stem cells. This delay is the time that Hes1 needs to affect Dll1 protein levels, which includes *Dll1* transcription time. We found in our model that increasing of $\tau 21$ by 0.1h affected the phase relationships between Hes1 and Dll1 protein oscillations, but not the oscillatory amplitudes nor period (Supplementary figure 4).

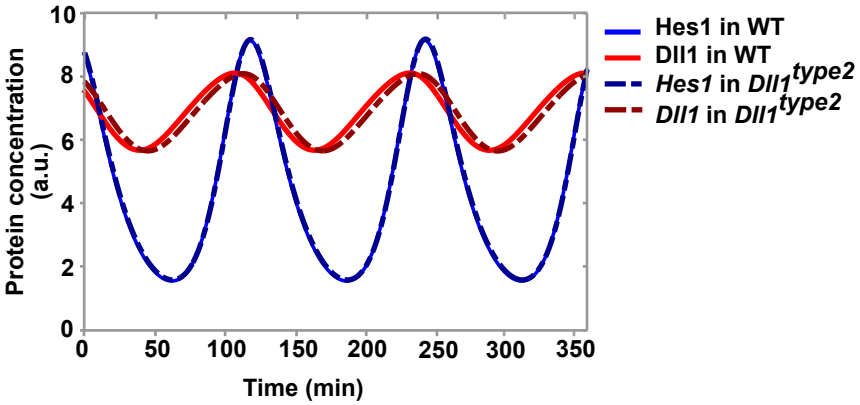

Supplementary figure 4. Oscillation dynamics of Dll1 and Hes1 in single wild type and *Dll1type2* mutant muscle stem cell with increased delay time $\tau 21$
Hes1 protein (Blue) and Dll1 protein (Red) are indicated. Equations (1-2) are used.

Next, we expanded the DDE model to two coupled cells according to the scheme of the regulatory network (Supplementary figure 5).

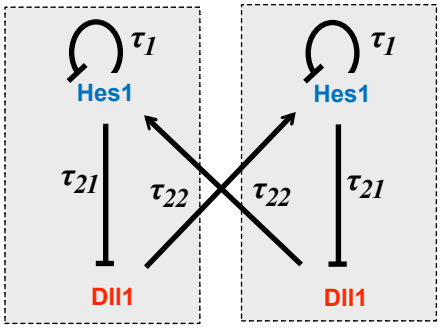

Supplementary figure 5. Scheme of the transcriptional regulation of Hes1 and Dll1 in two coupled cells

Hes1 protein (Blue) and Dll1 protein (Red) are indicated. Here, *τ1* is the time required for Hes1 protein to affect its production through the negative feedback loop. *τ21* is the time that Hes1 protein needs to reduce Dll1 protein through inhibiting the transcription of the Dll1 gene. *τ22* is the time that Dll1 protein needs to induce the Hes1 protein in the neighboring cell.

In this model, Dll1 expression in one cell induces Hes1 synthesis in the neighboring cell with a delay time *τ22*. We also set a coupling strength, which is specific for different cell types. The DDE equations in coupled cells are as follows:

$$\frac{\mathrm{d\,HP_1}}{\mathrm{dt}}(t) = k_1 \cdot \frac{k_2^2}{k_2^2+(\mathrm{HP_1}(t-\tau_1))^2} \cdot \frac{\mathrm{DP_2}(t-\tau_{22})}{k_7} - k_3 \cdot \mathrm{HP_1}(t) \quad (3)$$

$$\frac{\mathrm{d\,DP_1}}{\mathrm{dt}}(t) = k_4 \cdot \frac{k_5^2}{k_5^2+(\mathrm{HP_1}(t-\tau_{21}))^2} - k_6 \cdot \mathrm{DP_1(t)} \quad (4)$$

$$\frac{\mathrm{d\,HP_2}}{\mathrm{dt}}(t) = k_1 \cdot \frac{k_2^2}{k_2^2+(\mathrm{HP_2(t-\tau_1)})^2} \cdot \frac{\mathrm{DP_1}(t-\tau_{22})}{k_7} - k_3 \cdot \mathrm{HP_2(t)} \quad (5)$$

$$\frac{\mathrm{d\,DP_2}}{\mathrm{dt}}(t) = k_4 \cdot \frac{k_5^2}{k_5^2+(\mathrm{HP_2(t-\tau_{21})})^2} - k_6 \cdot \mathrm{DP_2(t)} \quad (6)$$

Here we used the same parameters *k1*, *k2*, *k3*, *k4*, *k5*, *k6*, *τ1*, and *τ21* as in the single-cell DDE model. In addition, we used *k7*=50, which corresponds to the coupling strength, and *τ22*=1.3h. We mapped the Hes1 and Dll1 protein dynamics in coupling cells with this model. We found that in coupled identical wild type cells, the Dll1 protein expressions in both cells oscillate in an out-of-phase manner. However, in the coupled mutant cells, in which *τ21* is increased by 0.1h, Dll1 protein oscillations in both cells are strongly dampened. Interestingly, Dll1 protein still oscillates with smaller amplitudes if one wild type and one mutant cell are coupled (Supplementary figure 6).

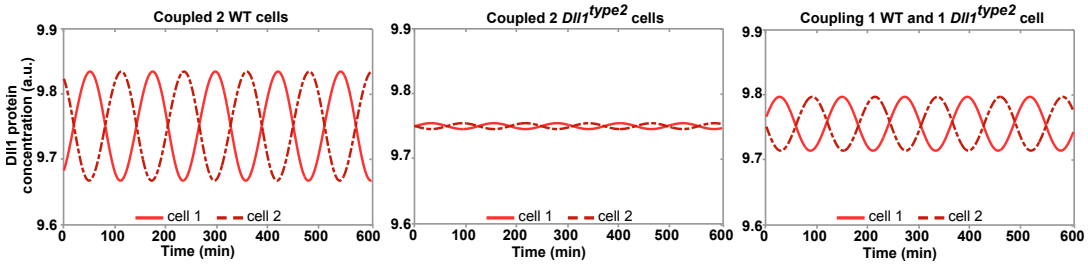

Supplementary figure 6. The dynamics of Dll1 in the two coupled cells

Dll1 protein dynamics in two coupled wild type(WT) cells (left), two coupled *Dll1type2* mutant cells (middle), and one *Dll1type2* mutant cell coupled with one wild type (WT) cell.

To systemically investigate the function of $\tau 21$ in coupled cells, we tested the influence of $\tau 21$ on the amplitudes of Hes1 and Dll1 protein oscillation and on their phase shift (Supplementary figure 7). The appropriate timing of Dll1 production is important for Dll1 dynamics. Here, we used $\tau 21$ = 0.35 for wild type cells, and the oscillations in two coupled cells showed an out-of-phase manner. When the delay is increased, the oscillations in coupled cells are dampened. We found that out-of-phase oscillations for two coupled cells with a certain $\tau 21$ range, while in another range the oscillations will be either quenched or in phase.

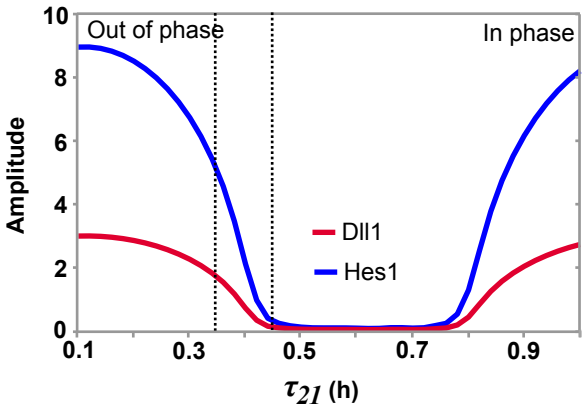

Supplementary figure 7. $\tau 21$ dependency of oscillation amplitude in two coupled cells.

To investigate $\tau 21$ dependency, the amplitudes of Hes1 and Dll1 oscillation were measured. Both cells showed the same oscillation amplitudes and periods. The dash lines showed the value of $\tau 21$ in wild type cell (0.35 h) and *Dll1type2* cell (0.45 h).

Thus, the delay time that Hes1 needs to regulate Dll1 protein production, which also includes the Dll1 transcription time, is important for the oscillation in coupled cells. Thus, the *Dll1type2* allele allowed us to investigate the functional importance of Dll1 oscillations in muscle stem cells.